Universidad de Valladolid

ESCUELA DE INGENIERÍAS INDUSTRIALES

UNIVERSIDAD DE VALLADOLID

ESCUELA DE INGENIERIAS INDUSTRIALES

Máster en Ingeniería Industrial

Estudio de la longevidad de las baterías de ion de litio en sistemas de almacenamiento solar fotovoltaico

Autor:

Gumiel Correa, Juan

Francisco Javier Rey Martínez

University of Malta

Valladolid, Julio 2021.

TFM REALIZADO EN PROGRAMA DE INTERCAMBIO

TÍTULO:	A study on Lithium-ion battery longevity in PV battery storage systems
ALUMNO:	Juan Gumiel Correa
FECHA:	2/07/2021
CENTRO:	Institute for Sustainable Energy
UNIVERSIDAD:	University of Malta
TUTORES:	Dr. Cedric Caruana Dr. Ing. Charles Yousif

Resumen

Título: Estudio de la longevidad de las baterías de iones de Litio en sistemas de almacenamiento solar fotovoltaico

Autor: Juan Gumiel Correa

Palabras clave: Batería de ion de Litio, Degradación batería, Sistema de almacenamiento de energía en batería, Cycle aging, Calendar aging

Las baterías de ion de litio (Li-ion) son una tecnología clave en los sistemas solares fotovoltaicos, permitiendo minimizar el desajuste entre generación y consumo y maximizar el autoconsumo. Este trabajo busca ofrecer un análisis exhaustivo de todos los parámetros operacionales que pueden impactar en la vida de las baterías de Li-ion, para identificar las tendencias asociadas a cada uno de ellos y buscar la estrategia optima para extender su vida útil y rendimiento efectivo.

Con este fin se estudiaron distintos parámetros y estrategias para cuatro casos representativos mediante simulaciones usando dos softwares diferentes. A partir de esto, se determinó una serie de pautas generales para extender la vida útil de la batería y se compararon con las que se dan en la literatura.

Abstract

Title: A study on Lithium-ion battery longevity in PV battery storage systems

Author: Juan Gumiel Correa

Keywords: Lithium-ion battery, Battery degradation, Battery Energy Storage System, Cycle aging, Calendar aging

Lithium-ion (Li-ion) batteries are recognized as a key energy storage technology for solar photovoltaic systems, when used to minimize mismatch between generation and consumption and maximize self-consumption of the user. This dissertation aims to offer a comprehensive analysis of all operational parameters that can impact Li-ion lifetime, to identify the tendencies associated with each one of them and offer guidelines on the optimal approach to extend its operational lifetime and effective performance.

To this end different parameters and operating strategies were studied for four representative scenarios through simulations using two different software. From this, a list of guidelines to extend battery lifetime were determined and compared to the ones given in literature.

A STUDY ON LITHIUM-ION BATTERY LONGEVITY IN PV BATTERY STORAGE SYSTEM

Juan Gumiel Correa

Institute for Sustainable Energy

University of Malta

July 2021

A STUDY ON LITHIUM-ION BATTERY LONGEVITY IN PV BATTERY STORAGE SYSTEM

A dissertation presented at the

Institute for Sustainable Energy of the University of Malta, Malta

in partial fulfilment of the requirements of the award of

Bachelor of Industrial Engineering

at the

Universidad de Valladolid, Spain

under the Erasmus Plus Student Exchange Programme 2020/21.

Declaration

No portion of the work referred to in the dissertation has been submitted in support of an application for another degree or qualification of this or any other university or other institute of learning.

Signature of Student

Name of Student

Juan Gumiel Correa

July 2021

Copyright notice

Abstract

Lithium-ion (Li-ion) batteries are recognized as a key energy storage technology for solar photovoltaic systems, when used to minimize mismatch between generation and consumption and maximize self-consumption of the user. Therefore, determining the key parameters that can impact the performance of this type of batteries is fundamental for its optimum performance.

This dissertation aims to offer a comprehensive analysis of all operational parameters that can impact Li-ion lifetime, to identify the tendencies associated with each one of them and offer guidelines on the optimal approach to extend its operational lifetime and effective performance.

To this end four representative scenarios were studied using two different software. The scenarios included are two corresponding to one person either working or unemployed and another two corresponding to a family of four members, two parents and two children, with both parents either working or unemployed.

The cumulative impact of different performance loading showed that parameters such as state of charge (SOC) range and ambient air temperature beyond the recommended operational rang tend to decrease the lifetime of the battery, while strategies such as oversizing the battery while keeping the same usable capacity could extend it. The more efficient dispatch models that achieved a higher cycle of the battery suffered more from degradation. Out of the two chemistries common for residential storage, the Lithium-Ion Phosphate-based battery showed a better performance in terms of lifetime.

Lastly, a list of guidelines to extend battery lifetime were determined and compared to the ones given in literature. For example, the state of charge between 20-80% is ideal for the modelled operation. An increase from 20% to 40% state of charge only adds 1 to 2 years more to the overall expected lifetime. Although oversizing is beneficial to the battery lifetime, this increases the capital costs. Finally, batteries should not be operated under high temperature (>25°), as they lose capacity and life. If placed under the solar PV panels, they would be in the shade and protected from overheating.

Acknowledgments

I would like to express my sincere gratitude to my supervisor Dr. Cedric Caruana and my co-supervisor Dr. Inġ. Charles Yousif for their commitment, patience and dedication. Their valuable contributions and ideas have been fundamental for the successful completion of this dissertation.

I would also like to thank the University of Valladolid and the University of Malta Erasmus offices for giving me this opportunity of experiencing a study-abroad period in this beautiful country.

Lastly, I would also like to thank my family and friends for their continuous encouragement and help. Thanks to my parents, for making this trip possible and believing in me. Special thanks to Panzi and Paula, for their constant love and support despite the distance.

Table of contents

List of Figures

List of Tables

List of Abbreviations

BESS	Battery Energy Storage System
BMS	Battery Management System
DOD	Depth of discharge
LCO	Lithium Cobalt Oxide
LFP	Lithium Iron Phosphate
Li-ion	Lithium-ion
LiPo	Lithium Polymer
LMO	Lithium Manganese Oxide
LTO	Lithium Titanate
NCA	Nickel Cobalt Aluminium
NiCd	Nickel Cadmium
NiMH	Nickel Metal Hydride
NMC	Nickel Manganese Cobalt
PV	Photovoltaic
RFB	Redox Flow Batteries
SEI	Solid Electrolyte Interface
SOC	State of Charge
SOH	State of Health

1 Introduction

1.1 The drive towards solar energy

Since the beginning, humanity has had an ever-growing demand for energy. To keep up with this demand, non-renewable energy sources like coal, oil and gas started being massively used after the industrial revolution. However, these kinds of sources are limited in the long term. Furthermore, they involve strong environmental threats like pollution and global warming. Because of this, in the recent years there has been a strong drive towards renewable energies, with the objective of providing the demanded energy in a clean and sustainable way.

In Europe this drive resulted in the Renewable Energy Directive 2009/28/EC which was enacted in 2009 aiming to increase the share of renewable energy across the different sectors [1]. In 2018 the recast Renewable Energy Directive 2018/2001/EU entered into force setting the current objective of fulfilling at least 32% of the energy needs in the EU with renewable energies by 2030 [2]. In 2019 the European Green Deal was announced; whose aim is to make Europe a climate neutral continent by 2050. Being responsible for more than 75% of the EU's greenhouse emissions, the energy sector plays a key role in achieving this goal [3].

The transition towards renewable energies in Malta is challenging. With small land area and limited hydrological resources, some of the common approaches towards renewable energies in other countries are not viable. However, with an average of 300 days of sunshine per year, photovoltaic (PV) solar energy has a very strong potential. Because of Malta's small surface area, land for large PV installations is scarce and expensive and thus the installation of panels on rooftops for domestic usage is more appealing. To this end, in the recent years the Government of Malta has incentivized the installation of PV system through subventions and bonifications. This way consumers can benefit from savings in their electrical bills while the country transitions to renewable energies.

1.2 Energy storage in PV residential systems

As it occurs with other renewable energies, PV solar energy is dependent on the resource and its production is not consistent, because it depends on the availability of solar radiation and the overall climatic conditions such as clouding, which are constantly changing. Furthermore, the PV generation profile and residential load profiles do not match as shown in Figure 1. The PV generation follows the irradiation pattern, peaking around noon. The load profile on the other hand is tied to the consumers' lifestyle, generally experiencing increases at mealtimes and peaking in the evening. The load profile will be strongly influenced by the situation of the particular household, varying with the number of people, the employment situation and the general lifestyle of the residents.

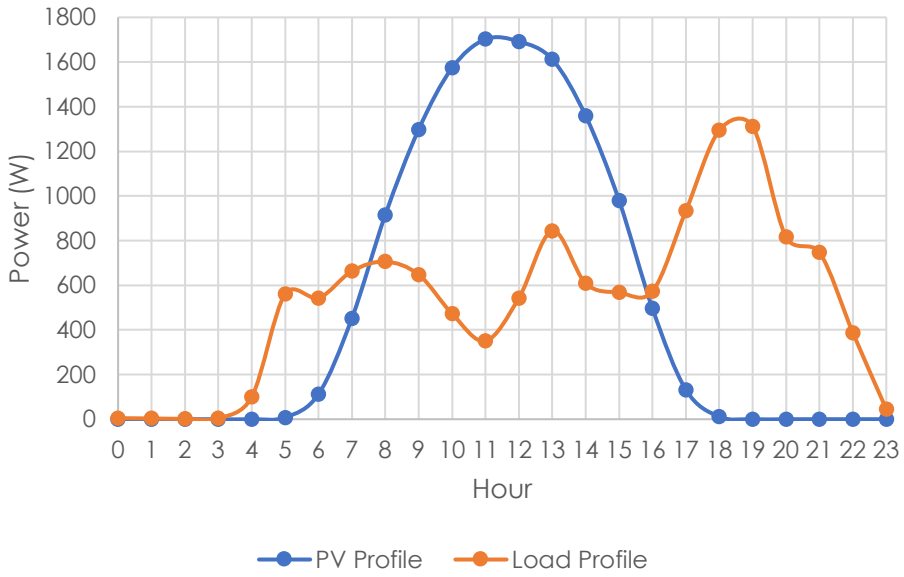

Figure 1. Average daily PV generation and load profile of a typical household.

A strategy to mitigate this mismatch is the use of energy storage. An energy storage acts as a buffer, allowing to store the excess power during central hours of the day and deliver it when the demand surpasses the production after sunset. Similarly, it helps to cover the demand when the atmospheric conditions are less favourable like during cloudy days.

In an off-grid system the energy storage must be big enough to ensure self-sufficiency. However, in an on-grid system, which is more common, the system can be much smaller as it only acts as a buffer. This way the use of energy storage allows a greater use of the PV production for increasing self-consumption. On the other hand, several operational parameters linked to battery usage such as cycling, and depth of discharge have a

significant impact on the performance of the battery bank such as lifetime and storage capacity.

1.3 Aim and Objectives

The aim of this dissertation is to determine the extent to which variable battery usage parameters impact the performance of Lithium-ion batteries, which are the most common type of batteries used for energy storage that is linked with PV systems. The main objectives of the dissertation are:

- Perform a detailed review of the failure mechanisms in Li-ion batteries and identify the operating parameters that affect Li-ion aging.
- Study the effect of the parameters affecting Li-ion aging through simulations, identifying the possible impact associated with each one of them.
- Extract general guidelines to extend Li-ion battery lifespan and compare them to the ones given by the manufacturers and in literature.

1.4 Dissertation structure

The dissertation consists of 5 chapters. Chapter 1 introduces the topic, explaining the motivation that has led to PV systems with batteries and setting the aim and objectives of the study.

Chapter 2 provides the necessary background about batteries and batteries in energy storage system to then focus on Lithium ions batteries and its degradation. After that it presents the literature review conducted about Li-ion lifetime.

Chapter 3 shows the methodology followed to carry out the simulations, describing the models employed and the scenarios studied.

Chapter 4 presents and discusses the results for the four scenarios studied, analysing the effect of each one of the studied parameters and comparing the scenarios against each other.

Chapter 5 summarizes the findings of the study, identifying the most relevant observations and providing guidelines to extend the lifetime of Li-ion batteries. Lastly, a number of recommendations for future work is provided.

2 Background Theory and Literature Review

This chapter provides the general background necessary for the dissertation and reviews previous works on Li-ion degradation. The first section provides a brief description of the main concepts about batteries that will be used throughout the dissertation. Then a brief description on batteries for energy storage is presented. After that Li-ion batteries are studied in more depth, discussing the general characteristics of this technology. The next section is focused on the degradation of Li-ion batteries. Lastly, previous works studying Li-ion degradation are presented and discussed.

2.1 General concepts about batteries

A battery is a device capable of storing electric energy through an electrochemical reaction. Batteries are generally classified in two groups. Primary batteries or non-rechargeable batteries are designed to be single used and cannot be charged. Secondary batteries or rechargeable batteries are reusable and can be both charged and discharged.

A battery is formed in a modular manner using basic electrochemical units known as cells. These cells are connected in series or parallel to build up to the desired battery specifications.

The basic components of a battery cell are shown in Figure 2, where the following can be noted:

- **Anode (negative electrode).** It is generally made of materials with tendency to lose electrons (electropositive).
- **Cathode (positive electrode).** It is usually made of materials with tendency to gain electrons (electronegative).
- **Electrolyte.** Is a material that makes possible the flow of ions between the electrodes. It can be solid or liquid.
- **Separator.** It is a barrier present when the electrolyte of each electrode is different to prevent the contact between them while being permeable to ions.
- **Cell container.** It is the casing for the cell that holds it together.

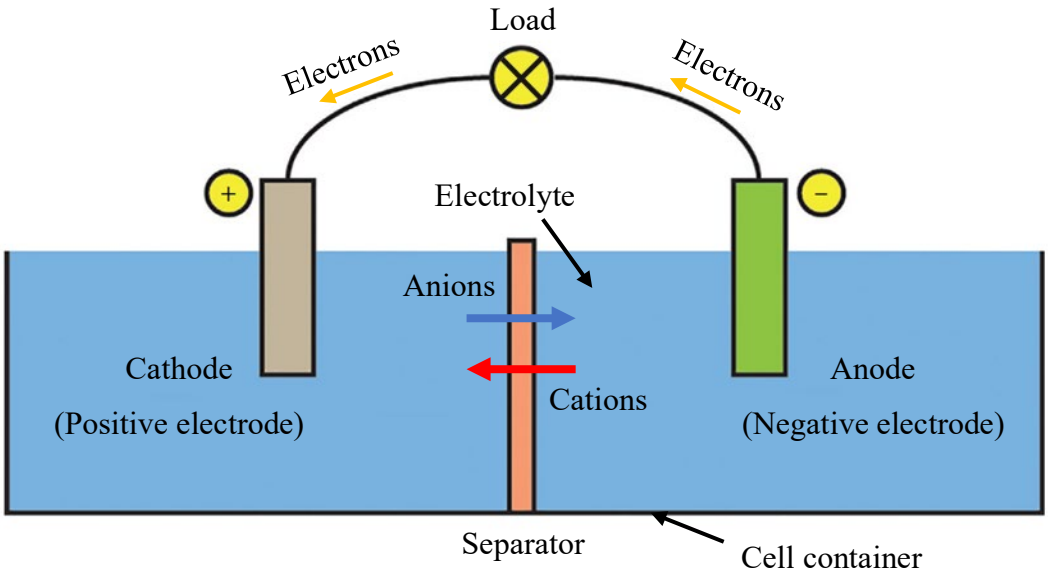

Figure 2. Basic components and principle of operation of a battery cell. Adapted from [4].

The electrochemistry of the battery is as follows. When the anode is connected to the cathode through an external circuit the cell discharges. During discharge the anode material oxidizes, releasing electrons. These electrons travel through the external circuit to the cathode, driving the load connected to the battery. In the cathode, the cathode material reduces, accepting the electrons. Simultaneously, the negative ions (anions) move through the electrolyte to compensate the resulting positive charge of the anode after losing electrons and the positive ions (cations) move to compensate the negative charge of the anode after gaining the electrons, thus closing the circuit. In secondary batteries this process can be reversed applying an external potential source to the battery, i.e., re-charging it.

In order to indicate the characteristics and behaviour of batteries there are several concepts and variables that will be used throughout this work. The main ones used to describe the battery condition and its technical specifications are listed below. Table 1 shows a recap of this terms.

Battery technical specifications [5]–[7]

This section describes the main technical specifications from a battery, generally specified in its datasheet:

- **Chemistry**. It describes the way of storing electric energy in the battery and the electrochemical reactions involved. Batteries are further classified according to their chemistry, as they can present very different behaviours.
- **Nominal Voltage**. It is the reference voltage the battery has been designed to operate at. The voltage of batteries drops as they discharge; therefore, the nominal value provides the most "typical" value under load. Voltages are highly dependent on the chemistry employed. Typical nominal voltage values are 2 V/cell for lead acid, 1.2 V/cell for Nickel based batteries and 3.6-3.7 V for Li-ion batteries [8].
- **Cut-off Voltage.** It is the minimum allowable voltage of the battery at which it is considered fully depleted. Typical values for end voltage are 1.8 V/cell for lead acid, 1.0 V/cell for Nickel based batteries and 2.8-3.0 V for Li-ion batteries [8].
- **Charge voltage.** It is the maximum allowable voltage at which the battery is considered fully charged. Typical end charge voltages values are 2 V/cell for lead acid, 4.2-4.3 V for Li-ion batteries while Nickel based batteries have a very flat voltage curve and the voltage is only slightly above the nominal 1.2 V/cell when fully charged [8].
- **Charge and discharge rate.** Indication of the charge and discharge currents. Usually, the manufacturer gives multiple specification for normal, rapid, pulse or maximum currents, which may also be different during charge and discharge.
- **Capacity.** It is the amount of charge stored in the battery and represents the energy that can be extracted from the battery. The capacity may vary depending on the operating conditions and fades away with the use. Because of this and in the same way as with the voltage, the term nominal capacity refers to the original design capacity of the battery. Generally, it is measured in Ah or mAh, representing the discharge current that the battery could supply for an hour.
- **Specific energy and energy density.** Specific energy is the energy stored in the battery per unit of battery mass. In the same way, energy density is the energy stored in the battery per unit of battery volume. They indicate how compact the battery is and are very important in applications where mass and/or volume are limited. Figure 3 shows the range of energy density and specific energy for the main secondary batteries' chemistries.

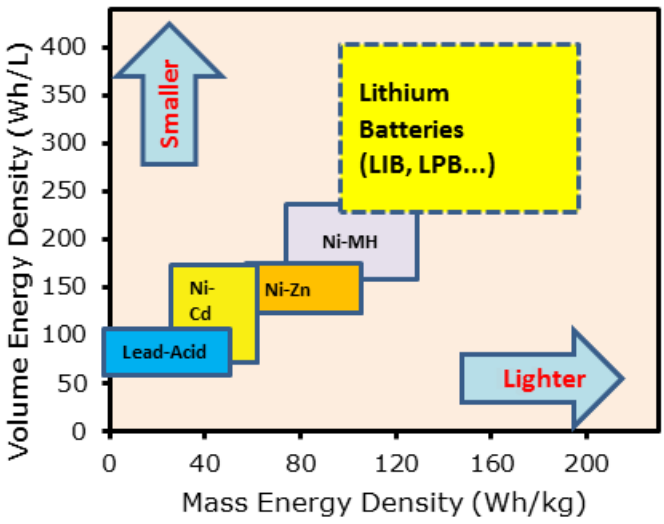

Figure 3. Energy density and specific energy for various battery types [9].

- **Specific power and power density.** It is the available power from the battery per unit of mass or volume respectively. It is important as it represents the limit on how fast the energy from the battery can be consumed. The difference between power density and energy density is important as often the charge/discharge time is key. Some applications require storing big amounts of energy and others need the ability charge or discharge the stored energy quickly. This way a mobile phone is optimized for energy density, lasting for long periods but not providing great power and taking relatively long to charge. On the other hand, a power tool might draw a lot of current, requiring lot of power during a short period, so the battery will be optimized for power density.

  An EV will need both power density and energy density, as it needs autonomy as well as power.
- **Shelf discharge and shelf life.** The self-discharge rate is the rate at which the battery loses the stored energy due to undesired secondary reactions. It is generally quantified as the percentage of capacity loss for a given amount of time. On the other hand, shelf life is the time it would take a fully charged battery for self-discharge completely.
- **Temperature Range.** Batteries have a range of temperatures at which they can operate. This range can be different for different operating modes such as charge, discharge and storage. Temperature has a strong influence on most of the parameters of the battery, which is highly dependent on the battery's chemistry.

- **Coulombic efficiency.** It is the ratio between the charge delivered and the charged supplied in secondary batteries. It shows the energy loss by the battery in the storage process.
- **Cycle life.** It is a measure of the lifespan of the battery. It is defined as the number of cycles the battery undergoes until it meets a deterioration criterion. The three main indicators to determine the deterioration of the battery are capacity decrease, internal resistance increase and self-discharge increase. The importance of each effect depends on the battery chemistry. For example, usually for Li-ion batteries the cycle life is referred to when its capacity falls below 80% of the original.

Battery condition [5]–[7]

This section describes some parameters used to define the instantaneous conditions of a battery:

- **Voltage**. It is the supplied voltage by the battery. It drops as the battery discharges, defining the discharge profile of the battery. These curves depend on the type of battery as shown in Figure 4. There is a distinction between Terminal Voltage and Open-circuit Voltage depending on whether the battery is loaded or not, respectively. From Figure 4**Figure 1**, it is seen that Lithium-ion (Li-ion) based batteries tend to have a higher and more stable voltage across the full cycle. This is similar to Nickel-Cadmium (NiCd) and Nickel Metal Hydride (NiMH) batteries, albeit having a lower voltage. Other more common use batteries such as the Lead Acid batteries tend to have more drop in voltage towards the end of the discharge cycle.

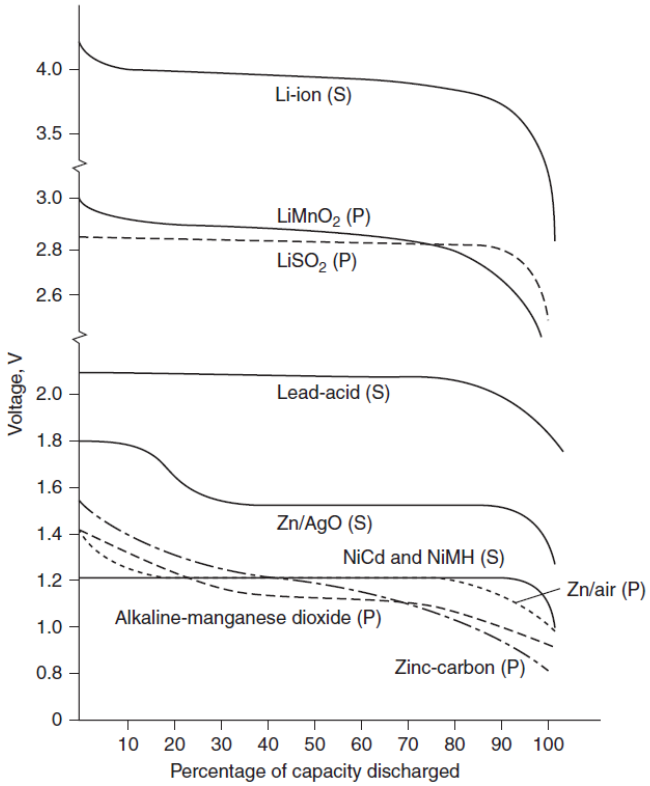

Figure 4. Discharge open-circuit profiles for primary (P) and secondary (S) batteries [8].

- **Charge and discharge rate.** It represents the speed at which the battery is charged or discharged.

  It is measured in Amps, although it is often given by the C-rate. The C-rate is defined as the current through the battery divided by the current at which the battery would deliver its nominal capacity in one hour. For example, a fully charged battery of 2Ah at 1C would provide a current of 2A for one hour. The same battery at 2C would provide 4A for half an hour or at 0.5C would provide 1A for two hours. However, at increased C rates, the total charge delivered will be less as there are increased losses. So, for example, at 4C it will deliver the 4A for a time slightly shorter than 30 minutes. The C-rate is useful as it allows to compare rates and provide guidelines for different sized batteries.

- **Internal resistance.** This is the resistance of the battery resulting from the resistivity of the components of the battery, especially the ion flow permeability of the electrolyte. In general, it varies with the operating conditions of the battery and tends to increase as the battery ages. This is a source of inefficiency, as part of the energy from the battery is lost as heat because of the Joule's effect and this affects both the charging and discharging cycles.

- **State of Charge (SOC)**. Represents the remaining capacity as a percentage of the maximum capacity of the battery.
- **Depth of Discharge (DOD)**. Expresses the battery capacity that has been discharged as a percentage of the total capacity of the battery.
- **State of health (SOH).** It is a variable used to estimate the deterioration that the battery suffers after cycling. For example, for the purpose of this work, in Li-ion batteries the capacity loss is the most important effect, so the SOH is generally calculated only from it. Therefore, SOH is defined as present maximum capacity as a percentage of the original maximum capacity of the battery. Figure 5 shows how SOH is related to SOC and DOD. This way the battery is divided in three zones, the zone where the energy is stored as SOC, the part that can be filled as empty and the no longer usable part that cannot be restored as degraded capacity.

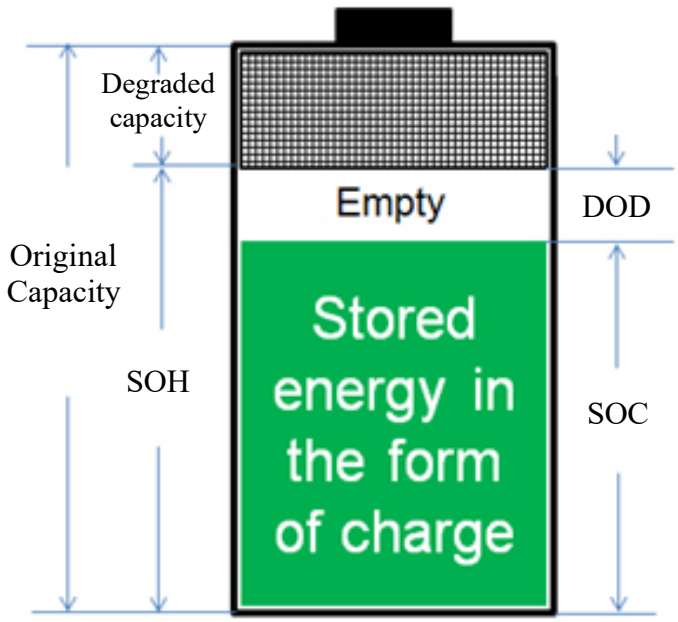

Figure 5. Relation between SOH, SOC and DOD. Adapted from [6].

Table 1. Main characteristics of batteries.

	Variable	Abbr.	Units
Battery condition	Voltage		V
	Rates		C-rate, mA, A
	Internal resistance		mΩ
	State of Charge	SOC	%
	Depth of Discharge	DOD	%
	State of Health	SOH	%
Technical specifications	Nominal Voltage		V
	Cut-off Voltage		V
	Charge Voltage		V
	Rate (Charge/Discharge)		C-rate, mA, A
	Capacity		mAh, Ah, C, Wh
	Specific energy		Wh/kg
	Energy density		Wh/l
	Specific power		W/kg
	Power density		W/l
	Shelf-discharge		%/month
	Shelf life		months, years
	Coulombic efficiency	CE	%
	Cycle life		cycles

2.2 Batteries for energy storage

One of the recent uses of batteries stems from the aforementioned mismatch between the solar PV generation profile and the consumer load profile, thus calling for energy storage to level off this mismatch and make the energy available at a later time when the sun has set. In so doing, one also benefits from a lower dependency on the grid for feeding the excess energy as well as for drawing energy from it during the night. The use of rechargeable batteries as a storage medium is usually the most convenient option for the domestic sector.

Figure 6 shows a comparison between the most popular battery technologies for energy storage. Not all of them are suitable for domestic energy storage, as the space may be

limited, the safety is critical and there is a need for batteries to be low maintenance after installation. This excludes some of the batteries that have gained popularity in the stationary energy storage sector such us the sodium sulphur, which operates at high temperatures. The most suitable battery types for residential use are detailed in the next sub-sections.

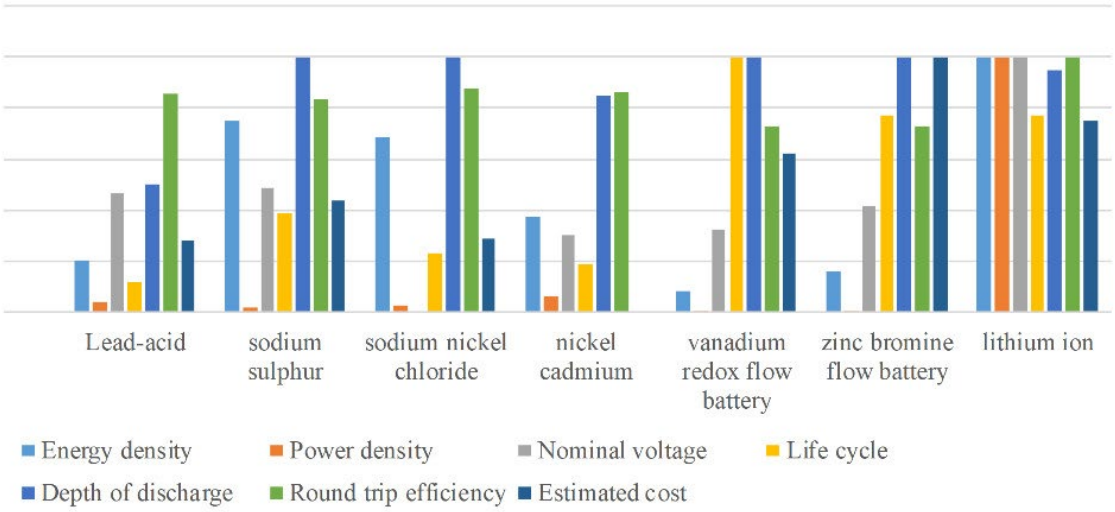

Figure 6. Comparison of the main battery technologies used for energy storage [10].

2.2.1 Lead Acid Batteries [4], [8]

Lead acid is a mature and very developed technology, being the first type of rechargeable battery invented. Therefore, it is widely used and still is the dominant type of battery for many applications.

Lead-acid batteries use lead oxide (PbO_2) as cathode and lead (Pb) as anode. These are submerged in an electrolyte formed by an aqueous solution of sulphuric acid (H_2S0_4) as shown in Figure 7.

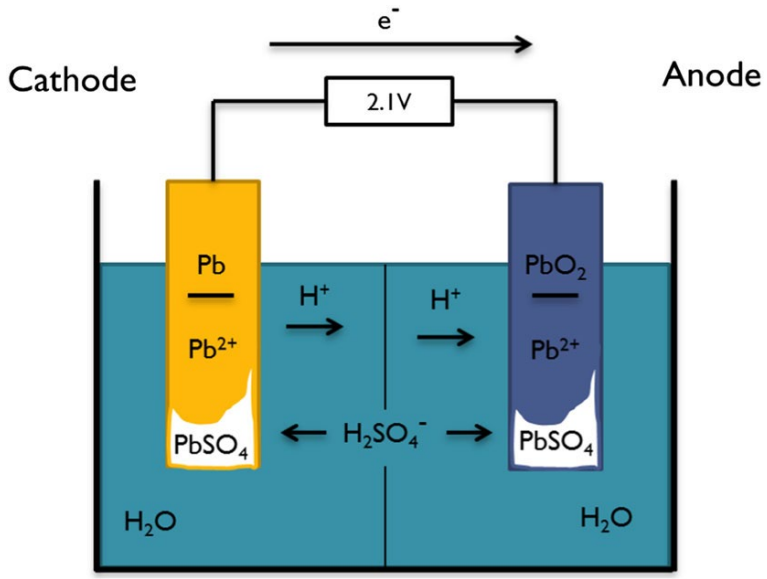

Figure 7. Schematic diagram of a lead acid battery [11].

During discharge, lead sulphate ($PbSO_4$) is formed on both electrodes and the electrolyte loses much of its sulfuric acid concentration, becoming mostly water. During charging, lead sulphate in the anode forms lead dioxide and lead at the cathode, while increasing the concentration of sulfuric acid in the electrolyte.

Lead acid batteries are the most inexpensive among the energy storage solutions. It is a reliable and safe technology, low maintenance and able to work in a wide range of temperatures. Furthermore, it is fully recyclable and as it is a mature technology the infrastructure to produce and recycle lead acid batteries is fully developed.

On the other hand, it has some disadvantages, mainly low energy density compared to other technologies. It also has a lower cycle life and its available DOD is limited to avoid severe damage to its lifespan, being in general about 60%. Although it is a very safe and stable type of battery it may generate hydrogen through secondary reactions so the area around it has to be well ventilated.

2.2.2 Lithium-ion Batteries

Lithium ion is a relatively new technology being discovered in the 1980s. It is the current leading choice for domestic energy storage because of its high energy density, high cycle life and full DOD range. It will be described in depth in the next section, because it is the battery on which this dissertation is focusing.

2.2.3 Nickel based Batteries [4], [8]

Nickel based batteries came after the lead acid batteries and gained a lot of relevance, as they offer a higher energy density and higher cycle life option. The most popular technology was Nickel Cadmium (NiCd), but it would be later partially replaced by Nickel metal hydride (NiMH) as Cadmium is extremely toxic. In the present, Nickel-based technologies have lost popularity in the domestic energy storage sector and are being replaced by Li-ion batteries, which have overall better specifications. One main flaw of Nickel based batteries is the "memory effect". When the battery is partially charged the battery acts as if "remembers" this smaller capacity as its new total capacity, thus limiting its original storage potential. Because of this, partial charging is very harmful for this technology.

NiCd batteries use nickel oxyhydroxide as cathode and metallic cadmium as anode, submerged in an alkaline electrolyte such as potassium hydroxide. During discharge the Cadmium oxides reduces to Cadmium hydroxide and the nickel reduces to nickel hydroxide. During charge the process is reversed.

NiCd offers a long cycle life, a very flat discharge profile and higher energy density than lead acid. This type of battery is very reliable, safe, low maintenance and can resist physical abuse, and has found a niche area of application such as in aerospace uses. However, it presents some major disadvantages, the memory effect, relatively low energy density and the use of toxic cadmium.

On the other hand, NiMH replace cadmium in the anode with a metal hydride. During discharge the metal hydride in the cathode dissociates into the pure metal and water, while in the anode the same reaction described for NiCd batteries takes place. Again, the process can be reversed applying an external voltage.

NiMH has a much higher energy density than NiCd and does not use toxic compounds. However, it is less stable and the charging process is delicate and complex. NiMH also has higher self-discharge rate.

2.2.4 Flow Batteries [4], [8]

Flow technology or Redox flow batteries (RFB) is a relatively new technology in the energy storage marketplace. It is a promising technology, where its main advantage over Li-ion and lead acid technologies is that it has full DOD available, with no harm in the lifespan for bigger DOD operation.

Redox flow batteries consist of a cell stack and two external tanks connected with pipes as shown in Figure 8. This way the positive electrolyte and negative electrolyte (catholyte and anolyte respectively) are stored in external tanks with a different oxidation state. The liquid electrolyte of each cell is pumped and flows through each half of the cell stack, separated by a membrane that allows the exchange of ions, enabling the oxidation and reduction, hence the "redox flow battery" name. After the reaction, the spent electrolytes return to the tanks. Right now, vanadium flow battery is the most promising.

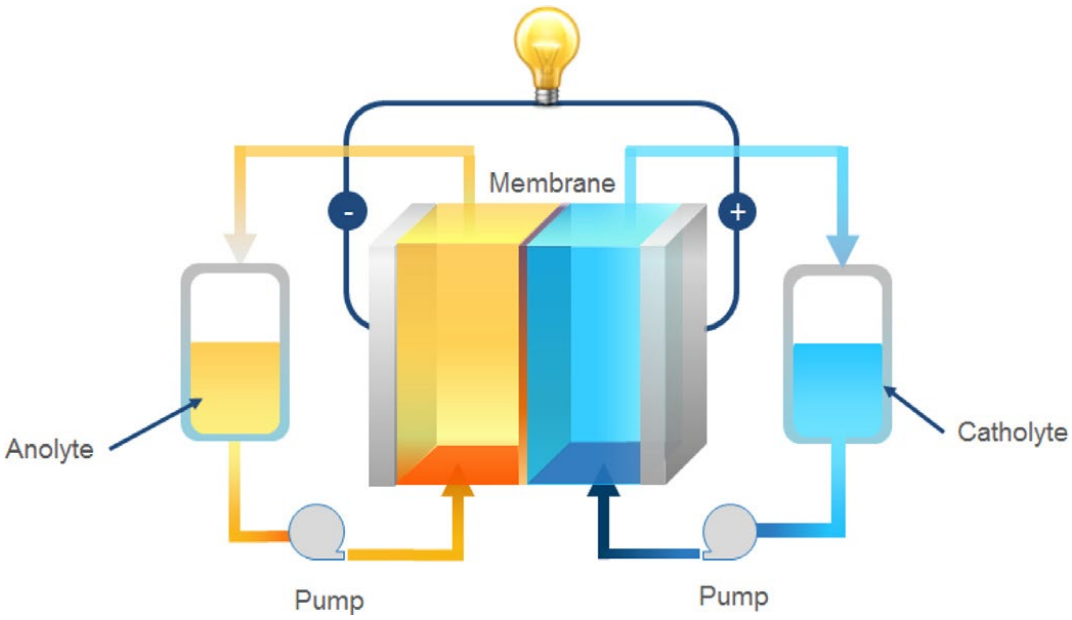

Figure 8. Schematic diagram a redox flow battery [12].

One main advantage of this type of battery is that power and capacity are independent. In this way, it is possible to increase the power by increasing the membrane surface or increase the capacity by increasing the size of the electrolyte tanks. Furthermore, it is a very safe technology as the electrolytes are stored in different tanks and has a long lifespan, not being affected by DOD.

On the other hand, it's energy and power density are quite low and still is a very expensive technology. However, it is expected to gain relevance in the coming years.

2.3 Lithium-ion Batteries

Li-ion batteries were first commercialised in 1991 by Sony. Since then, Li-ion batteries have experienced a great growth consolidating as the leading technology in a wide range of applications, as they are the best technology in terms of power and energy density.

In Li-Ion batteries electrochemical energy is stored through the intercalation of lithium ions into the structure of the electrode material. Ions move from the positive to the negative electrodes during charging and back when discharging.

2.3.1 General characteristics

Li-ion batteries' characteristics vary with the chemistry employed, although they share some common traits. This way by selecting the suitable chemistry, Li-ion batteries can cover a wide range of applications. Table 2 summarizes the advantages and disadvantages of Li-ion batteries relative to other technologies.

Table 2. Main advantages and disadvantages of Li-ion batteries.

Advantages	Disadvantages
High single-cell voltage High specific power and energy High energy efficiency High-rate discharge and charge High cycle life Lower cost thermal management Partial state of charge excellence/No memory effect Low self-discharge rate/High shelf life Broad temperature range of operation Sealed cells/maintenance free Design flexibility (Many possible chemistries)	Moderate cost Safety (Flammable electrolyte) Degrades at high temperature Unsafe when rapidly charged at low temperatures Need protective circuit

Li-ion batteries offer high energy and power densities, making them attractive for volume or weight sensitive applications. Li-ion intercalation reactions are very efficient and there are very limited side reactions, leading to high Coulombic efficiency. Li-ion cells in general operate between 2.5 and 4.3 V, which is much higher than other types of batteries thus needing less cells to build a battery of a given voltage. Li-ion batteries have long cycle life (over 1000 cycles), low self-discharge (2 to 8% a month) and they can also operate in a wide range of temperature (0°C-45°C) [8]. Li-ion batteries can also charge and discharge at high rates. As these batteries are sealed, maintenance is not required and they can operate in a wide range of environments. Furthermore, they do not contain toxic heavy metals like other technologies and are safe for disposal.

On the other hand, Li-ion batteries are not very flexible when operated outside their designated ranges. Rapidly charging the battery at freezing temperatures (<0°C) is

unsafe and exposing the battery to high temperatures may damage it. Li-ion batteries might degrade when discharged below their limits and may vent when overcharged. Therefore, they need protective circuitry to avoid going out of their safe operating region.

One significant disadvantage of Li-ion batteries that has held them back in favour of other technologies is their cost. Li-ion batteries are more expensive than other types of batteries, although this cost has decreased dramatically in recent years.

Li-ion batteries are a safe technology, although they use flammable electrolyte, which may cause safety concerns like thermal runaway. This process consists of a rapid increase of temperature of the battery, which may cause it to ignite or explode. This might happen if the battery is punctured or damaged, if it is overcharged or if it suffers a short circuit.

2.3.2 Working principle and cell components

The general working principle and components of Li-ion battery is the same as discussed before for common batteries. Lithium is a very attractive material to make a battery. Its configuration with only one electron in the outer atom layer makes it easy to lose an electron and form a positive ion. This leads to high negative redox voltage, resulting in high voltage per cell.

Lithium is a very small and light element as well, which allows to construct batteries with high energy density. As lithium has a very small ionic radius it can diffuse through the anode and cathode and allocate inside them through intercalation. This way lithium ions are inserted into the host without causing significant structural change in a reversible way. On the other hand, because of this ease to form ions, lithium is a very reactive material so the cell components must be chosen accordingly and side reactions may occur. The cell must be sealed to avoid contact with external elements, such as oxygen or moisture, as they would react with lithium [5], [8], [13], [14].

The reaction mechanism is described in Figure 9. During discharge, Lithium ions move from the negative electrode (anode) to the positive electrode (cathode), where they are intercalated. At the same time, electrons move through the external circuit in the same direction to compensate the resulting positive charge at the cathode. This way electrons drive the load applied to the circuit.

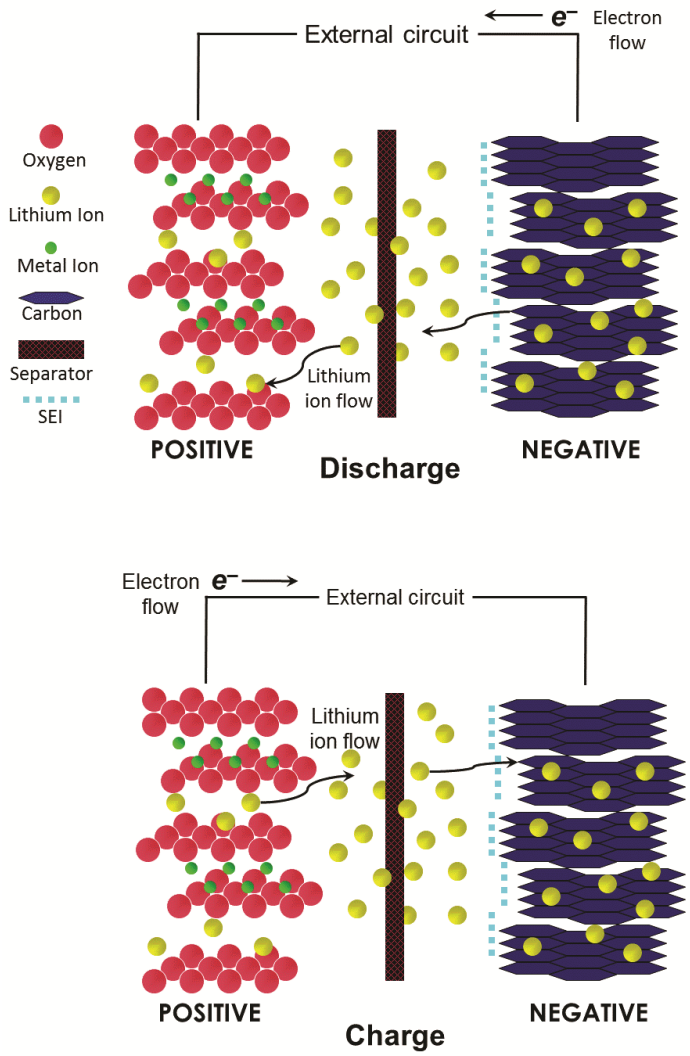

Figure 9. Reaction mechanism of Li-ion batteries [15].

During charge the process is reversed. The external voltage applied make Lithium ions move from the positive electrode (cathode) to the negative electrode (anode), where they allocate through the same process of intercalation.

The anode and the cathode are separated by the electrolyte in order to prevent any uncontrolled reaction between them. The electrolyte must prevent the contact of the electrodes while enabling the flow of ions through it. As lithium is a very reactive material and Li-ion cells operate at significantly higher voltages than other types of cells, this electrolyte must be chosen carefully. It is not possible to use aqueous solutions as with other cells because under a high voltage these compounds would dissociate and react with other components of the battery [14]. Because of this Li-ion cells generally use liquid organic solvent with Lithium salts dissolved to allow the ionic flow. However,

this causes the main safety concern of Li-ion batteries, as these organic solvents are highly flammable.

Despite all this the electrolyte will not be completely inert, as side reactions with the electrolyte will play a key role in the cell degradation. During the first charge cycle, a solid electrolyte interface (SEI) layer forms on the surface of the anode, preventing it from reacting with the electrolyte. The SEI is critical for the safety, stability and cycle life of the cell [13], [15].

The active materials used for each component generally are:

- **Positive electrode or cathode**. In general consists of an aluminium foil coated in both sides with a metal oxide that contains lithium [13]–[15].
- **Negative electrode or anode**. In general consists of a copper foil coated with graphite [13]–[15].
- **Separator and electrolyte**. In general, consists of a polymeric membrane of polypropylene or polyethylene saturated with the liquid electrolyte formed by a Lithium salt dissolved in a flammable organic solvent [13]–[15].
- **Current collectors**. In addition to supporting the electrodes, the aluminium and cooper foils act as current collectors, bridging the cell with the external circuit.

2.3.3 Types of Li-ion batteries

Li-ion batteries' characteristics depend heavily on the composition chosen for the cathode, the anode and the electrolyte. This section covers the commercially available chemistries for Li-ion batteries. However, the technology of Li-ion battery is not mature, with several more chemistries as well as blends of the existing ones being researched. Therefore, this list could be subject to change in the coming years.

2.3.3.1 Anode and Cathode chemistries

Usually, batteries are classified according to their cathode composition, given that most of them have the same graphite anode. Table 3 summarizes the main cathode chemistries. The exception to this is Lithium Titanate anode batteries. Table 4 summarizes the two main anode options.

Table 3. General characteristics of common cathode chemistries [13], [15]–[17].

Material	Abbreviation	Description
Lithium Cobalt Oxide	LCO	– High energy density – Low cycle life – Poorer safety – Expensive
Lithium Manganese Oxide	LMO	– Good power and energy density – Poor cycle life. – Good thermal stability and safety
Nickel Manganese Cobalt	NMC	– Good overall – High energy density – Good power density – Good cycle life
Lithium Iron Phosphate	LFP	– Very safe – High power density – Low energy density. – High stability
Nickel Cobalt Aluminium	NCA	– Highest energy density per unit mass – Lower thermal stability – Expensive

Table 4. General characteristics of common anode chemistries [13], [15]–[17].

Material	Abbreviation	Description
Graphite		– Most common – Cheap – Higher energy density and voltage
Lithium titanate	LTO	– Can be used with LMO or NMC cathodes – More expensive – Very high cycle life – Excellent thermal stability – Excellent safety – Good low temperature operation – Much lower voltage output – Much lower energy density

Lithium Cobalt Oxide (LCO) [13], [17]

Lithium Cobalt Oxide (LCO) was the first lithium battery chemistry introduced in 1991. LCO consists of a Lithium Cobalt Oxide ($LiCoO_2$) cathode and a graphite anode. Figure 10 summarizes LCO's characteristics in a hexagonal spider graphic, which shows that it excels in energy density. However, the drawback of LCO batteries is a relatively low cycle life, poorer safety and a limited power density. Because of these drawbacks, its main application is consumer electronics like mobile phones, cameras, laptops, etc where specific energy is key but have less demanding power performance than industrial applications. In the recent years it has lost popularity in favour of Manganese or Aluminium alternatives with a cheaper cost than Cobalt and improved performance.

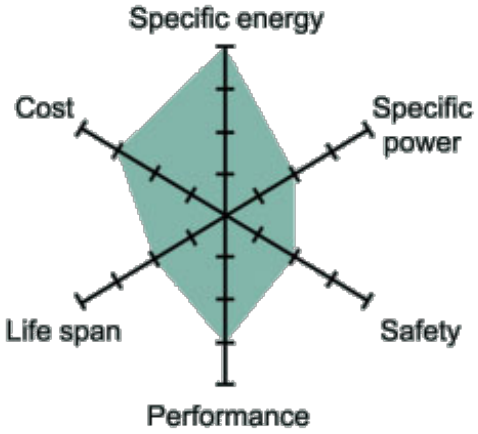

Figure 10. Snapshot of LCO [17].

Lithium Manganese Oxide (LMO) [13], [17]

Lithium Manganese Oxide (LMO) was first commercialised in 1996 offering better power density than LCO. LMO consists of Lithium Manganese Oxide ($LiMn_2O_4$) cathode and a graphite anode. Figure 11 summarizes LMO's characteristics using a similar graphic to Figure 10. LMO batteries have better power density than LCO but about a third less energy density. They have good thermal stability and safety, but still have relatively low lifespan. Its use is in applications that require more power than LCO like power tools or medical devices. However, they have lost relevance and have been replaced by blending the manganese oxide with nickel and cobalt.

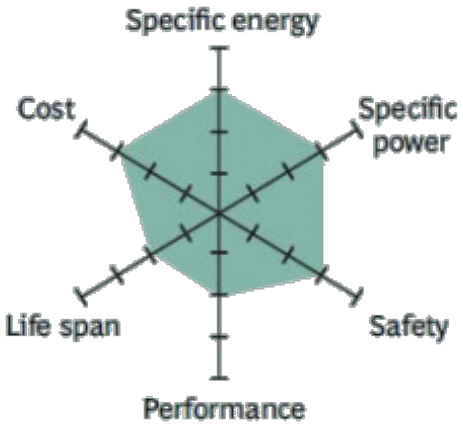

Figure 11. Snapshot of LMO [17].

Lithium Nickel Manganese Cobalt Oxide (NMC) [13], [17]

Lithium Nickel Manganese Cobalt Oxide (NMC) was introduced in 2008. It is a combination of Manganese, Nickel and Cobalt. Figure 12 shows that NMC has good over all characteristics, excelling in energy density. This is achieved by combining the high energy density of Nickel with the good thermal stability of Manganese, while Cobalt helps further stabilising Nickel. The cathode is generally formed by one third Nickel, one third Cobalt and one third Manganese, although other combinations are possible to target the desired qualities as well as to try to reduce Cobalt content, which is an expensive material. It is used in applications where high energy density as well as good power capabilities are desired like power tools or electric vehicles. However, it is also used in industrial applications or energy storage, as it is a balanced cell. Therefore, NMC popularity has greatly risen in the recent years.

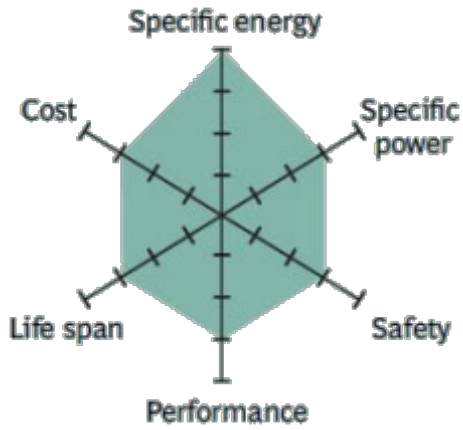

Figure 12. Snapshot of NMC [17].

Lithium Iron Phosphate (LFP) [13], [17]

Lithium Iron Phosphate (LFP) was introduced in 1996. LFP consists of a Lithium Iron Phosphate ($LiFePO_4$) cathode and a graphite anode. Figure 13 summarizes LFP's characteristics in a similar graphic to the previous ones. LFP batteries have a really good specific power, being able to work at high ratings as well as long life cycle. LFP batteries are more robust than other Li-ion batteries, having a good thermal stability and tolerance if abused, which makes them very safe. On the other hand, LFP batteries have a rather low energy density, having a lower voltage per cell of 3.2 V/cell. They also have elevated self-discharge. Its use is restricted to applications with power and safety requirements, expected to have a long lifespan and where energy density is less relevant, like industrial applications or energy storage. It has experienced a moderate growth in recent years in the energy storage sector.

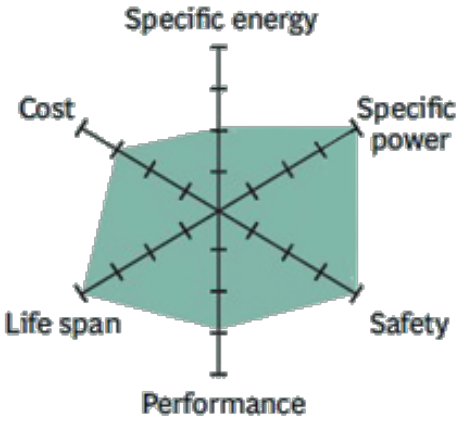

Figure 13. Snapshot of LFP [17].

Lithium Nickel Cobalt Aluminum Oxide (NCA) [13], [17]

Lithium Nickel Cobalt Aluminium Oxide (NCA) was introduced in 1999 as an option with good specific and power. NCA consists of a Nickel Cobalt Aluminium Oxide ($LiNiCoAlO_2$) cathode and a graphite anode. Nickel grants high energy density while Aluminium contributes to the cell stability. Figure 14 outlines NCA's characteristics. NCA batteries are similar to NMC cells, offering good lifespan and specific power and excelling at specific energy. However, they have lower thermal stability and high cost. It was outclassed by NMC, although in the recent years it has regained relevance in the

electric powertrain industry, used by Panasonic and Tesla, as it offers the highest energy density.

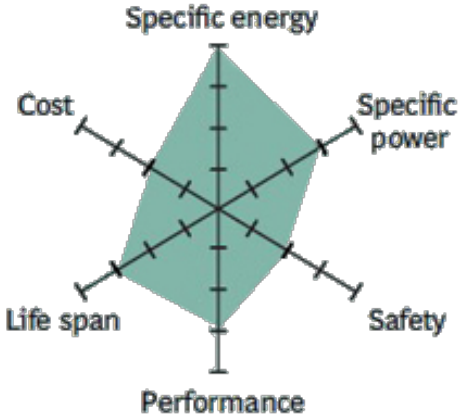

Figure 14. Snapshot of NCA [17].

Figure 15 shows the popularity of the main cathode chemistries in 2018 and it expected evolution for 2030.

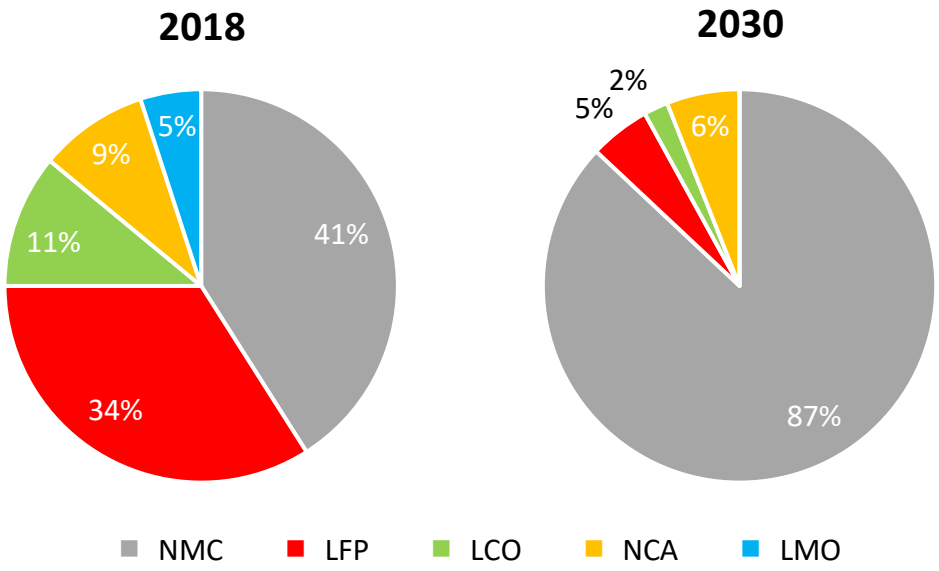

Figure 15. Cathode materials distribution in 2018 and forecast for 2030 [18].

These pie charts show that in the present NMC batteries are the most popular and are expected to keep growing in the near future, becoming the prevalent Li-ion cathode active material. Other chemistries like LFP and LMO are expected to slowly lose popularity, outclassed by NMC. NCA is expected to have a mild rise as a chemistry used by some electric vehicle battery manufacturers.

Carbon based anodes [13], [15]

Graphite is used as anode for the majority of the lithium-ion batteries. It can be natural graphite or artificial graphite. Lithium ions intercalate between the carbon sheets during charge and are released during discharge. Graphite is rather inexpensive compared to the cathode or to other anode alternatives materials and it is the most extended option as it has an overall good performance.

Lithium Titanate (LTO) [13], [17]

Lithium Titanate (LTO) was introduced in 2008. LTO consists of a NMC or LMO cathode but replacing the graphite anode with Lithium Titanate (Li_2TiO_3). Figure 16 shows that LTO's characteristics are rather different than the ones from previous graphite anode chemistries. The great advantage of LTO batteries over graphite anodes is that they do not form SEI in the anode, allowing for greater charge and discharge rates, very long lifespan and avoiding the precipitation of metallic Lithium on the anode during charging known as lithium platting when charged at low temperatures. Despite its great life cycle, safety and good power capabilities, LTO batteries have a very low energy density, having 2.8 V/cell and they are extremely expensive, as Titanium is a rare material. Common uses are UPS, street lightning and electric powertrains.

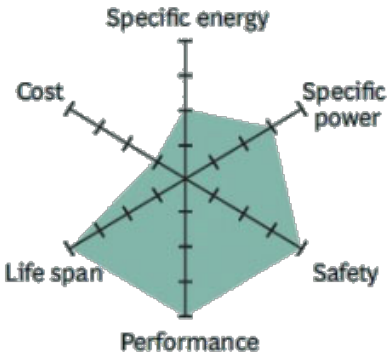

Figure 16. Snapshot of LTO [17].

Table 5 summarizes the main characteristics of the different types of Li-ion batteries.

Table 5. Comparison of the main li-ion chemistries [13], [19].

Positive electrode	LCO	LMO	NMC	LFP	NCA	LMO or NMC
Negative electrode	Graphite	Graphite	Graphite	Graphite	Graphite	Lithium titanate
Optimized for	**Energy**	**Power**	**Energy or Power**	**Power**	**Energy**	**Cycle life**
Operating voltage range	3 - 4.2	3 - 4.2	3 - 4.2	2.5 - 3.65	3 - 4.2	1.8 - 2.8
Nominal voltage	**3.6**	**3.7 - 3.8**	**3.6 - 3.7**	**3.2 - 3.3**	**3.6**	**2.4**
Specific energy (Wh/kg)	150 - 200	100 - 150	150 - 220	90 - 120	200 - 260	70 - 80
Charge rate	**0.7–1C (3h)**	**0.7–1C (3h)**	**0.7–1C (3h)**	**1C (3h)**	**1C**	**1C (5C max)**
Discharge rate	1C (1h)	1C, 10C possible	1–2C	1C (25C pule)	1C	10C possible
Cycle life (ideal)	**500–1000**	**300–700**	**1000–2000**	**1000–2000**	**500**	**3,000–7,000**
Thermal runaway	150°C (higher when empty)	250°C (higher when empty)	210°C (higher when empty)	270°C (safe at full charge)	150°C (higher when empty)	One of safest Li-ion batteries
Ambient temperature during charge (°C)	**0-45**	**0-45**	**0-45**	**0-45**	**-20-45**	**-20-45**
Ambient temperature during discharge (°C)	-20-60	-30-60	-20-60	-30-60	-30-60	-30-60

2.3.3.2 Electrolyte chemistries

As shown in previous sections, the electrolyte role in Li-ion batteries is more demanding than in other types of batteries, as it needs to withstand higher voltages while not reacting with the lithium ions. Therefore, the effort in the recent years has been to substitute the flammable organic liquid electrolyte with safer options. Table 6 shows the main commercially available electrolyte options.

Table 6. Main types of electrolytes [13], [15].

Type	Description
Liquid organic electrolyte	– Polymeric membrane saturated with liquid electrolyte (lithium salt in organic solvent) – Most extended – Flammable (Safety)
Gel polymer electrolyte (LiPo) / Solid State electrolyte	– Gelled electrolyte or a solid polymer electrolyte – Less flammable because of the elimination of organic solvent, increasing safety – Very expensive

The lithium polymer batteries' (LiPo) electrolyte, also referred to as solid-state electrolyte, gel polymer electrolyte or solid polymer electrolyte, replaces the organic liquid electrolyte with a solid polymer or gelled electrolyte. A solid polymer consists of inorganic lithium salts dissolved in polymeric framework like polyethylene oxide. However, it has low conductivity at room temperature and nowadays most of the LiPo batteries use gelled electrolyte. A gelled electrolyte uses lithium salts suspended in a polymer gel [13], [20].

The main advantages of this system are the elimination of organic solvent, not using flammable components and increasing the safety of the cells. In Li-ion batteries the anode and cathode swell and contract during charge and discharge. Conventional compositions need to have applied external pressure in order to keep the electrolyte in contact with the electrodes, while in LiPo batteries the electrolyte binds the anode and cathode together [13], [15], [20]. However, the ionic conductivity is worse than the liquid electrolyte alternatives and the cost remains extremally expensive, which have limited its commercialization [13].

2.3.4 Battery architecture

Li-ion batteries are formed by the aggregation of cells to store energy and all the auxiliary systems that ensure its correct and safe operation.

2.3.4.1 Cell construction

In many cases the voltage output of a single cell will be less than the required for a certain application. Therefore, cells are stacked in series to build up the total desired voltage of the battery. Similarly, cells can be stacked in parallel in order to increase its

capacity. This section shows the different strategies available to combine the individual cells in order to build the battery pack.

Cylindrical cells [13], [15], [21]

In cylindrical cells multiple cells are stacked and rolled to form a cylinder-shaped battery, as shown in Figure 17. This aggregation is then sealed by a rigid metal housing, which will prevent any exterior pollutant such as oxygen or moisture.

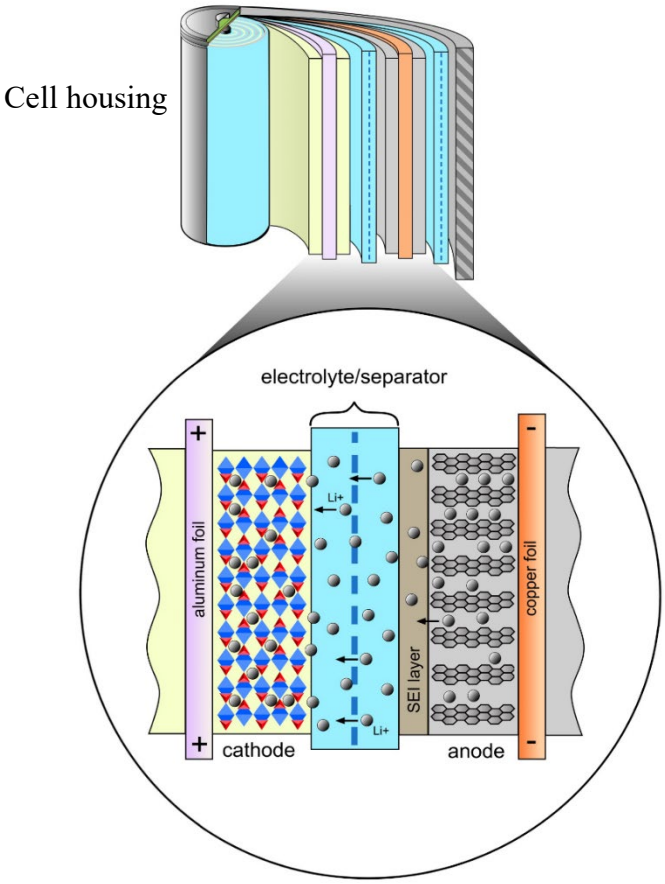

Figure 17. Lithium-ion battery construction for a cylindric cell [13].

Cylindrical packaging offers good mechanical stability, as the cylinder shape helps to withstand the internal pressures without swelling and resists well external abuse. It further allows the allocation of added safety features like short circuit protection or pressure relief mechanisms, making it generally the safest configurations. Cylindric cells production can be easily automated, making it the cheapest configuration to manufacture. Its main drawback is a less ideal packaging, as empty space cavities exist in the cell.

Its main applications are portable application like power tools, medical applications, portables and e-bikes.

Prismatic cells [13], [15], [21]

In prismatic cells the battery is shaped in the form of a prism. The aggregation is then sealed with a similar construction to that in cylindrical cells. There are multiple strategies to achieve this as depicted in Figure 18. Generally, in small format batteries the cells are rolled in a pseudo-prismatic way or folded like an accordion and in large format batteries individual larger cells are stacked on top of each other.

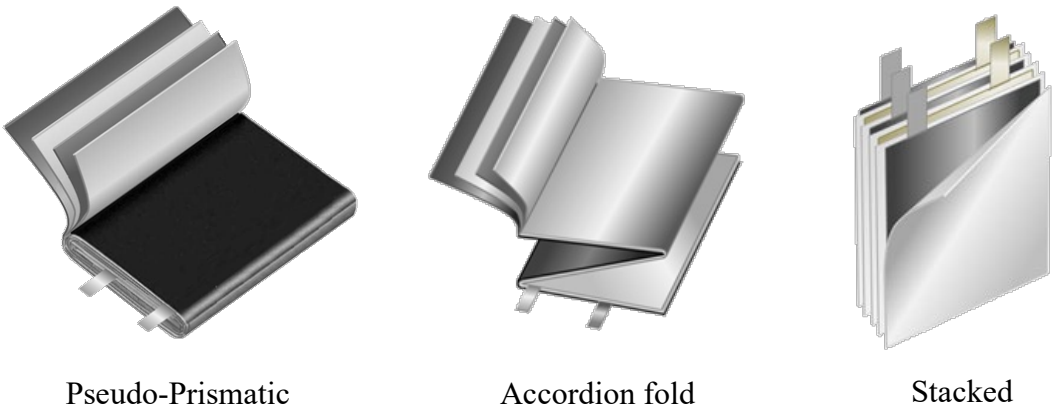

Figure 18. Different prismatic cell constructions [15].

Prismatic batteries are similar to cylindrical cells but achieve a better packaging as there is a better use of space and almost no empty space exist inside. Further this strategy allows to reduce the thickness of the cell and the prismatic shape fits better in many applications. On the other hand, prismatic cells are less robust than cylindrical cells and some swelling may occur as a consequence of internal pressure. The lack of empty spaces makes it less efficient in thermal management and the manufacturing of prismatic cells is more complex, making them costlier to produce than cylindrical cells. Small format prismatic cells are used for mobiles, tablets and low-end portables while large format batteries are mainly used in electric powertrain in electric and hybrid vehicles.

Pouch cells [13], [15], [21]

Pouch cells use a similar laminated architecture to large format prismatic cells, innovating in the packaging. Instead of a using a rigid metal case they use a flexible lightweight bag sealed by heat as shown in Figure 19.

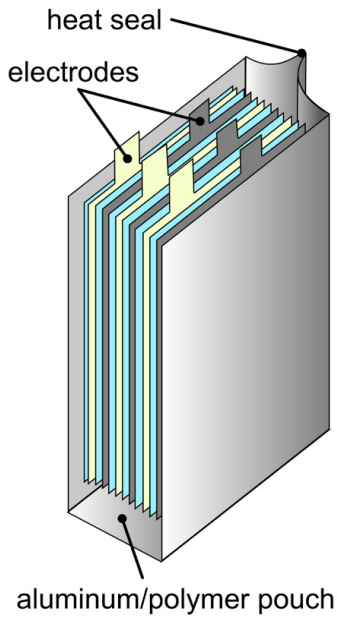

Figure 19. Pouch cell structure [13].

This type of cell achieves great density for both power and energy as the space is greatly used with almost no empty interior space and the elimination of the metal housing, greatly reducing the weight of the cell. The downside is a reduction in the mechanical resistance. This type of case will not properly protect the battery from external abuse and the possibility of allocating safety features is more limited.

Because of the flexible case, pouch cells will suffer more moderate swelling during the charge and discharge cycles. Unlike cylindric and prismatic cells, pouch cells cannot apply pressure to the electrodes to keep them together, requiring an additional mechanism for this purpose. Because of this, pouch packs are commonly used for Li-Polymer, as this type of battery naturally does not need pressure as the polymer electrolyte binds together the cathode and the anode.

Pouch cells are still a relatively new technology and their manufacturing costs are still higher than cylindric cells. Pouch cells serve similar applications to prismatic cells with special emphasis in stationary applications, as their poorer safety is a lesser inconvenient for these.

Figure 20 shows the popularity of each type of packaging through the years. Prismatic cells are expected to progressively be replaced by pouch cells, as they serve similar purposes and pouch cells have better power and energy density and are expected to further develop to overcome their disadvantages. Cylindric cells will experience a more moderate growth, as a solid option in their field of application.

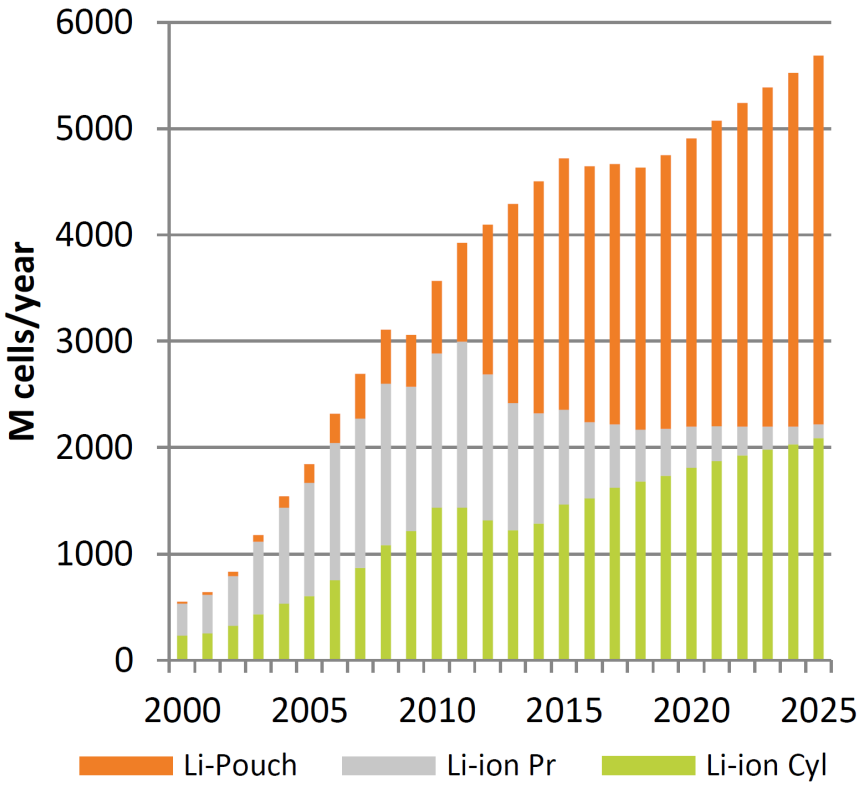

Figure 20. Number of batteries produced per year of each type of packaging strategy and expected evolution [18].

2.3.4.2 Battery management system

The Battery Management System (BMS) monitors the state of the battery and controls the ancillary systems to ensure its correct operation. Figure 21 shows an example block diagram for the BMS.

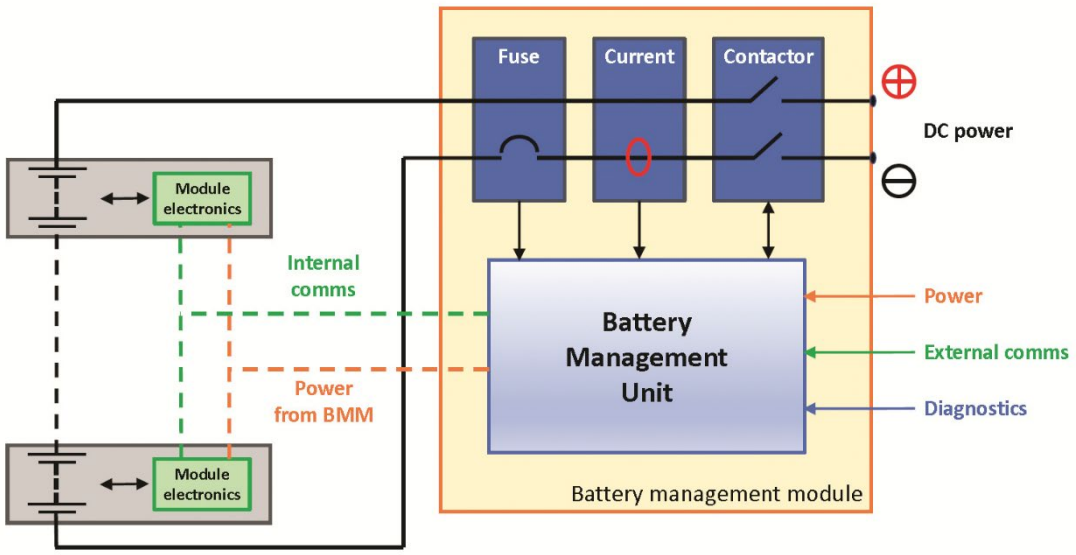

Figure 21. BMS block diagram [15].

The complexity and number of functions of the BMS may vary the with the size and role of the battery but some of its main functions are [15]:

- **Monitoring.** The BMS receives and interprets the signal from sensors to monitor the state of the battery measuring parameters like cell voltage, battery voltage, cell temperature, string current, and ambient temperature among others.
- **Cell protection.** Through the monitoring of the battery variables the BMS can detect potentially dangerous situations and modify the operation or shut down the battery for protection.
- **Cell balancing.** In batteries formed by multiple cells, each cell will charge and discharge at slightly different rates, as each cell is unique. In order to avoid the overcharge or over discharge of any of them the BMS will monitor the voltage of each cell and keep them balanced.
- **Charge and discharge control.** The BMS controls the charge and discharge process, regulating the voltages and currents and communicating with the charger.
- **Determination of SOC and SOH.** The BMS will determinate the current SOC and SOH from the variables monitored and may communicate it to an external system.
- **Communication.** The BMS is in charge of managing the communication with other components from the battery, other auxiliary system like thermal management or safety systems if they are present, the charger during the charge processes and external communication with the system the battery is part of.

This way the BMS is behind all the control and operation of the battery and a correct BMS operation not only ensures the proper functioning of the battery but can further extend its lifetime.

2.3.4.3 Thermal management system [15]

This system is not present in all batteries, being in general only necessary when the battery is susceptible to high charge and discharge rates. Therefore, many batteries monitor the temperature to avoid safety concerns and only rely on passive heat transfer in order to maintain the cell temperature.

The objective of thermal management system is to use active strategies to extend the lifetime of the battery and keep it in the range of temperature for optimal performance. In general, the mission of thermal management system will be to refrigerate the battery as it heats up during operation. However, the heating of the battery at low temperatures is also possible, as these may be very harmful during charging.

2.3.4.4 Safety systems [15]

As seen previously, most Li-ion batteries are flammable and present safety concerns. Because of this, batteries have basic short circuit and overcharge protections. This is done through the BMS operation, fuses and voltage driven or current driven switches. Additional safety features may be required with increasing capacities or operating rates.

Once it starts, a thermal runaway is almost impossible to stop and the best option is to let the battery burn away in a well vented place. Therefore, the main objective of the safety systems is to detect and shut down the battery before this happens.

In the event of a thermal runaway, it is important to vent the accumulated gas in order to avoid more violent reactions. Because of this, cylindric and prismatic cells may be equipped with vent valves while pouch cells will be vented by the rupture of the foil pouch. Similarly, larger battery banks may have fire extinction systems.

2.3.5 Operation of Li-ion batteries

The operation of Li-ion batteries must be maintained within defined conditions. Overcharging a Li-ion battery can lead to a fire or explosion, and over discharging below the minimum voltage (usually because of self-discharge during storage) can cause the copper from the anode to dissolve in the electrolyte, disabling the cell [13], [15].

Li-ion batteries are usually charged in two steps as shown in Figure 22. The first step is a high constant-current charge (~0.5-1C) until the battery reaches its maximum voltage (~4.1-4.2 V/cell). After that, the battery is charged at constant voltage until the current drops below a threshold (~0.02C-0.1C), or for a fixed amount of time (~2h). Precise voltage regulation is necessary as the tolerance for overcharging in Li-ion batteries is very narrow (≤50 mV) [13]. These values are indicative and are common for cobalt blended batteries. For other chemistries like LFP or LTO the charging process is similar but the voltage thresholds are different and generally allow for higher charging rates.

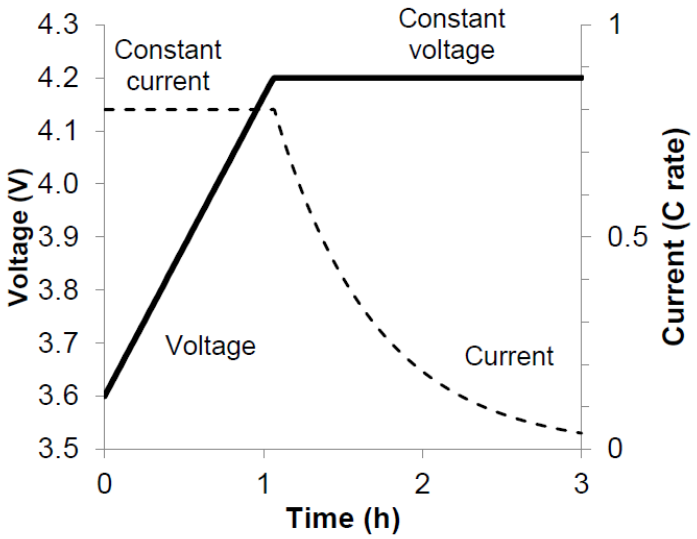

Figure 22. Approximate evolution of current and voltage of the battery during charging [13].

When multiple cells are connected, their voltage must be balanced by the BMS such that none of them exceeds the maximum. Surpassing the charge rates indicated by the manufacturer can lead to the formation of lithium dendrites in the anode, which may eventually cause a short circuit. Even higher rates can lead to the formation of oxygen in the cathode, decomposition of the electrolyte or catastrophic failure [13], [15].

Discharging of Li-ion batteries is less delicate and can be done at any rate within the manufacturer's specifications. In general, the manufacturer will give indication of recommended discharge patterns like peak, pulsed or nominal. Unlike previous technologies, Li-ion batteries do not have a memory effect and do not need full discharge cycles, in fact benefiting from partial discharge cycles.

2.3.6 Li-ion batteries for PV application

A battery in a PV system is exposed to frequent cycling as it is designed to charge and discharge every day. Moreover, the charging power or time is limited and therefore the battery has long operation at partial states of charge. Li-ion batteries are suitable for this application as operation in partial state is not harmful [15]. Furthermore Li-ion batteries require very little maintenance once installed.

For home storage applications, safety and space limitations are generally assumed to be the most defining parameters. In this context LFP and NMC are the most popular chemistries. NMC batteries offer high energy density, and good overall characteristics while LFP batteries offer very safe operation.

Table **7** summarizes the main characteristics of some popular commercial models. To allow for easier cost comparison, the total cost of each battery is divided by the total energy it would deliver during its lifetime according to the warranty.

Table 7. Characteristics of popular Li-ion battery models for PV energy storage [22]–[29].

Model	Type	Nominal Capacity	Max Steady Power	Cycle life	Cost per warranted kWh (1 cycle a day)
LG Chem RESU 6.5	NMC	6.5 kWh	4.2 kW charge and discharge	3200 cycles 90% DOD (60% SOH)	$0.30 (+inverter cost)
Tesla Powerwall 2	NMC	14 kWh	5 kW charge and discharge	2800 cycles 100% DOD (70% SOH)	$0.31 (+inverter cost)
Varta Pulse 6	NMC	6.5 kWh	2.5 kW charge 2.3 kW discharge	4000 cycles 90% DOD (80% SOH)	$0.48
SENEC Home V3 Hybrid 5	NMC	5 kWh	1.5 kW charge 2 kW discharge	12000 cycles 80% DOD (60% SOH)	$0.43
ReLiON RB48V100	LFP	5 kWh	5 kW charge 10 kW discharge	7000 cycles 80% DOD (70% SOH)	$0.29 (+inverter cost)
BYD B-BOX 5	LFP	5 kWh	5 kW charge and discharge	6000 cycles 100% DOD (80% SOH)	$0.35 (+inverter cost)
SimpliPhi PHI 3.4	LFP	3.4 kWh	1.5 kW charge 3 kW discharge	5000 cycles 90% DOD (80% SOH)	$0.42 (+inverter cost)
Power Plus Energy L. Pr.	LFP	3.3 kWh	6 kW charge 3 kW discharge	5000 cycles 75% DOD (70% SOH)	$0.37 (+inverter cost)

2.4 Degradation Mechanisms of Li-ion batteries

In theory, Li-ions batteries use a completely reversible mechanism and should last for an infinite number of cycles. Unfortunately, there are a number of undesired chemical and mechanical processes that limit their lifetime. Aging in li-ion batteries involves a loss of available capacity and an increase in internal resistance. Of the two, capacity loss is the most significant and usually used to characterize the aging.

2.4.1 Degradation mechanisms

There are several degradation mechanisms that cause Li-ions batteries to age. The dominant degradation mechanism can change with the chemistry chosen or the operation conditions of the battery [30]. Figure 23 summarizes the main degradation mechanisms for Li ion batteries. These can be further classified by the component affected.

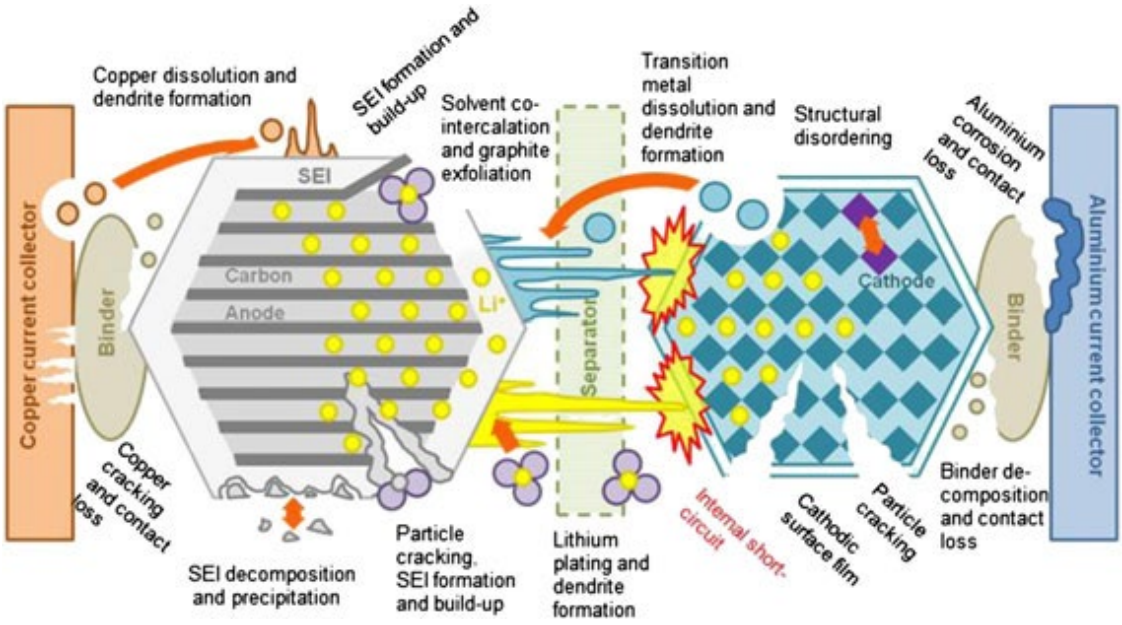

Figure 23. Main degradation mechanism of Li-ion batteries [31].

Anode degradation

Figure 24 shows some of the degradation mechanism that affect the anode. This analysis is focused on graphite-based anodes as they are the most common. Some of the main ones are:

- **SEI formation.** SEI growth is generally considered one of the dominant aging mechanisms in Li-ion batteries. Although SEI can be formed in anode and in the cathode, it is more significant in the anode due to the low potentials within cell charging [31]. SEI is formed due to the reaction of Li-ions with the electrolyte. This reduces the number of cyclable Li-ions available (less capacity) and makes the SEI layer thicker (more internal resistance) [31]–[34].
- **Lithium plating.** Lithium plating happens when the metallic Lithium precipitates to the surface of the anode. These usually happens when the intercalation of Li-ions in the anode slows down because of low temperatures.

This reduces the amount of cyclable Li-ion and may produce shorts [30], [35] Because of this a lithium battery should never be charged below 0°C [36].

- **Structural changes and mechanical stress.** In combination with SEI growth, this is generally the other main degradation mechanism responsible of Li-ion aging. The constant cyclic intercalation and de-intercalation of Li-ions in and out of the active material causes structure changes, cracks and wear in the anode electrode and reduction of the surface of active material as well as the loss of mechanical and electrical contact, deteriorating transfer [31]–[34].

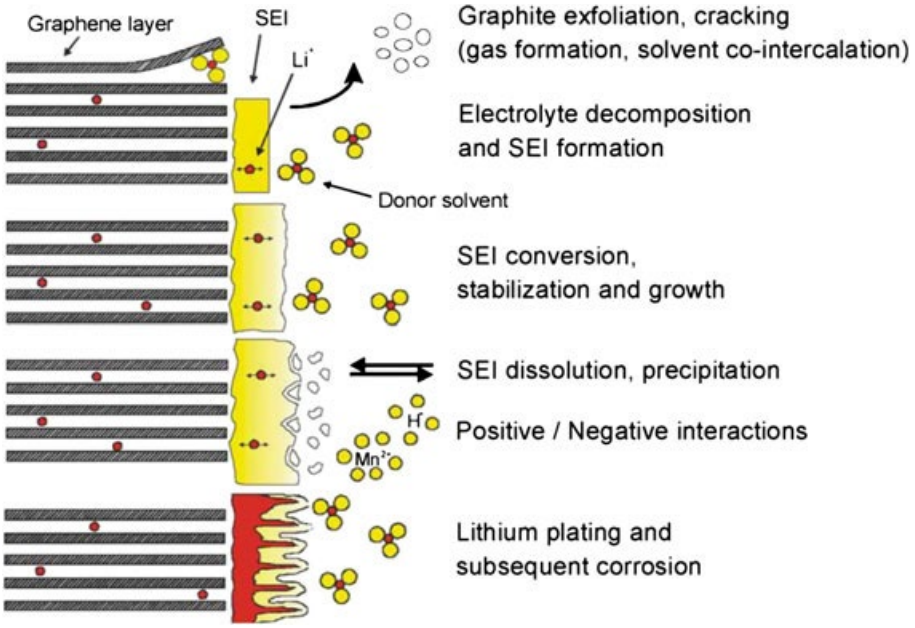

Figure 24. Anode degradation mechanisms [31].

Cathode degradation

Cathode degradation mechanism are somewhat similar to the anode ones. Figure 25 summarizes the known mechanism that cause the cathode to age. There are several cathode chemistries and each one of them will have particular degradation modes but in general terms are:

- **SEI growth.** Although much less significant than in the anode, in the cathode some SEI is formed due to the reaction with the electrolyte [31]–[34].
- **Structural changes and mechanical stress.** As with the anode, the constant cycling of the battery will cause cracking and structural disorder in the cathode. This may lead to the isolation of the active materials and weaker contact, reducing the capacity and increasing resistance [31]–[34].

- **Active material dissolution.** This is a characteristic of Manganese based cathodes. In these, the Manganese will dissolve in the electrolyte and may migrate to the anode and deposit in the SEI [31].

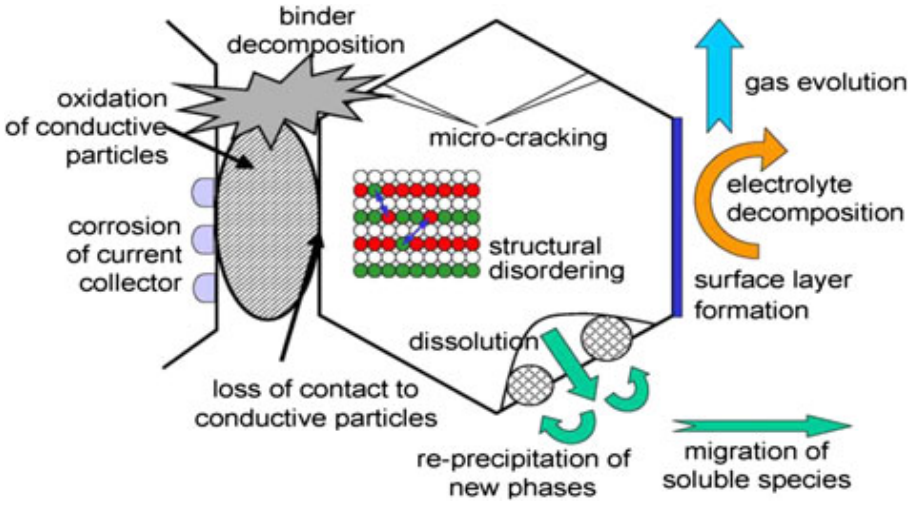

Figure 25. Cathode degradation mechanisms [31].

Separator degradation

Although the separator films are inert and do not react with the battery components, its physical degradation can disrupt the ion flow, increasing the overall resistance. This is usually consequence of the obstruction and deformation of the pores with cycling. A worse flow through the separator can also favour the electrolyte decomposition and its consequent reaction with the anode and cathode [31].

Current collector degradation [31]

The main degradation of the aluminium and copper current collectors is the corrosion by the electrolyte. Aluminium is relatively inert due to the passive layer formed in its surface. However, some corrosion may happen with cycling due to pitting corrosion. On the other hand, copper may dissolve in the electrolyte at very low voltages, reacting with it so the voltage of the cell should never wall below the manufacturer's minimums.

2.4.2 Calendar aging and Cyclic aging

The overall cell aging of lithium-based batteries is usually classified in two categories distinguishing between time-based and cycling-based effects:

Calendar aging

The calendar aging is the aging due to the passage of time, regardless of whether the battery is being used or not. It is mainly driven by time and influenced by the temperature and SOC [37]. The calendar aging is mainly a diffusion driven mechanism. This way, when the battery is idle at a SOC high there is a significant potential and concentration difference across the electrolyte. This difference will cause the diffusion of lithium ions from the electrode to the electrolyte. This will expose more electrode material and will also cause the lithium ions to react with the electrolyte to form more SEI [30]–[32]. The temperature increases diffusion, accelerating this process.

High SOC are more harmful as the battery is at a higher energy state. However, if the SOC in storage is too low, the battery could become severely depleted via self-discharge, which may cause permanent damage and make it unsafe to charge [13].

Cyclic aging

Cycling aging is the aging due to battery use. Is influenced by the depth of discharge (DOD), current rate (C-rate) and temperature [37].

There is a limit to the rate at which lithium ions can be accepted by the electrode. Because of this, at high rates a small portion of Li-ions are deposited on the surface of the electrode instead of intercalating into it, where they react with the electrolyte forming more SEI. This limit is tighter in the anode as there is already SEI formed and the ions must diffuse through it, which implies that the rate will be more limited during charging than discharging [15]. This effect is aggravated at low temperatures as the diffusion through the SEI and intercalation in the electrode becomes slower, further limiting the rate, or at higher temperatures, that may lead to the dissociation of the electrolyte easing its reaction [15], [32]. High temperatures will also accelerate the kinetics of side reactions and diffusion, accelerating the aging processes [30].

As seen before, low temperatures may also lead to lithium plating.

LTO anode batteries do not form SEI in the anode so they will be significantly less affected by the rate of charge, being able to charge and discharge at the same rate [15].

Higher DOD induce a greater volume change in the graphite during the intercalation process, increasing stress and microcracks. This exposes more active material, enabling further reaction with the electrolyte to form more SEI [30].

2.4.3 Guidelines to extend Li-ion battery lifetime

The manufacturers and literature give a number of instructions to extend the lifetime of batteries. These guidelines are a direct consequence of trying to minimize the aging processes studied above and can be summarized in the following points:

General

- Avoid extreme temperatures and high moisture environments when using or storing Li-ion batteries [38].
- Avoid any type of mechanical damage or stress [13], [38].

Storage

- In most cases, batteries should be stored near or below room temperature and at 20-50% state of charge [13], [36], [39].

Charging

- Use moderate charge rate and avoid fast charge when possible [38].
- Select a lower float voltage and avoid saturation charge, as fully charging stresses the battery. The optimal charge voltage is estimated to be the corresponding to about a 70% SOC, as going lower may not gain further extend of lifetime. It is important to try to keep the average SOC not too high as well, charging the battery only the amount predicted to be needed [36], [38]–[43].
- Most Li-ion batteries should not be charged at ambient temperatures below 0°C or above 40-50°C [13], [36], [38].

Discharging

- Fully discharging a Li-ion battery will reduce its life, and discharging the battery below 2.5-3 V/cell can cause permanent damage or short-circuiting [36], [38], [39], [42].
- Use partial discharge cycles, with small DOD [36], [38]–[40], [42], [44].
- Avoid high discharges rates [38].

2.5 Li-ion degradation and lifetime analyses in the literature

This section aims to review previous studies concerning Li-ion degradation and lifetime.

2.5.1 Lifetime studies based on experimental data

The study of degradation experimentally is challenging, as it often requires the operation of multiple batteries in a controlled environment for years. This often leads to compromised results because of the use of short time studies, the usage of accelerated aging conditions that can stimulate faster degradation or not considering the current developments in new materials [37].

Dubarry et al. studied the degradation in a real Battery Energy Storage System (BESS) during a three-year period [45]. The 1MW/250 kWh Lithium titanate BESS was used under heavy duty conditions, cycling an average of 8 times a day and spending 85% of the time above 90% of the rated power. In the three-year period the BESS suffered a 5-10% capacity degradation after more than 5000 equivalent full cycles.

Gailani et al. tested batteries from three different manufacturers, studying calendar aging and cycle aging [37]. Calendar aging was studied for two different manufacturer LFP batteries during 30 months under different SOC and temperatures. In both cases, calendar aging increased with increasing temperatures and SOCs. Cycle aging was studied to the two previous LFP batteries and one NMC battery under different DOD, temperature and C-rate limit. In all cases the capacity fade increased for increasing DODs, temperatures and C-rate limit. However, the NMC battery outperformed both LFP batteries and degrade slower for the same conditions, reaching 80% SOH after 3000 cycles at 1C rate, 35°C temperature and 70% DoD.

Grolleau et al. studied calendar aging in Li-ion batteries for EV application [46]. For that the degradation of NMC batteries at different SOC and temperatures was studied for 24 months, showing as previous studies increased aging for hight temperatures or high SOC. After that, the degradation of batteries which expended most of the time at rests subjected to small cycling was studied for different charging scenarios, showing that even very reduced cycling caused a strong negative effect on Li-ion lifetime.

Preger et al. [30] performed a three year cycling study of commercial LFP, NCA and NMC cells. The cells were cycled with varying temperature, DOD and discharge rate. LFP had the highest lifetime across all conditions. The trends in temperature, DOD

and rates were chemistry specific, with the capacity fade increasing with temperature for LFP cells but decreased for NMC cells, indicating different dominant degradation mechanisms. The discharge rates did not show a clear tendency in aging. The capacity fade increased with increasing DOD ranges for all chemistries, with NCA and NMC showing a stronger dependence than LFP.

2.5.2 Lifetime modelling for Li-ion degradation

By the time of writing this dissertation, the exact conclusions about Li-ion battery degradation remain unknown and the existing lifetime prediction models are empirical or semiempirical. This will irremediably result in some limitations to the available models and increased dependency on experimental data. However, these models still give reasonable predictions that in most cases match with reality, making them useful tools. The degradation models used in this dissertation will be discussed in detail in the methodology chapter. Many authors have proposed different models.

The model proposed by Smith et al. is highly empirical, consisting of trial functions statistically regressed to Li-ion cell life datasets [34]. Grolleau et al. proposed a calendar aging model fitting their experimental data following a similar approach [46]. Pérez et al. proposed a model for obtaining the Li-ion degradation under erratic operation from the manufacturer's degradation data for constant DOD ranges [33].

Other models like the one proposed by Goebel et al. follow a more semiempirical approach [47], trying to mathematically model the degradation mechanisms using physical and chemical laws and using the experimental data to adjust these expressions and make them fit the experimental data.

2.5.3 Lifetime studies based on simulations

Because of the limitations of experimental studies, many authors choose to use lifetime models to simulate different scenarios. Although these stem from the experimental data, they allow to simulate complex scenarios and obtain results much quicker and at a lower cost.

Mishra et al. studied the impact of different chemistries and climatic conditions on a battery in a residential energy storage system under different operating conditions [41]. In the study high temperatures, high DODs and high average SOCs showed to be detrimental to the lifetime. The LFP chemistry showed less sensitivity to temperature

and DOD and achieved better lifetime predictions than the NMC one. Lifetime was also improved by oversizing the battery and cycling it within tighter SOC limits.

Tian et al. performed an economic analysis of the lifetime of a BESS under multiple SOC ranges [48]. It showed that although wider SOC ranges led to higher revenue from the market, the lifetime of the BESS was reduced reducing the overall value of the BESS. Thus, the optimum SOC range is smaller, finding the balance between the BESS revenue and degradation. Won et al. and Goebel et al. also follow a similar approach analysing a BESS system and looking for the operational dispatch to maximize its rentability considering the degradation cost associated [44], [47].

Beltran et al. studied time expectancy for commercial Li-ion batteries implemented as home solar storage systems [49]. Each battery was studied at three different load patterns, in three different locations, with two sizes of PV system and three different battery sizes. The simulations showed that NMC batteries were affected more by cycle aging than the LFP ones. However, as the battery size increased calendar aging gained relevance and the two chemistries converged. Additionally, the degradation experienced by different load profiles and PV generation profiles did not vary significantly.

Overall, the literature shows similar results. In most of the studies the LFP chemistry outperforms NMC one in cycling aging and is less affected by the DOD and rate. Temperature showed a strong effect in all scenarios, with higher temperatures accelerating aging both in calendar and cyclic aging. The higher charge and discharge rates accelerated cyclic aging as well in most of the studied reviewed. Lastly, the SOC showed a strong influence on calendar aging with higher SOC leading to faster aging.

3 Methodology

This chapter discusses the methodology followed to perform the analysis of the lifetime of Li-ion batteries. The main parameters affecting the lifespan of Li-ion batteries were identified in the literature review and their effect was studied through simulations in three different modelling software. The analysis was performed for 4 different scenarios, corresponding to four different household, with two different sized PV systems associated.

3.6 Scenarios considered

In order to cover a wider range of situations and to study the effect of the household type, four scenarios were studied:

- One person unemployed
- One person working
- Family, two children, both parents unemployed
- Family, two children, both parents working

These cases were chosen to study simple cases, where the duty of the battery is expected to be significantly different. One working person within a household will usually spend most of the day away from home, so the battery will play a key role in using the PV energy outside that time window. On the other hand, a family with both parents unemployed will very likely have energy consumption during the PV's working hours and the battery's contribution will be less critical. Thus, a broad battery use scenario is covered.

This way the working and unemployed scenario for multi-person and one-person households were studied. Multi person scenarios are expected to have a higher and more varied load pattern, while working cases expected to have higher mismatch between PV and load than their unemployed counterparts.

The battery and PV system employed was kept the same in the working and unemployed variants, being the difference between them the load profile. On the other hand, different battery and PV systems were considered for the person and family case, as the family is expected to have a higher demand and thus use a larger system.

3.1 Consumption profiles

In order to simulate the operation of the battery it is necessary to know the time evolution of the demand and the PV generation, i.e., the consumption and generation profile.

Both the consumption and generation profiles were obtained from Polysun software to serve as a starting point [50]. This software is very renowned and has been first developed at the Institute for Solar Technology, University of Applied Sciences Rapperswil, Switzerland, back in 1992. Later on, a spin-off company was formed to offer the software on a commercial basis.

Polysun has an extensive database of consumption profiles for more than 70 household types. Out of these the "one-person" and "family with two children" scenarios were chosen as simple and somewhat common cases for one-person and multi-person scenarios. Considering the unemployed and working variants, the four consumption profiles were obtained with a data resolution of 1 hour.

These profiles were then scaled to reflect the typical consumption in Malta. This was based on the data from a report on energy consumption in households from the National Statistics Office of Malta [51]. The data considers four types of dwellings as presented in Table 8.

Table 8. Summary of energy consumption per household type [51].

Appliance	Daily average (kWh/d)			
	Apartment	Maisonette	Terraced house	Villa
Refrigeration	1.92	2.47	2.51	2.46
Kettle	0.11	0.09	0.14	0.19
Dishwashers	0.00	0.10	0.00	0.00
Electric Ovens and Hobs	0.22	0.20	0.06	0.36
Microwave Ovens	0.09	0.07	0.06	0.07
Water Heating	2.52*	2.52	2.87	2.53
Space Heating (non-A/C)	0.00	0.14	0.00	0.36
Airconditioning	0.00	0.07	0.00	0.00
Televisions	1.08	0.99	0.95	0.92
Hi-Fi Equipment	0.00	0.01	0.00	0.02
Computers	0.36	0.59	0.50	0.17
Washing Machines	0.24	0.26	0.25	0.33
Tumble Drier	0.00	0.06	0.00	0.02
Solar Heating	0.00	0.05	0.00	0.00
Pool Pump	0.00	0.00	0.00	1.02
Lighting and Other	2.94	3.15	3.69	4.27
Main Incomer	9.47	10.76	11.02	12.72
Yearly average (kWh/y)	3455	3929	4023	4644

*The study reported that the water heating figure for Apartments was abnormally high so the same value as maisonettes was used instead.

The four households identified earlier were associated with an appropriate dwelling from those considered in the report. In this way, an apartment was considered for the one-person households while a villa was chosen for the family households. The corresponding yearly average consumption values were then used to scale the respective Polysun profiles.

3.2 Photovoltaic System and generation profiles

Each household was assumed to own a PV system. The PV systems were designed using Polysun software, setting up two different sized PV systems; one for the single person and one for the family households. The criterion used to size the PV system in both cases was to have an annual generation that is close to the annual consumption identified from Table 8. All of the chosen components were state-of-the-art with good efficiencies so the analysis would be valid for newer projects. The photovoltaic modules selected were monocrystalline panels, mounted with a south-orientation and a tilt angle of 30° to the

horizontal. The number of panels was adjusted in each case to achieve the desired total energy generation.

The weather data was obtained from the Polysun software itself with the location set to Valletta (Malta). Polysun obtains this data using the webservice of Meteonorm. In this way, the data of a typical meteorological year was obtained using data from the 1996-2015 period for radiation parameters and from 2000-2019 for temperature, dew point temperature, wind, precipitation and days with precipitation.

Using the designed PV systems and the obtained weather data, the generation profiles were obtained with 1 hour resolution. Table 9 shows a brief summary of the designed system but this will be further elaborated in the next chapter.

Table 9. Summary of the PV system designed.

	One person	Family
Total annual consumption [kWh]	3455	4644
Total annual generation (AC) [kWh]	3384	4504
PV peak power [kWp]	2.25	2.92
Battery size [kWh]	4.5 kWh	6 kWh

3.3 Battery sizing

The Association of European Automotive and Industrial Battery Manufacturers (EUROBAT) suggests a typical battery size of 2 kWh per installed kWp of PV for household installations [52]. Weniger et al. studied the sizing of Li-ion batteries for PV residential application and recommended similar capacities [53]. Consequently, the batteries were sized to the closest commercially available capacities following this rule. Thus, as indicated in Table 9, 4.5 kWh and 6 kWh batteries were chosen for the single person and family households respectively. Further characteristics and selection of operational parameters for the batteries will be discussed in the next subsections.

3.4 Lifetime models and battery operation strategies

Three different models were used in this dissertation, Polysun lifetime prediction [50] SAM software [54] and simSES [55].

3.4.1 Polysun lifetime prediction [56]

Polysun offers a first approximation of the battery lifetime, considering the cycling and calendar aging.

For Li-ion batteries the number of cycles to fail C_F at different DOD is modelled as a Wohler curve as shown in (1):

$$C_F = \alpha_1 \cdot \mathrm{DOD}^{-\alpha_2} \tag{1}$$

Where $\alpha_1$and α_2 are parameters obtained from empirical lifetime test data, intrinsic to the battery model used. Then the data obtained from the modelled battery is divided into 20 DOD ranges of the same size and the number of cycles in each range, M_i, is computed. Using M_i and the number of cycles to failure at each range $C_{FL,i}$ obtained from (1), the annual damage D to the battery is computed according to (2):

$$\mathrm{D} = \sum_i \frac{M_i}{C_{FL,i}} \tag{2}$$

The total cycling life is then obtained from the annual damage.

On the other hand, calendar life is given in the respective battery catalogue entry. In most cases this value is 20 years. Finally, the combined lifetime estimation will be the minimum of the calendar life and cycling life.

3.4.2 SAM Software[54]

SAM (System Advisor Model) is a free techno-economic software for the renewable energy industry developed by the National Renewable Energy Laboratory (NREL) of the United States.

The utility used in the program was the battery storage system analysis. Introducing the generation and consumption profiles obtained from Polysun it allows to analyse the performance of the battery. SAM software has several dispatch models for the battery:

- **Peak shaving:** This strategy attempts to reduce the peak power injection into the grid, considering the solar resource and the load during the day. Two approaches are available:

    - **Peak-shaving one-day look ahead:** For each day, the battery dispatch is based on the solar resource and load data over the next 24 hours. The look-ahead option gives the ideal case as it is based on a perfect prediction of the future load and solar resource data.
    - **Peak shaving one-day look behind:** Similar to the previous approach but the dispatch is based on the previous 24 hours. This is a more realistic case as it does not predict the future and leads to some mismatch between the assumed and actual profiles.
- **Input targets:** This strategy tries to operate the battery in response to specified targets. Two targets are available, as follows:
    - **Grid input power:** In each time step the demand from the grid is compared to the set target. The battery charges when the overall load is less than the target, and discharges when the overall load is greater than the target.
    - **Input battery power targets:** In each time step, an attempt is made to charge to the negative power value introduced, or discharge to the positive power value introduced.
- **Price signal forecast:** This option operates the battery to minimize the electricity bill over the next 24 hours by considering the load, system power output, and electricity rates.
- **Manual dispatch.** In this option the timing of battery charges and discharges as well as the maximum amount it can be charged in each time slot is manually introduced. A manual dispatch was set to be equivalent to the operation strategy "Greedy" from simSES. In this mode the battery can charge and discharge as much as possible at any given time.

Out of these options the "Manual dispatch greedy" was used, as there is no grid power or battery power target and this work does not cover the economic aspect. The peak saving options show very little operation of the battery, with it spending most of the time idle and not actively participating.

To analyse the battery lifetime, SAM also differentiates between cyclic aging and calendar aging. The cyclic degradation model relies on the curves of capacity fade versus number of cycles elapsed at distinct average DODs like the one shown in Figure 26.

These curves can be found in the datasheet of the battery or use the default curves for the main Li-ion chemistries provided by SAM.

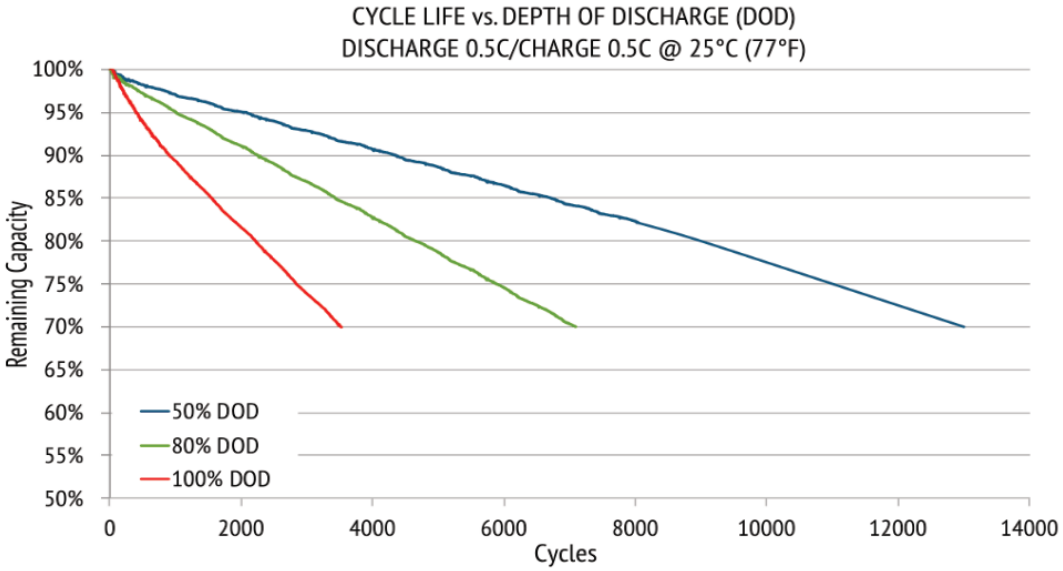

Figure 26. Capacity fade versus number of cycles of the ReLiON RB48V100 LFP battery [26]

Counting the number of cycles in a Li-ion battery is complex, as partial DOD cycles degrade the battery slower, and thus do not accumulate to form a full cycle. This way for instance five partial 20% DOD would account for less than a full 100% DOD cycle. To track the number of cycles that the battery has undergone SAM applies a rainflow counting algorithm [57]. This algorithm is often used in cycle counting in fatigue processes, allowing to transform a complex, irregular discharge history into a series of constant amplitude events. To achieve this the algorithm defines the cycles as closed hysteresis loops [58]. After obtaining the number of cycles, the aging is determined by interpolating the curve at the current cycle number and average cycle DOD at the corresponding timestep.

On the other hand, the calendar aging follows the model proposed by Smith et al. [59]. This model calculates the parameter k_{cal} as a function of the SOC and temperature as shown in (3), where the parameters a, b and c are fitted to the empirical data.

$$k_{cal} = a \cdot e^{b\left(\frac{1}{T}-\frac{1}{T_{ref}}\right)} \cdot e^{c\left(\frac{SOC}{T}-\frac{1}{T_{ref}}\right)} \quad (3)$$

With k_{cal} the resulting remaining capacity (measured in SOH terms) of the battery is calculated as a function of the square root of time t according to (4), where q_0 is the initial SOH of the battery.

$$q = q_0 - k_{cal}\sqrt{t} \quad (4)$$

Finally, the total resulting aging is obtained as the value that gives the lowest remaining capacity out of calendar and cyclic aging in each time step.

In SAM, a reference set of parameters for each scenario was analysed more in detail as it will be explained in the simulations section. For these cases the general characteristics like cycling, average DOD and SOC were studied as well as the SOC and DOD distributions, plotting the histograms of the corresponding data arrays. The performance of the battery for the reference parameters in each scenario was studied by analysing the self-consumption fraction achieved. The aging in all scenarios was analysed representing the SOH time evolution. For the reference parameters this aging analysis was further split into aging and calendar aging Some additional outputs were studied to help understanding the results like the C-rate distribution, which was obtained representing the histogram of the power data normalized with battery size.

3.4.3 simSES [55]

The simSES software (Simulation of stationary energy storage systems) is an open-source modelling framework for the simulation of stationary energy storage systems developed by the Technical University of Munich, Germany [55].

In simSES, the tool for residential storage was used. The same PV generation and load consumption profiles obtained from Polysun and previously used in SAM were used. In simSES, four operation strategies are offered for the battery:

- **Greedy**: This mode maximizes the self-consumption of the system. The excess power is stored in the battery and excess demand is supplied by the battery. There is no forecast or consideration of system limits, as the available capacity is finite and limited by the SOC limits, thus the battery can get fully charged or discharged.
- **Self-Consumption Optimization avoiding Curtail**: The curtailment is the deliberate limitation of the power output of the PV system, generally in order to balance supply and demand, security or because of transmission limitations. This mode is similar to the Greedy strategy but incorporates a way to minimize curtailment losses. The expected curtailed energy is calculated and computed to corresponding SOC of the battery. SOC limit is temporarily changed to keep sufficient storing capacity to store the power above curtailment limit.

- **Feed-in damping:** This strategy was implemented according to Zeh et al. [60]. The power at which battery is charged is damped, depending on the remaining empty capacity of the battery and the predicted remaining time until sunset achieving a nearly constant charge power over the complete sunshine duration.
- **Dynamic feed-in limit.** This mode introduces a small improvement on the previous one. Energy for certain thresholds is roughly estimated to obtain a near-optimal reference feed-in limit.

The models used by simSES are different for each battery technology. For the NMC chemistry the capacity fade due to cycling is obtained through the exponential equation shown in (5), where n is the number of cycles and a, b, c and d are parameters obtained from fitting the data from the warranty sheet of the Tesla Powerwall with 6.4 kWh storage size.

$$f_{cyc} = a \cdot e^{b \cdot n} + c \cdot e^{d \cdot n} \tag{5}$$

The capacity fade due to calendar aging is obtained in the same way as shown in (6), Where now t is the time elapsed and a, b, c and d are fitted to the Powerwall's time degradation data.

$$f_{cal} = a \cdot e^{b \cdot t} + c \cdot e^{d \cdot t} \tag{6}$$

The combined effect of the two only considers the cyclic aging.

On the other hand, the model for LFP batteries is more detailed. This model is based on the model proposed by Wang et al. [61] and was implemented by Göbel et al. [47]. The capacity fade due to calendar aging f_{cal} is expressed as function of the duration d, the surface temperature T_s and the state of charge SOC. This relation is given by (7), where the parameters β_1, β_2, β_3, β_4, β_5, β_6 and β_7 are fitted to the empirical data.

$$f_{cal}(d, T_s, SOC) = \left(\beta_1 \cdot SOC^{\beta_2} + \beta_3\right) \cdot \left(\beta_4 \cdot T_s^{\beta_5} + \beta_6\right) \cdot d^{\beta_7} \tag{7}$$

Then, the capacity fade due to cycling f_{cyc} is obtained as a function of the capacity consumed measured in Ah, the surface temperature T_s and the C-rate at which the cell was cycled, r_c. (8) shows the resulting expression,

$$f_{cyc}(Ah, T_s, r_c) = \beta_8(r_c) \cdot e^{\left(\frac{\beta_9(r_c)}{R_{gas} \cdot (T_s + k_T)}\right)} \cdot (0.5 \cdot Ah)^{\beta_{10}} \tag{8}$$

where the variables β_8 and β_9 and the parameter β_{10} are fitted to the empirical data, R_{gas} is the gas constant and k_T is the conversion summation (273.15) from Celsius to Kelvin.

Finally, the resultant combined fade of the battery is the maximum of the cycling fade and calendar fade for each timestep.

In simsSES it was proceeded in a similar way than in SAM. The same general characteristics were analyzed in simSES for the reference parameters. The performance of the battery in each scenario in this case was studied by analysing the self-consumption fraction achieved. Similarly to SAM, the SOH evolution was used analyse the degradation of Li-ion batteries under multiple operation parameters, and the calendar and cycling aging for the reference parameters. simSES software does not offer the option to limit the ratings so this effect was only studied in SAM

3.5 Simulations

The main objective of the simulations performed was to identify the best operating strategies in order to extend the Li-ion batteries lifetime. In order to achieve this, the effects of the parameters affecting the battery lifetime' as identified in the literature review, were studied. These consisted of:

- **SOC operating range**: Limiting the maximum and minimum allowable SOC is a common strategy to prolong the lifetime of Li-ion batteries. This directly limits the maximum DOD.
- **Charge and discharge rates:** Higher charge and discharge rates cause accelerated aging. Therefore, establishing an upper C-rate limit for charging/discharging can prolong the battery lifetime. The C-rate limit also indirectly reduces the battery cycling as it limits the power exchange.
- **Battery Capacity:** Oversizing the battery is a possible strategy that could extend the lifetime as the same amount of energy in a larger battery will represent a smaller DOD with correspondingly less cycles than for a smaller battery. However, the effect of increasing the battery capacity is not trivial. A larger battery could keep operating in situations where a smaller battery would be either full or depleted, and thus experiencing the same or even higher number of cycles. This would of course improve the performance and self-consumption ratio of the system, but the lifetime could be decreased. In order to assure an increase in the lifetime, the usable capacity must remain the same using tighter SOC ranges.

- **Battery dispatch method:** The battery dispatch method will dictate how the battery operates, consequently conditioning the evolution of the SOC and the DOD. This way the dispatch method chosen will influence the lifetime. It is important to notice that the usual objective of the dispatch method is to maximize the performance and self-consumption of the system and often will not prioritise battery lifetime.
- **Battery chemistry:** The main Li-ion chemistries used for energy storage are NMC and LFP. Of the two, LFP usually has a longer lifespan, although the difference between the two has decreased in the recent years.
- **Temperature:** Temperature has a strong influence in aging and limiting the exposure of the battery to high temperatures can increase its lifetime.

As shown in the previous subsection the impact of each of the parameters will be conditioned by the model used. Therefore, firstly the effect of each parameter was explored to analyse its effect on the lifetime prediction for each model used in just one of the studied cases. The scenario studied extensively was family, both parents working as it was considered as the most common out of the four in which to consider installing a PV battery system. In order to do this a set of parameters was taken as a reference out of which one parameter was modified at a time, thus obtaining the SOH evolution as a function of the said parameter. The reference parameters were chosen according to the manufacturer and literature guidelines and are summarized in Table 10. The predictions obtained from the three models were then compared.

In simSES, the chemistry used as reference was LFP as the NMC model seems limited. Similarly, LFP batteries are used in SAM. For battery dispatch, the "Manual dispatch greedy" was used as it was the one which achieved the best use of the battery. In simSES "Greedy" mode was used, as it is equivalent to SAM's dispatch model.

Table 10. Reference parameters.

	SAM	simSES
SOC range	20-80%	
Charge/discharge rate limit	0.5C/0.5C	
Battery dispatch method	Manual dispatch greedy	Greedy
Battery chemistry	LFP	
Temperature	25°C	

The simulated period in all cases was set to 25 years, given that this is commonly taken as the expected service life of residential PV systems. The simulation step size used was one hour, as it offers enough resolution to obtain valid results. The battery replacement threshold used was a SOH of 80%, as it is the common reference in the literature.

Once the key parameters were identified, the analysis was extended to the rest of the cases. Lastly, the results of the different scenarios were compared. In summary, Figure 27 shows a flow chart describing the methodology used for exploring the effect of the parameter settings on the lifetime.

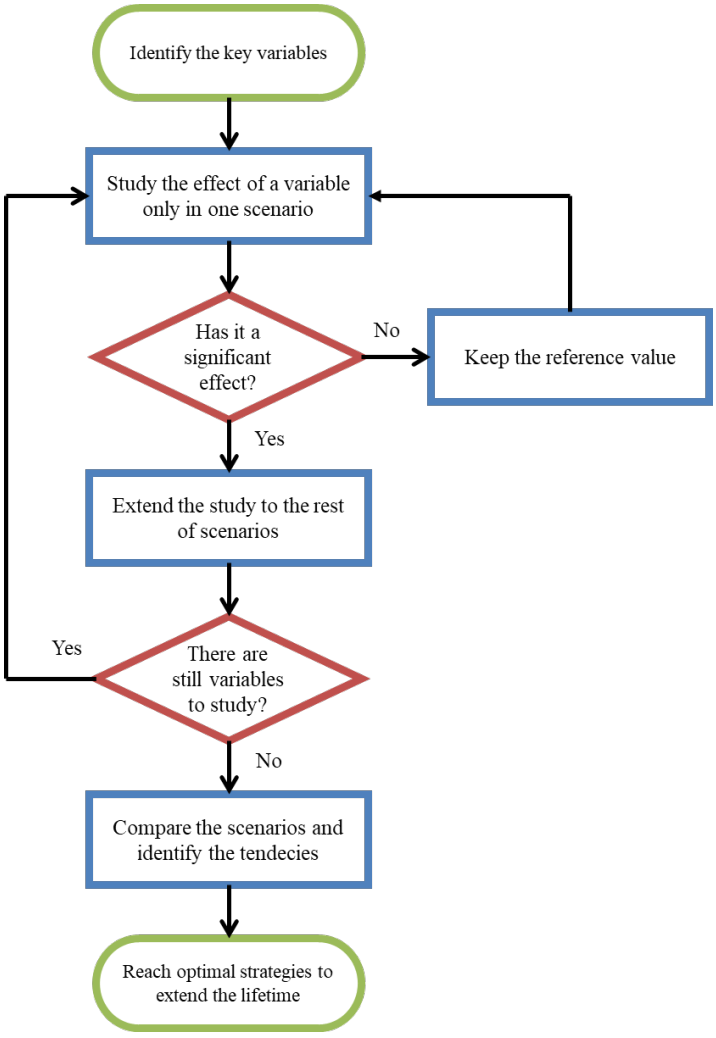

Figure 27. Flow chart of the methodology employed.

The chapter showed the methodology followed in order to perform this study. The motivation for the four scenarios studied was discussed, showing the criteria followed to dimension the PV system and the battery and thus obtain the consumption and generation profiles for each scenario. After that the models and dispatch methods of the

software used were described. Lastly, the methodology followed to perform the simulations was described, showing the main parameters studied.

4 Results and discussion

This chapter presents the results for the four scenarios studied. The first scenario was subjected to a deeper and more complete analysis while the following ones are studied more lightly, focusing on their particularities and differences between them.

4.1 Scenario 1: Family with both parents working

Both in SAM and simSES the simulations were set up introducing the "family with both parents working" consumption and generation profiles and adjusting the size of the battery. To showcase the profiles, a week of operation during the summer is presented in Figure 28 and a week during the winter in Figure 29.

The load in both figures is similar, showing a marked difference between the weekdays and the weekend, with the central hours of the weekdays having very little consumption, as everyone is away from home. In the weekends the consumption is greater and more distributed throughout the day, having more consumption during the PV production hours. Most of the days present three peaks corresponding to the mealtimes.

The PV system size for the family scenarios was 2.92 kWp. The PV generation during the summer is high and experiences very little variation from day to day, as in Malta the cloud coverage during summer is rare. In contrast, the generation during the winter is lower and more irregular as there are less sun hours and cloudy or rainy days are more common.

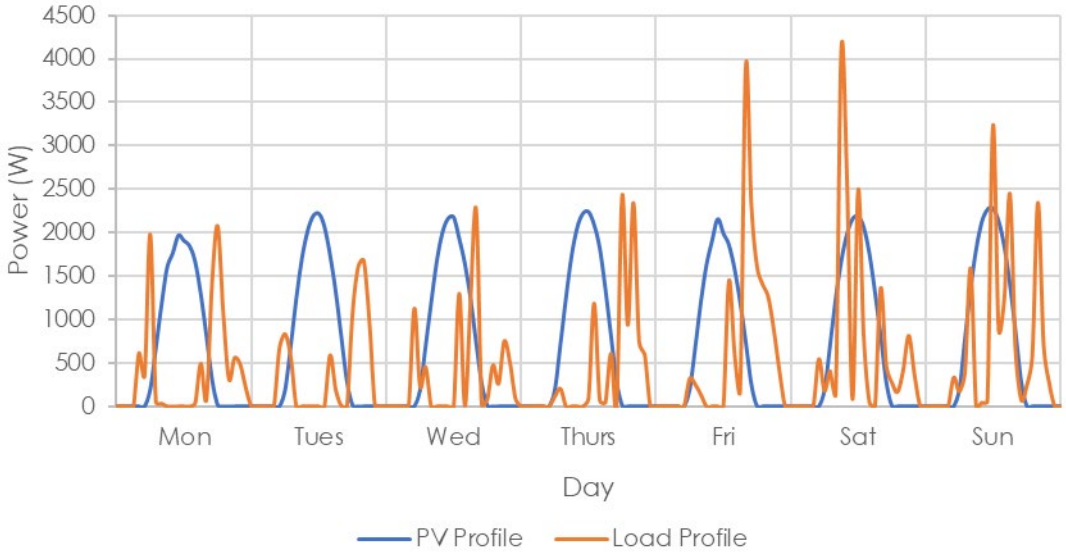

Figure 28. Consumption and generation profiles of Scenario 1 during a summer week.

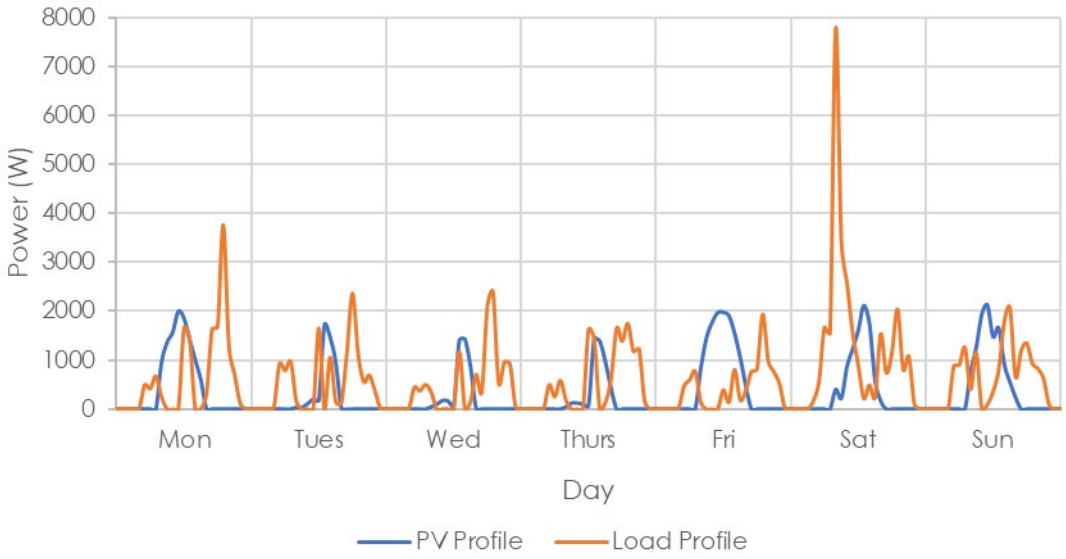

Figure 29. Consumption and generation profiles of Scenario 1 during a winter week.

4.1.1 Reference parameters

The summary of the simulations performed using both SAM and simSES is presented in Table 11. The number of cycles, average DOD and average SOC are very similar, as both models are using the same dispatch method. In SAM, the fist number of cycles value is measured in the same way as in simSES, as the number of times the accumulated discharge reaches 100%. The second value for number of cycles is the one obtained from the counting algorithm in SAM. This value was extremely high across all scenarios and was analysed in more detail, observing that the rainflow algorithm was being triggered by the small changes in state of charge, where the battery switches between

charging and discharging for short periods. As this value is used to compute cycle aging, the cycle aging in SAM is more pronounced.

Table 11. Summary of Scenario 1 with reference parameters

	SAM	simSES
Total Cycles (Counting algorithm)	5585 (16115)	5583
Average Cycles/day	0.61	0.61
Average DOD	34.25%	39.51%
Average SOC	40.68%	40.47%
Battery replacements	1 (16th year)	1 (14th year)
SOH Calendar Aging	96.87%	83.91%
SOH Cycling Aging	81.30%	86.39%
Total SOH	81.30 %	81.25%

To analyse the operation of the battery in both software their SOC evolution for the same weeks as the profiles of Figure 28 and Figure 29 is shown in Figure 30 and Figure 31. In both cases, the battery follows the profiles and is operated in a similar way. Generally, it charges early on in the day reaching the upper SOC limit and is discharged to the bottom limit in the evening. In the weekends when there is a higher demand in the central hours of the day the battery can alternate between charge and discharge. In the winter the PV production is more limited, and the battery sometimes does not fully charge during the day.

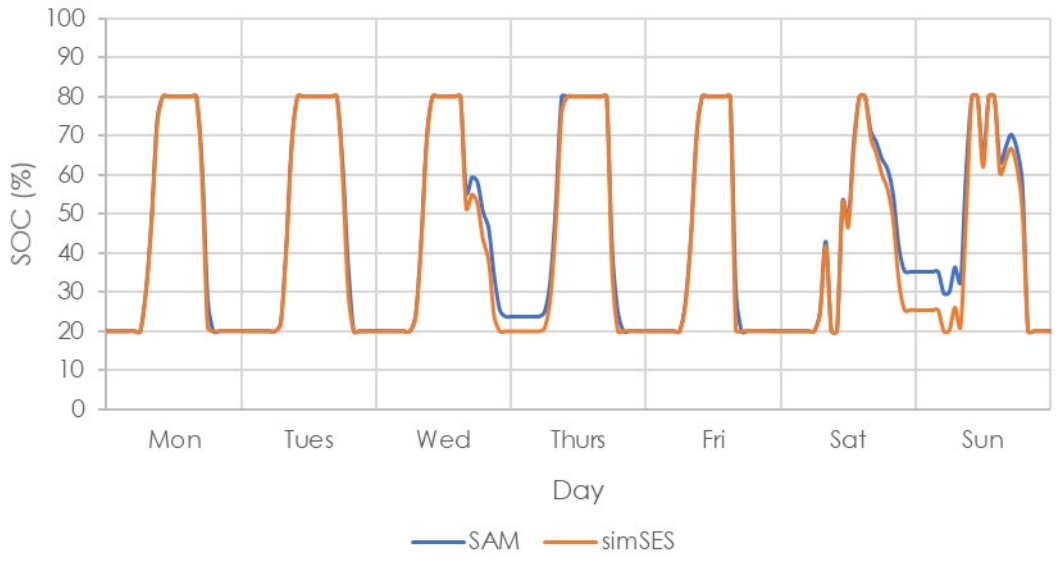

Figure 30. SOC in SAM and simSES at Scenario 1 during a summer week using the reference parameters.

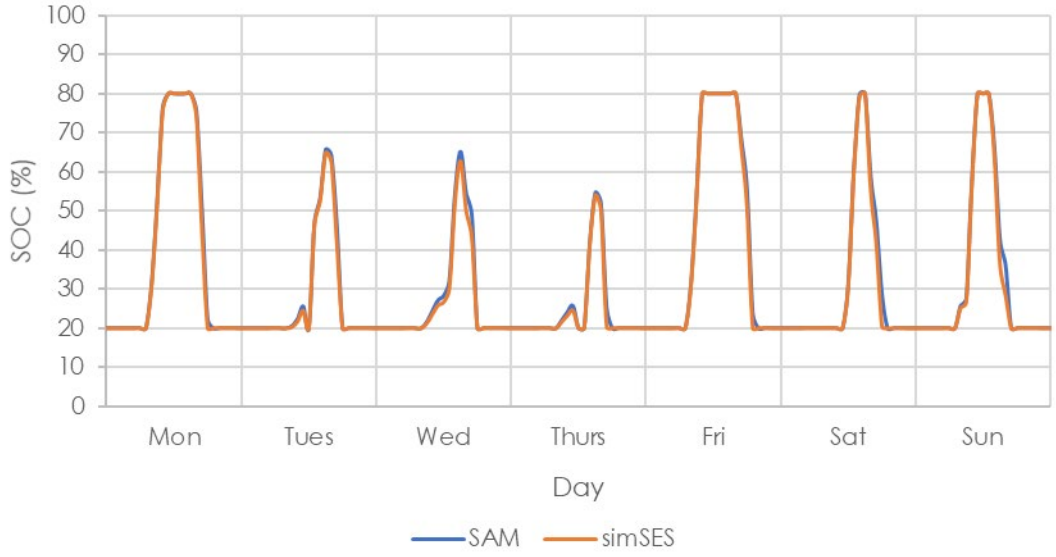

Figure 31. SOC in SAM and simSES at Scenario 1 during a winter week using the reference parameters.

Figure 32 shows the evolution of the SOH obtained from the two models. The simSES prediction is less favourable with the battery needing replacement before, although initially the aging happens faster in SAM.

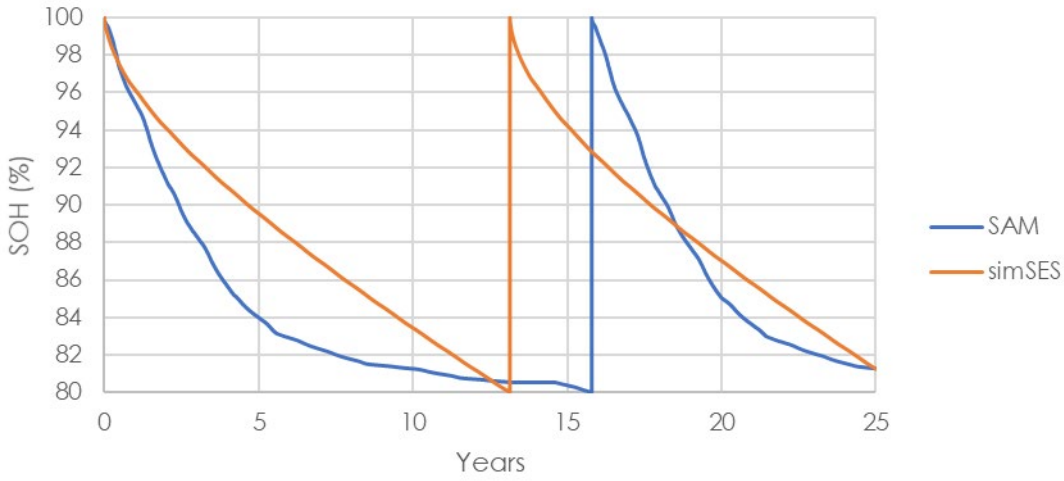

Figure 32. Evolution of the SOH in SAM and simSES at Scenario 1 using the reference parameters.

The calendar and cycling aging of both models is analysed in more detail in Figure 33 and Figure 34. Figure 33 shows that in SAM, as the number of cycles obtained from the counting algorithm was extremely high the cyclic aging dominates during the whole simulation.

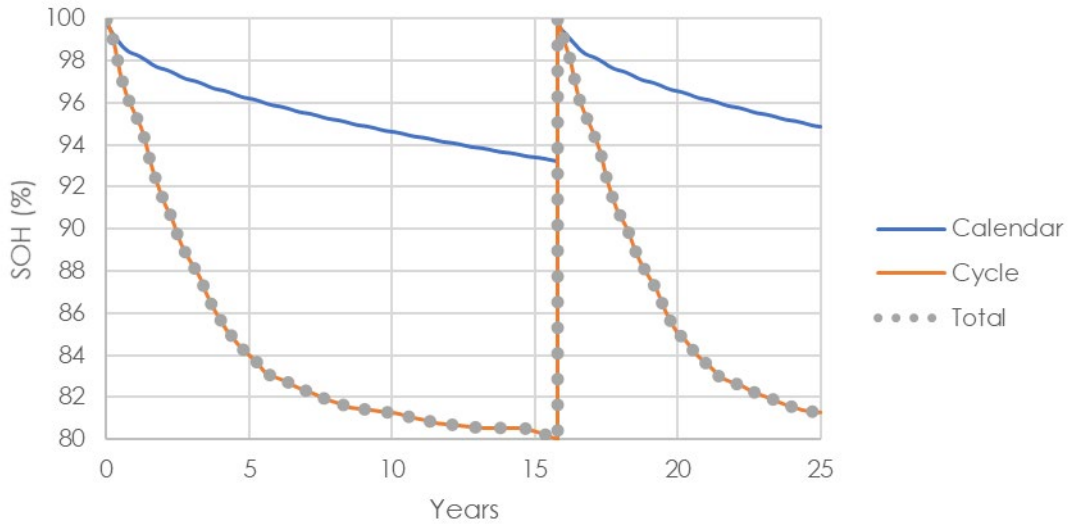

Figure 33. Calendar and cycling aging in SAM at Scenario 1 using the reference parameters.

On the other hand, Figure 34 shows that in simSES the dominant aging mechanism is calendar aging, with cycling aging only dominating at the start. In SAM the cycle and calendar aging are calculated separately and then the combined aging is the lowest value of the two at each time step whereas in simSES at each timestep the cycle and calendar aging is calculated, and the total aging takes the biggest drop of the two, leading to a smaller total aging than either cycling or calendar aging.

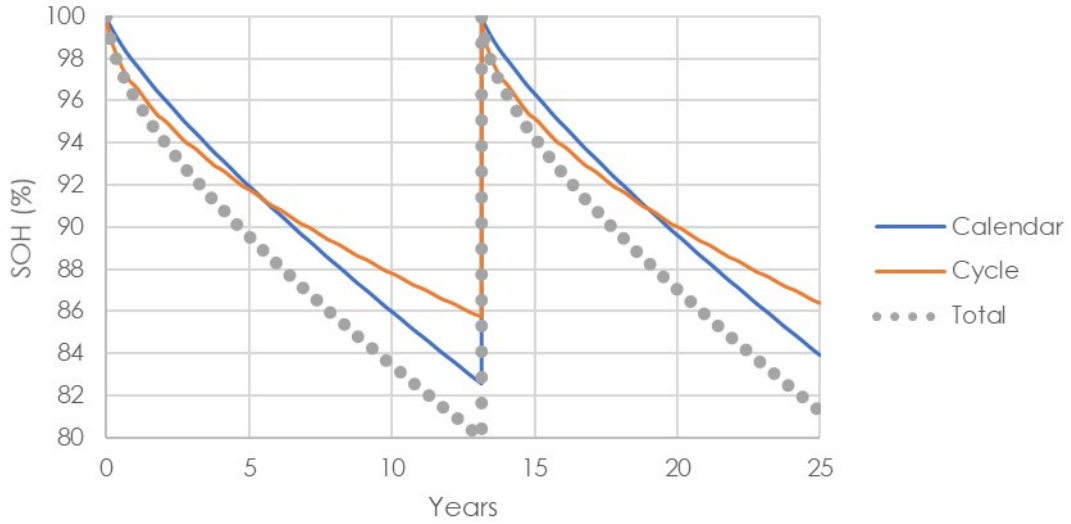

Figure 34. Calendar and cycling aging in simSES at Scenario 1 using the reference parameters.

Throughout the results section it will be shown that in SAM the cyclic aging dominates, as a consequence of the rainflow algorithm miscount. On the other hand, the simSES model takes a more conservative approach when predicting calendar aging than SAM and will be generally the dominant aging mechanism.

To further analyse the operation of the battery in each software the frequency of different SOCs and DODs was plotted. The histogram of Figure 35 shows that SAM and simSES have a very similar distribution, having tendency to the extreme SOC. This in agreement with Figure 30 and Figure 31, as once the battery reaches either the upper or lower limits it stays idle at it until the next power exchange takes place. This is a consequence of the 'greedy' algorithms in use.

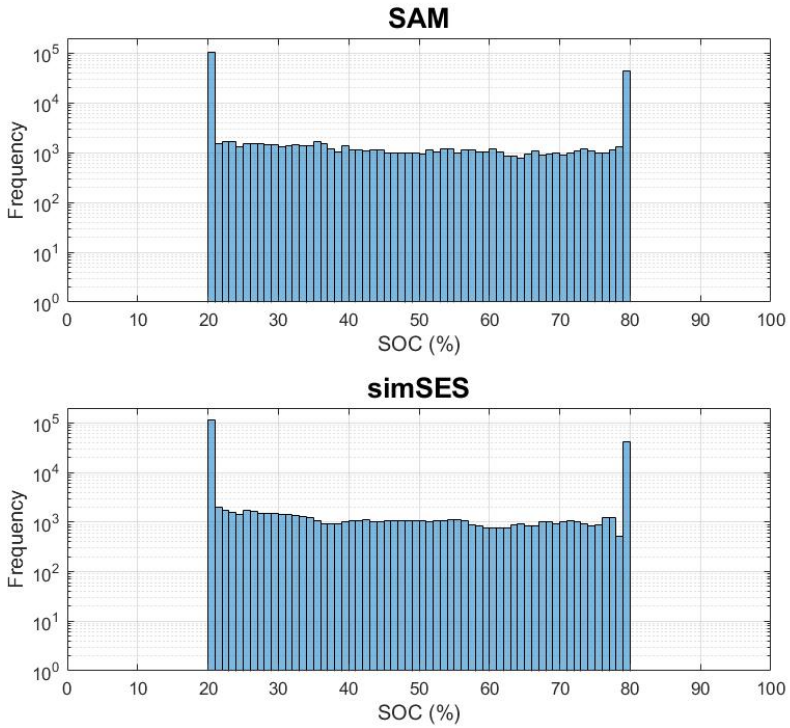

Figure 35. Frequency distribution of the different SOCs in SAM and simSES at Scenario 1 using the reference parameters.

On the other hand, Figure 36 shows the histogram of the different DOD. Again, both models show a close behaviour, with a greater tendency to 60% DOD (the maximum allowable with the SOC limit).

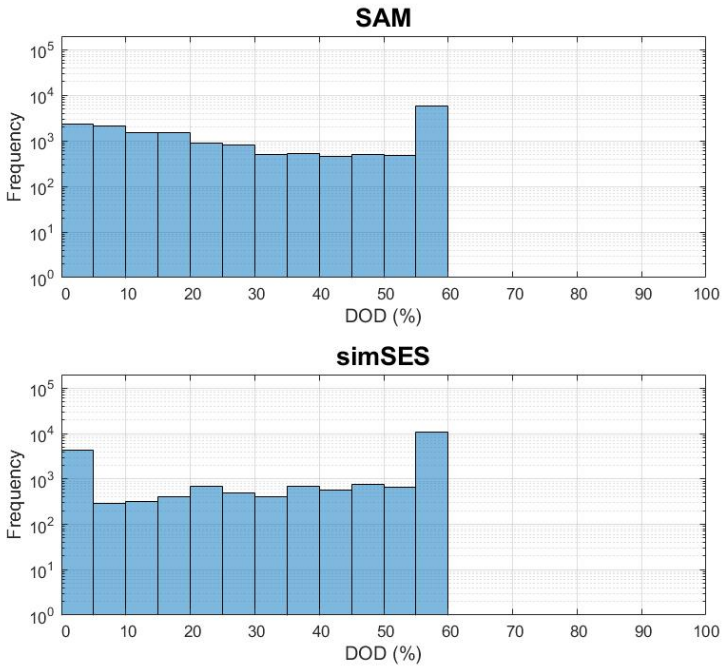

Figure 36. Frequency distribution of the different DODs in SAM and simSES at Scenario 1 using the reference parameters.

4.1.2 SOC Range

The influence of different SOC ranges was studied in Polysun, SAM and simSES.

The expected lifetime for each SOC range in Polysun is represented in Figure 37. As expected, the lifetime of the battery increases as the SOC interval narrows. Centred intervals show a very similar behaviour to non-centred ones and the key determining factor seems to be the width of the range. In this way, ranges smaller than 40% DOD are limited by the 20 years calendar aging limit.

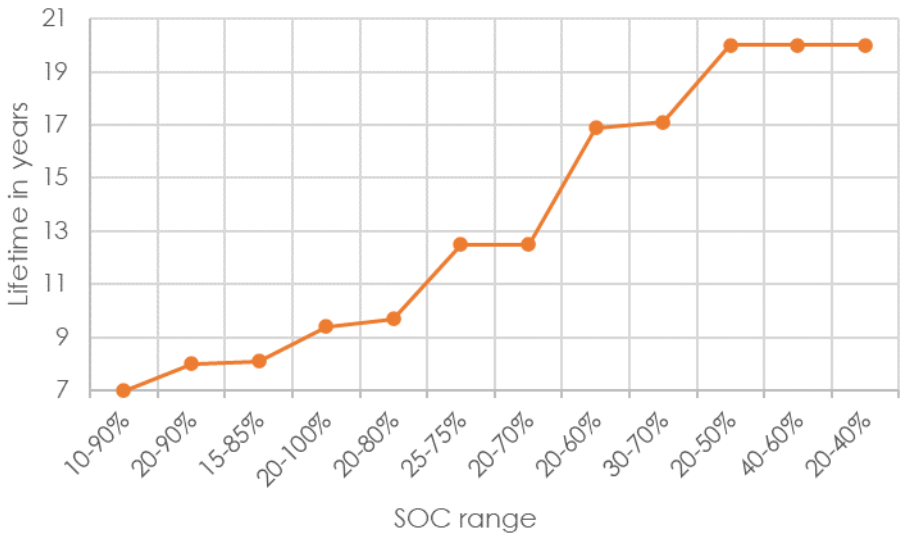

Figure 37. Expected lifetime in Polysun for different SOC ranges at Scenario 1.

The SOH evolution in SAM is represented in Figure 39. In the 20-100% and 20-80% ranges after the 6th year, because of the very elevated number of cycles, the cycle count exceeds the data of most of the curves of lifetime shown in Figure 38 that SAM uses to calculate the cycling aging. When this happens, it starts using the slower aging data of the small 10% and 20% DOD curves for bigger DOD, leading to an inaccurate deceleration in the aging. Because of this the 20-100% and 20-80% show a better performance than tighter ranges, as the aging for them has slow down. This will happen often in SAM and along with the very high cycle count greatly limits the legitimacy of SAM's results.

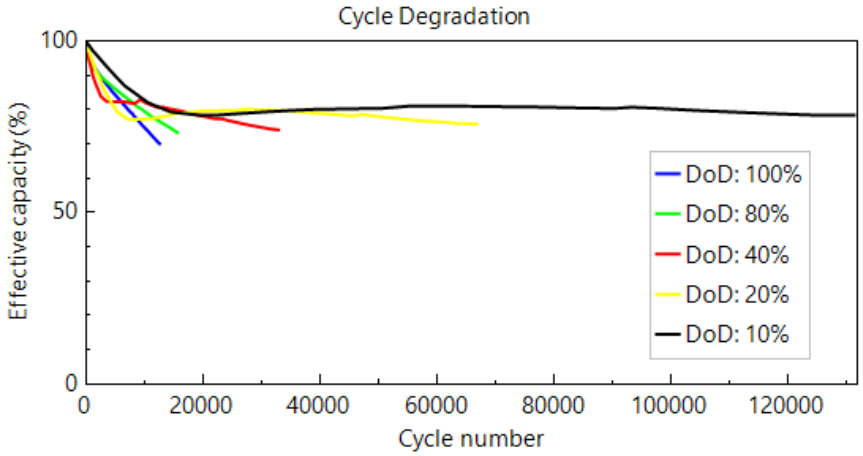

Figure 38. Lifetime curves used by SAM to model the cyclic aging for the LFP chemistry.

Observing before this effect took place, at the first five years, the results are the expected, with wider ranges aging faster. As cycling aging dominates in all the ranges studied, the position of the range has very little effect with the ranges 20-60% and 30-70% or 40-60% and 20-40% showing very similar results. Because of the high cycle counting, all SAM cases are subjected to extreme cycle aging, with the ranges of 20-60% and 30-70% needing two battery replacement and the ranges of 40-60% and 20-40% needing one.

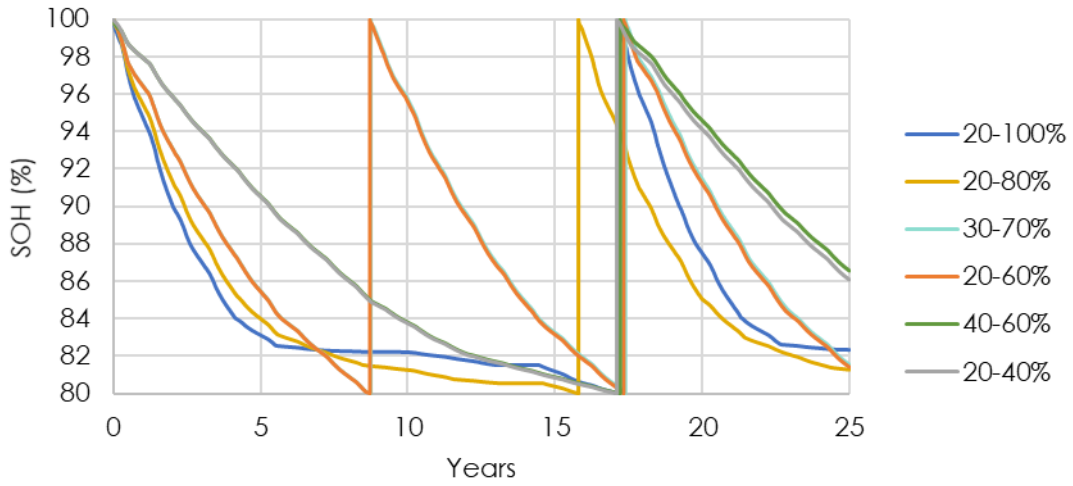

Figure 39. Evolution of the SOH in SAM for different SOC ranges at Scenario 1.

On the other hand, the evolution in simSES is depicted in Figure 40. As the predominant aging mechanism was calendar aging, the most important effect is how the ranges limit SOC. This way ranges with higher SOC perform worse, as it happens with the 40-60%, which despite having a shallower DOD than the 20-60% range performs worse, as it has a higher average SOC. All the ranges need at least one battery replacement, with the less favourable 20-100% range needing two.

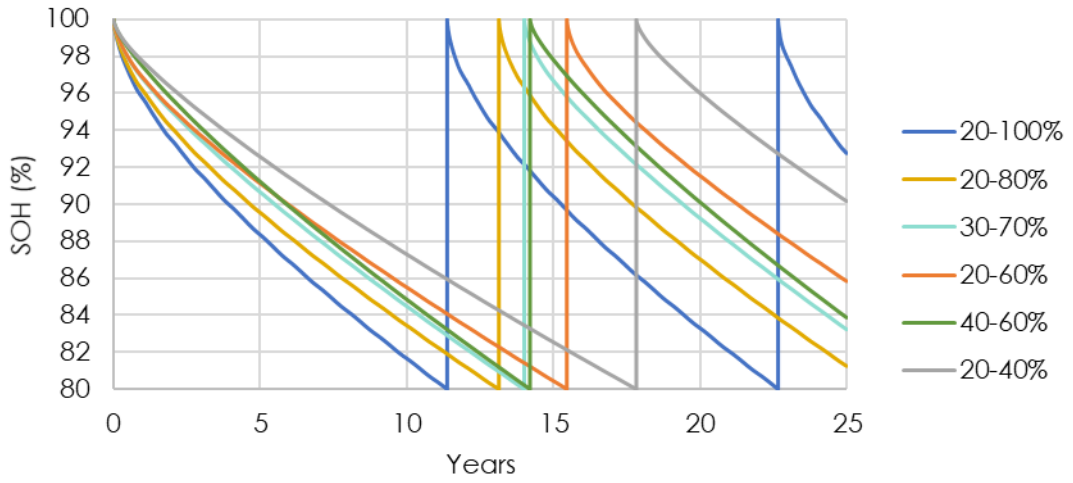

Figure 40. Evolution of the SOH in simSES for different SOC ranges at Scenario 1.

Lastly, the effect of either high or low SOC was studied. For that, the intervals of 0-20% and 80-100%, which have extreme SOC and very shallow DOD, were analysed. The results for both SAM and simSES are represented in Figure 41. In SAM the resulting SOH for the 0-20% interval is very similar to other 20% ranges. On the other hand, in simSES this interval performs substantially better than the previous ones, as the calendar aging modelled by simSES benefits from lower SOC.

SAM also punishes high SOC in calendar aging. The 80-100% in SAM is similar to the 0-20% one. However, in this case because of the very high SOC calendar aging dominates during the first years, although the difference with other 20% ranges is small, as cyclic aging remains relevant. In contrast, in simSES the difference is much more pronounced, with this range being the worst performing and even needing battery replacement twice.

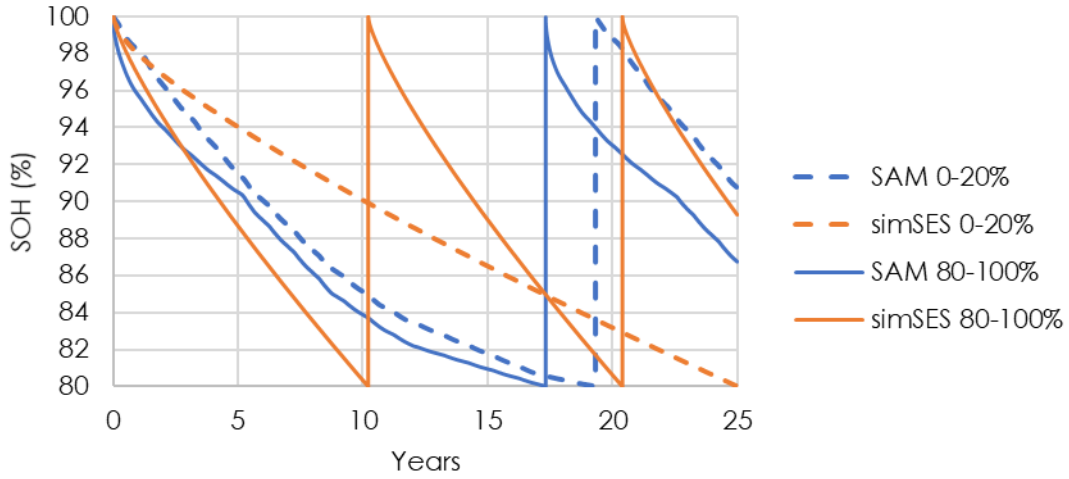

Figure 41. Evolution of the SOH in SAM and simSES for extreme SOC ranges at Scenario 1.

4.1.3 Charge and discharge rate

The influence of the charge and discharge rates was studied only in SAM, as simSES software does not offer an option to limit the ratings. Figure 42 shows how different C-rates affect the lifetime. The three rates show almost the same evolution.

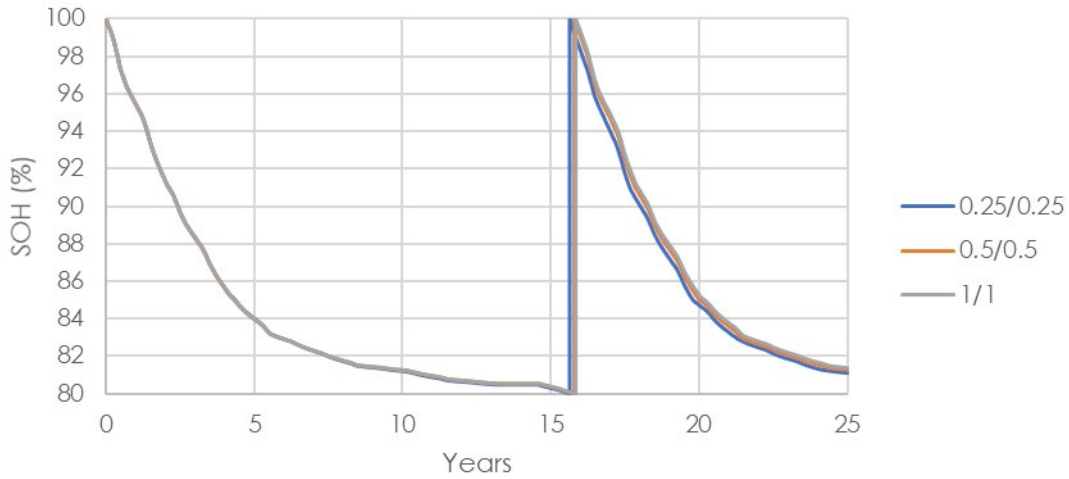

Figure 42. Evolution of the SOH in SAM for various C-rate limits at Scenario 1.

The histogram in Figure 43 shows the distribution of C-rates in SAM and simSES when there is no rate limit. Both histograms are very similar, with the most common rates

being very small and with the rates over 0.5C being very infrequent. Rates over 0.25C being are more frequent but still rather uncommon, what could explain the small effect of these limits.

It is important to notice that the battery capacity was sized to have double the size of the PV peak power and therefore the maximum possible charging power will be half of the battery size, i.e., a 0.5C rate. This way the charge C-rate, which is usually most restrictive, is limited by design to 0.5C.

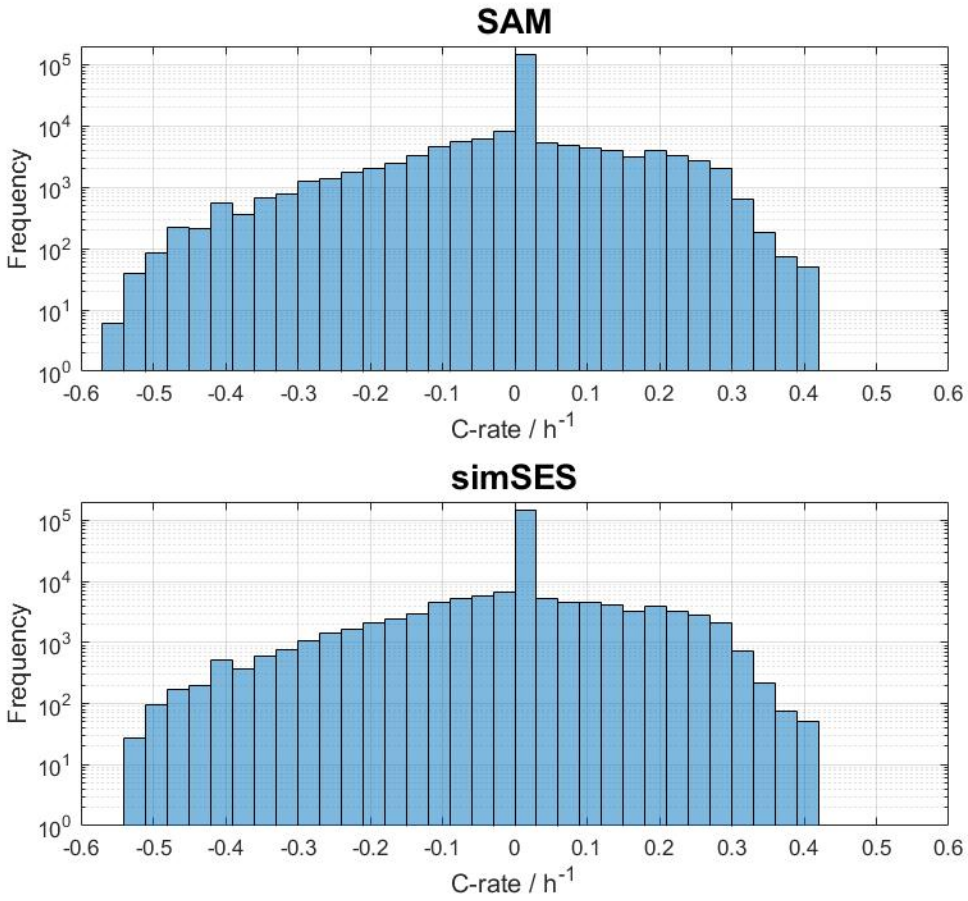

Figure 43. Frequency distribution of the different charge (positive) and discharge (negative) C-rates with no rate limit in SAM and simSES at Scenario 1.

4.1.4 Battery size

The battery size sensitivity was studied by testing batteries one third bigger and one third smaller than the design size. The result in SAM is shown in Figure 44. This plot shows very similar results for the three battery sizes, in favour of the smaller batteries. As discussed before, bigger batteries work in situations where a smaller battery would be either depleted or full, and thus cycle more. This way the bigger batteries can experience

a faster cycle degradation. However, is important to consider the error introduced by SAM's model once surpassed the lifetime curves ranges, as before that point the three sizes had a very close performance.

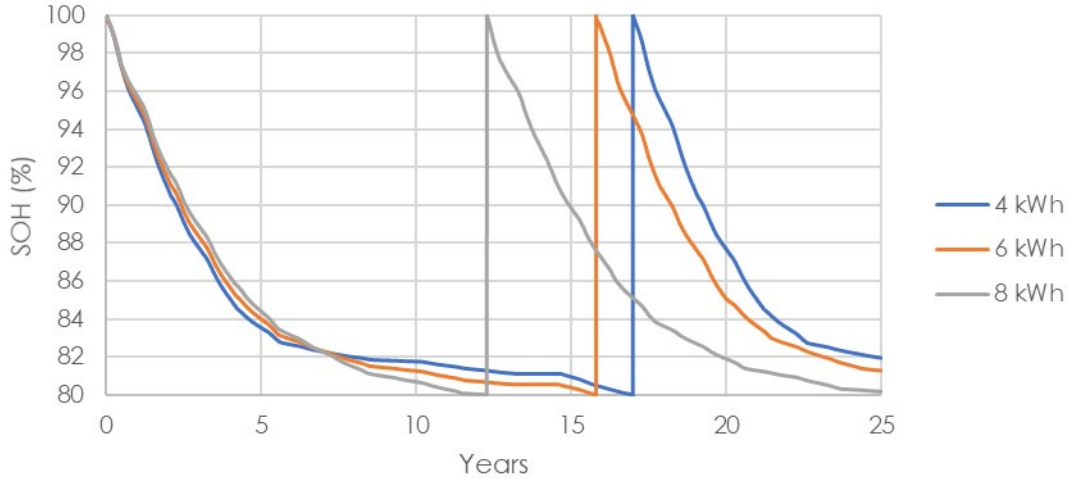

Figure 44. Evolution of the SOH in SAM for different battery sizes at Scenario 1.

In order to extend the lifetime instead of the performance, when increasing the battery size, it is necessary to keep constant the total usable capacity and modify the DOD ranges accordingly. In this way the original design 6 kWh battery, which cycled between 20-80% would have 60% of its capacity as usable (3.6 kWh). This 3.6kWh usable capacity represents 45% of the 8kWh battery and 90% of the 4kWh battery. Figure 45 shows the SOH evolution when cycling the 4kWh battery from 5% to 95%, the 6kWh battery with the original 20% to 80% and the 8kWh battery from 27.5% to 72.5%.

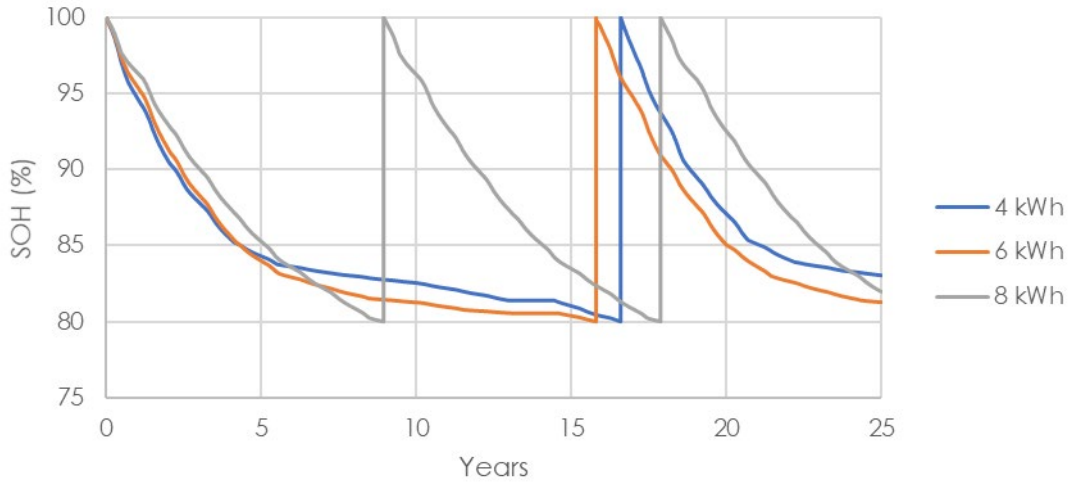

Figure 45. Evolution of the SOH in SAM for different battery sizes while keeping the same usable capacity at Scenario 1.

Once again, the cycle count surpassing the lifetime data range on the less favourable ranges makes them perform better than they should. Focusing on the four first years, the expected evolution with the increase of battery size improving the lifetime is observed.

On the other hand, in simSES the results are almost identical when operating with the same SOC range as shown in Figure 46. This might be due to calendar aging being the dominant degradation mechanism for most of the run. This way the change in cycling does not have an effect and the calendar aging is only slightly affected by the small changes in the SOC distribution.

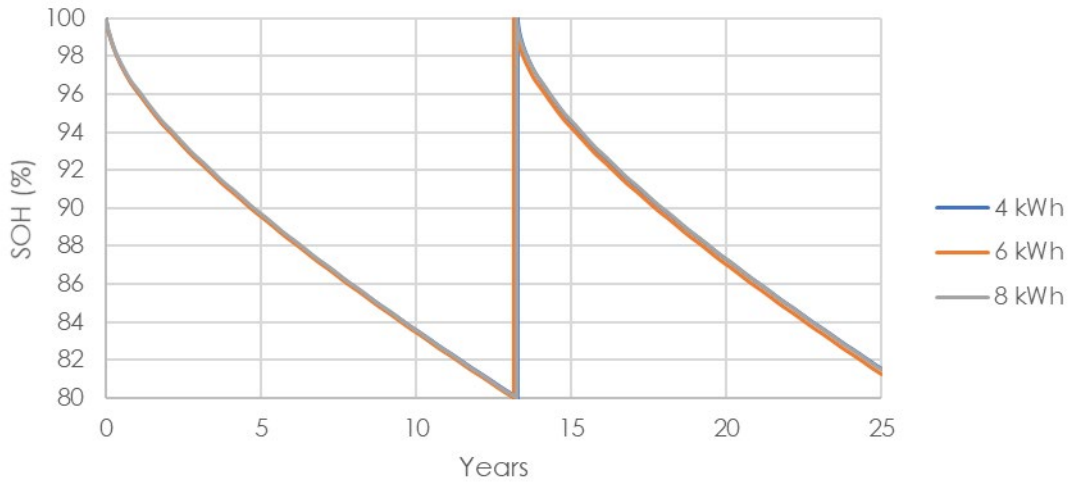

Figure 46. Evolution of the SOH in simSES for different battery sizes at Scenario 1.

Figure 47 shows the results when the SOC ranges are changed to keep the same usable capacity. It shows that now batteries of a greater size are seen to perform better than the smaller ones. As calendar aging is the dominant mechanism probably the reason is the smaller SOC limits. All batteries have the same usable capacity and cycle in the same way, but the higher SOC limit in bigger batteries is smaller. Presumably this effect would be more relevant in cycle dominated cases, as the maximum DOD would be smaller.

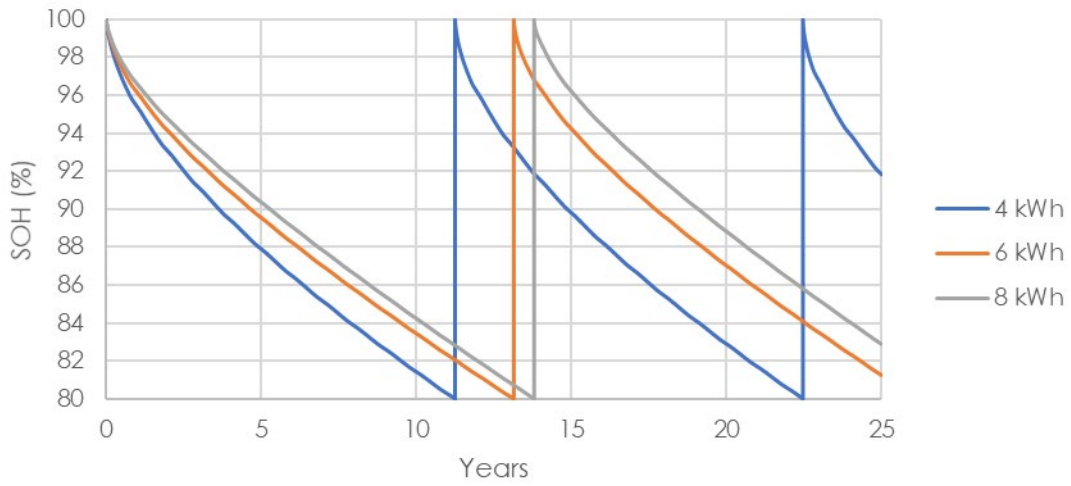

Figure 47. Evolution of the SOH in simSES for different battery sizes while keeping the same usable capacity at Scenario 1.

In the following scenarios only the battery capacity increases with constant usable capacity will be studied as it showed to be the most interesting case from a lifetime perspective. The study was done in simSES due to the limitations identified in SAM.

4.1.5 Dispatch method

This section studies the effect in the lifetime of the different dispatch methods available in each software. The three dispatch methods tested in SAM are shown in Figure 48.

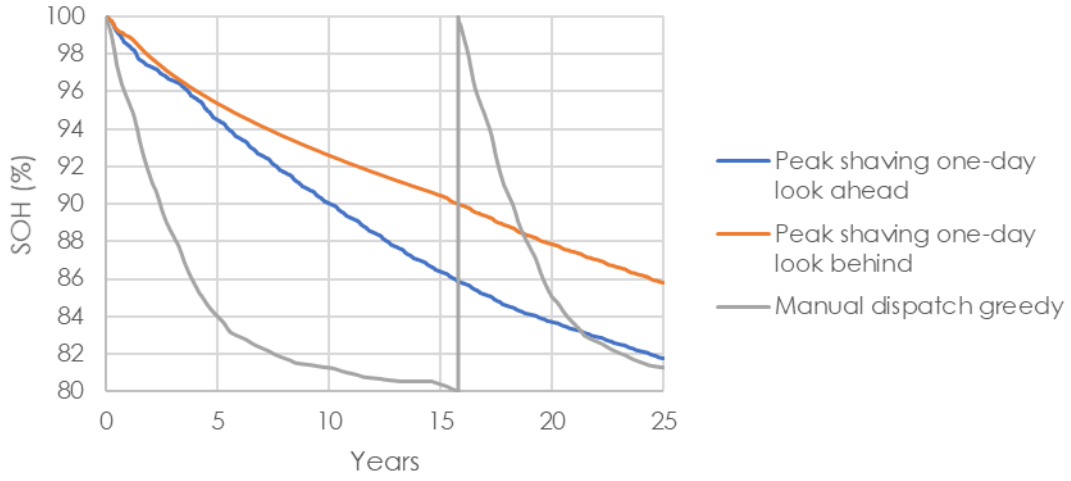

Figure 48. Evolution of the SOH in SAM under different dispatch methods at Scenario 1.

The "Manual dispatch greedy" suffered a stronger aging than the two "peak shaving" methods, especially during the first years, as it suffers the very high cycle aging due to the fault in cycle counting observed previously. "Peak shaving" methods showed very little operation of the battery, with the battery spending most of the time idle and thus suffered much less from cyclic aging. This way both dispatch methods do not even need

battery replacements in the period studied, although their operation of the battery was really inefficient. “Peak saving one-day look ahead” achieves a higher cycle of the battery than “Peak saving one-day look behind” as it has the perfect forecast for the following day, and thus suffers more from cycle aging.

Figure 49 shows the state of health evolution under different dispatch methods in simSES. The four of them exhibit very similar results, probably because the calendar aging is the dominating aging mechanism and dispatch models mostly affect cyclic aging. “Greedy” and “Maximize Self-Consumption” obtain the exact same result as the difference between them is PV curtailment, and neither in this scenario nor in any of the following ones put a limit on the PV output power.

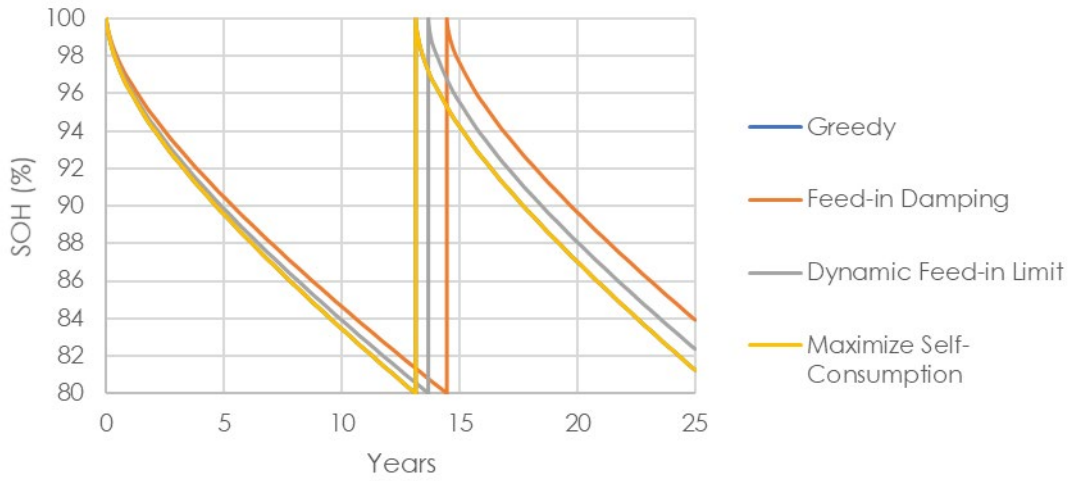

Figure 49. Evolution of the SOH in simSES under different dispatch methods at Scenario 1.

4.1.6 Chemistry

The next effect studied was the influence of the battery chemistry. Figure 50 shows the result for SAM. The LFP chemistry performs much better in terms of lifetime as the NMC needs to be replaced multiple times. This probably happens because the lifetime curve used to calculate NMC cyclic aging includes the same amount of data for each DOD and thus not experiences the slower aging observed with the LFP one. Observing the first five years of simulation, before this phenomenon takes place, it would seem that the evolution of both chemistries could be similar.

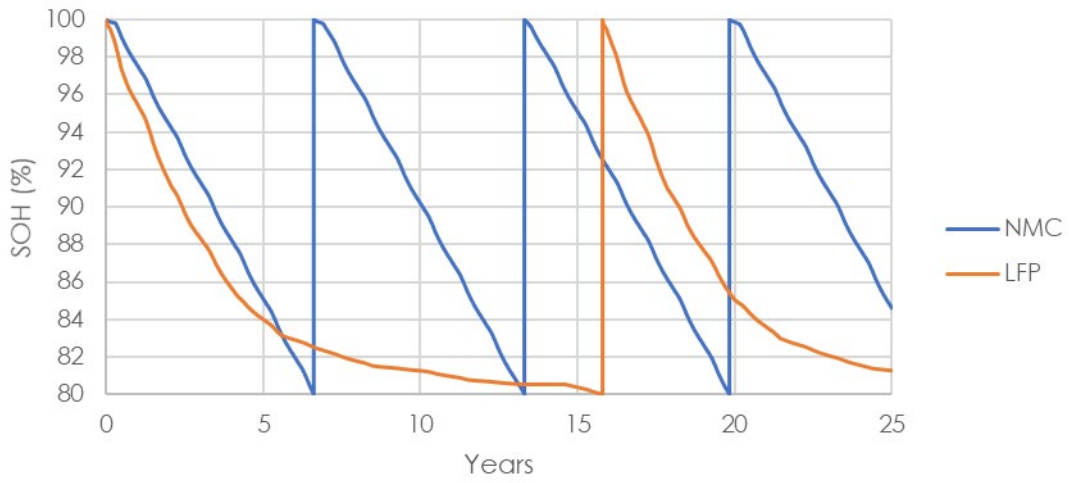

Figure 50. Evolution of the SOH in SAM for different battery chemistries at Scenario 1.

On the other hand, the result from simSES is shown in Figure 51. When comparing the results of the two chemistries it is important to remember that the NMC model is more limited as it is a much simpler model and does not consider calendar aging. In this case, the NMC battery performs much worse than the LFP one. Considering that it does not include calendar aging and the literature the NMC chemistry performs only slightly worse than the LFP one, this low life is unexpected and probably a consequence of the limitations identified for the NMC model in simSES.

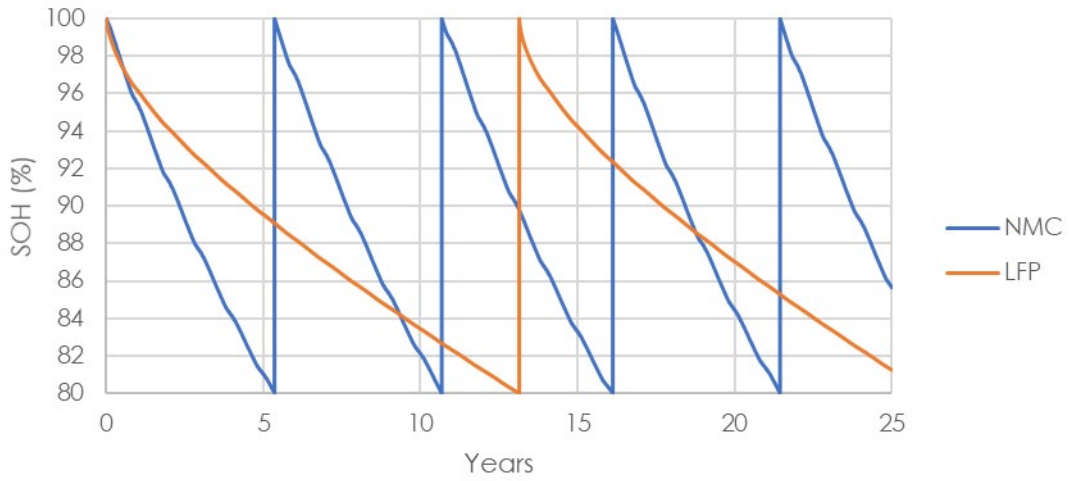

Figure 51. Evolution of the SOH in simSES for different battery chemistries at Scenario 1.

4.1.7 Temperature

Lastly, the lifespan of the battery at various ambient temperatures was studied. Figure 52 shows the SOH's evolution obtained in SAM. In SAM temperature only affects calendar aging. This way, calendar aging is eclipsed by the extreme cycling and is only dominant at high temperatures cases at beginning.

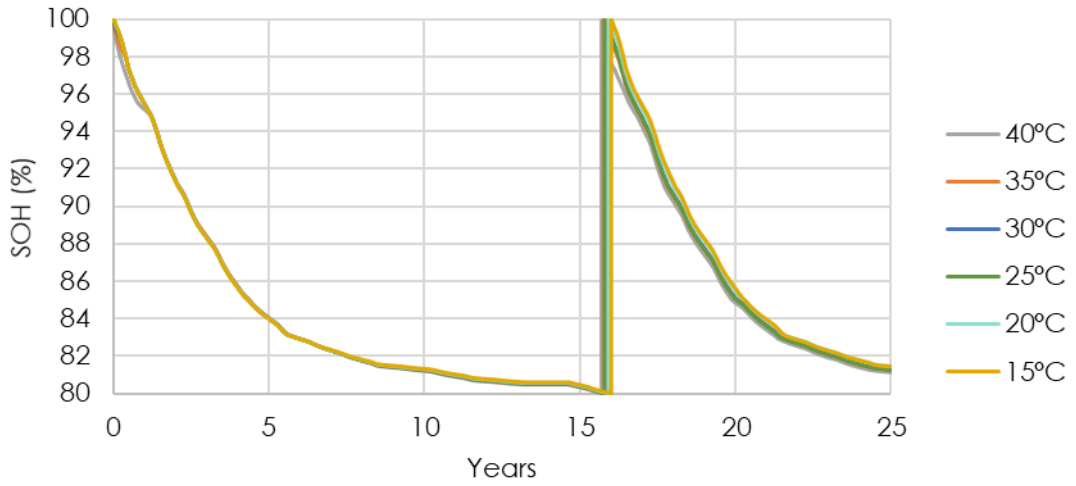

Figure 52. Evolution of the SOH in SAM at different ambient temperatures at Scenario 1.

On the other hand, the results from simSES are shown in Figure 53. Temperature shows a strong effect on the SOH evolution and as temperature increases the battery ages faster. This way high temperature cases like 40°C or 35°C need many battery replacements.

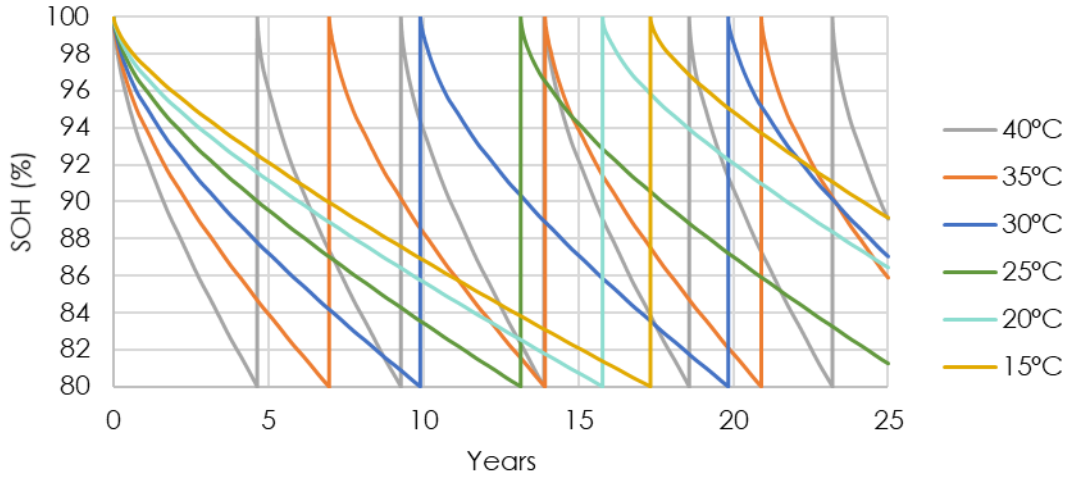

Figure 53. Evolution of the SOH in simSES at different ambient temperatures at Scenario 1.

4.2 Scenario 2: Family with both parents unemployed

As in the Scenario 2, the simulations in SAM and simSES were set up introducing the corresponding "family with both parents unemployed" consumption and generation profiles and adjusting the size of the battery. The same weeks as in the Scenario 1 are represented in Figure 54 and Figure 55.

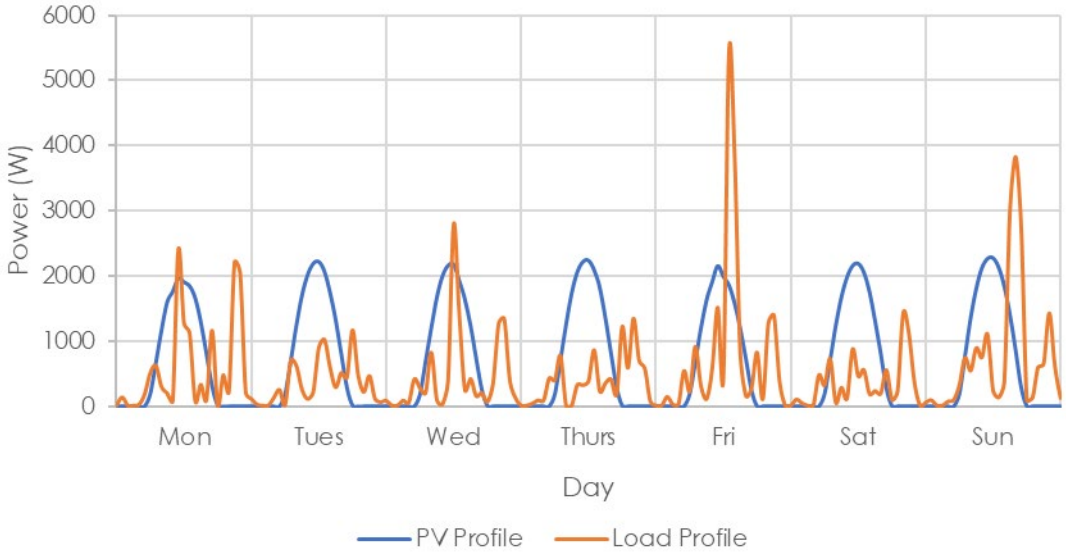

Figure 54. Consumption and generation profiles of Scenario 2 during a summer week.

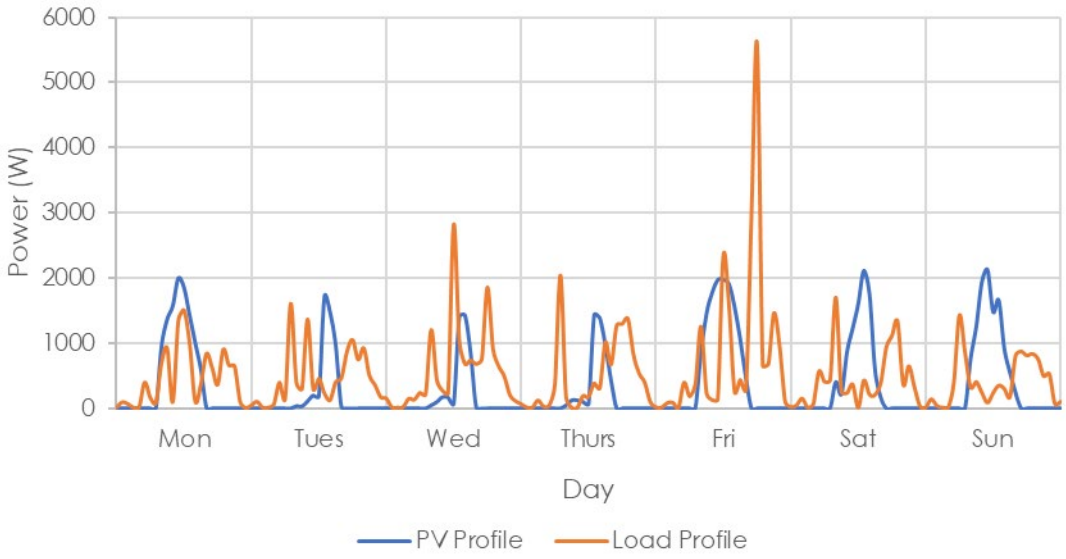

Figure 55. Consumption and generation profiles of Scenario 2 during a winter week.

Comparing these figures with Figure 28 and Figure 29 from Scenario 1 it is shown that in the unemployed scenario the demand is more distributed throughout the day, with a greater consumption during the hours that have PV production. It also no longer shows a marked difference between the weekdays and the weekend, as now the parents are unemployed.

4.2.1 Reference parameters

The summary of the simulations performed using both SAM and simSES is presented in Table 12. As for scenario 1, both models obtain similar values for cycle, average SOC and average DOD, while the counting algorithm obtains a very high cycle number.

Table 12. Summary of Scenario 2 with reference parameters

	SAM	simSES
Total Cycles (Counting algorithm)	5203 (14861)	5246
Average Cycles/day	0.59	0.60
Average DOD	35.01%	39.07%
Average SOC	39.81%	38.79%
Battery replacements	1 (18^{th} year)	1 (14^{th} year)
SOH Calendar Aging	95.51%	84.08%
SOH Cycling Aging	82.28%	86.85%
Total SOH	82.28%	81.37%

The SOC evolution for the summer and winter week is shown in Figure 56 and Figure 57. When compared with the equivalent Figure 30 and Figure 31 from Scenario 1 it is observed that now due to the most common consumption during the central hours of the day the battery is even used while there is PV production, when the consumption in the profiles (shown Figure 54 and Figure 55) surpasses the generation. The figures also show that the battery is not fully charged during the day more often, especially during winter, as a greater share of the PV production is being directly consumed.

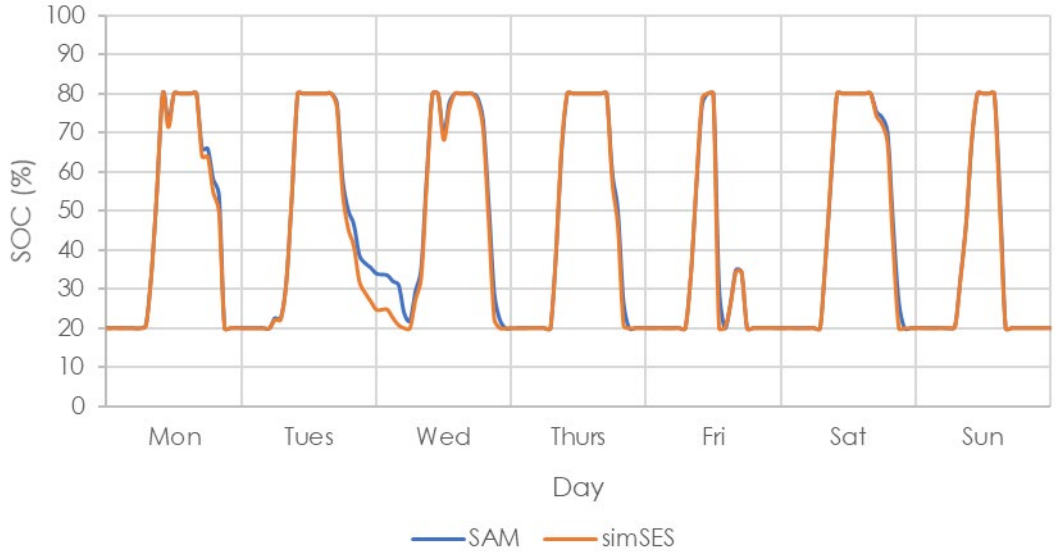

Figure 56. SOC in SAM and simSES at Scenario 2 during a summer week using the reference parameters.

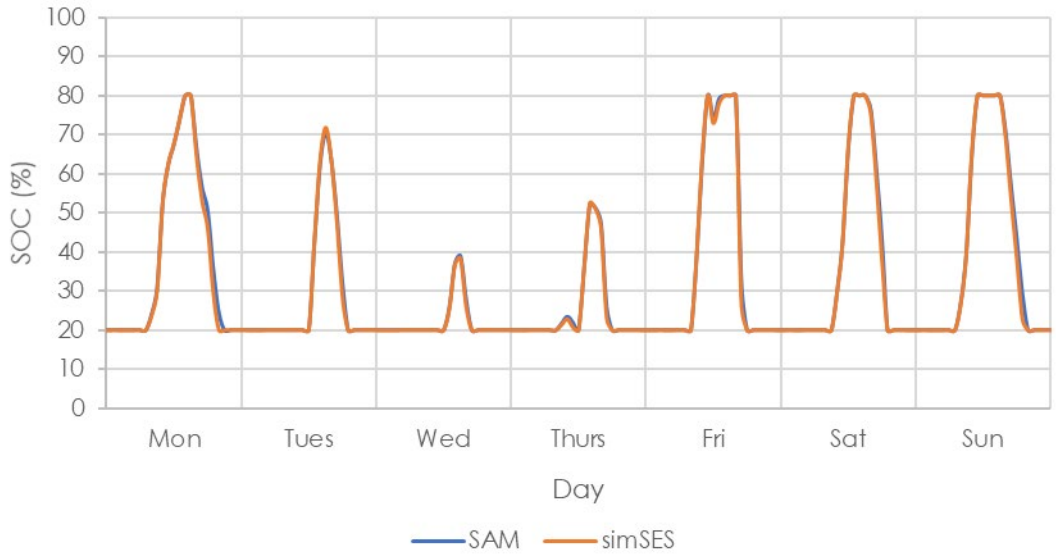

Figure 57. SOC in SAM and simSES at Scenario 2 during a winter week using the reference parameters.

On the other hand, the difference in aging is similar to the previous scenario. Figure 58 shows the evolution of the SOH obtained from the two models. This evolution is very close to the corresponding Figure 32 from Scenario 1. The aging comparison between scenarios will be discussed in more depth in the last sub-section.

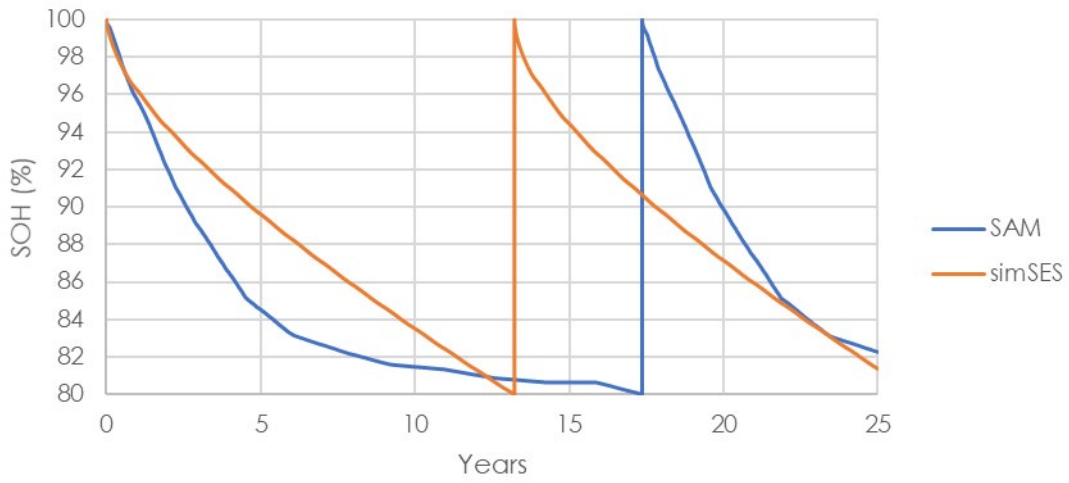

Figure 58. Evolution of the SOH in SAM and simSES at Scenario 2 using the reference parameters.

The calendar and cycling aging of both models is analysed in more detail in Figure 59 and Figure 60. Figure 59 shows that in SAM the cycle aging is the dominant mechanism. Comparing with the Figure 33 from Scenario 1, the evolution is very similar as the same very high cycling happens.

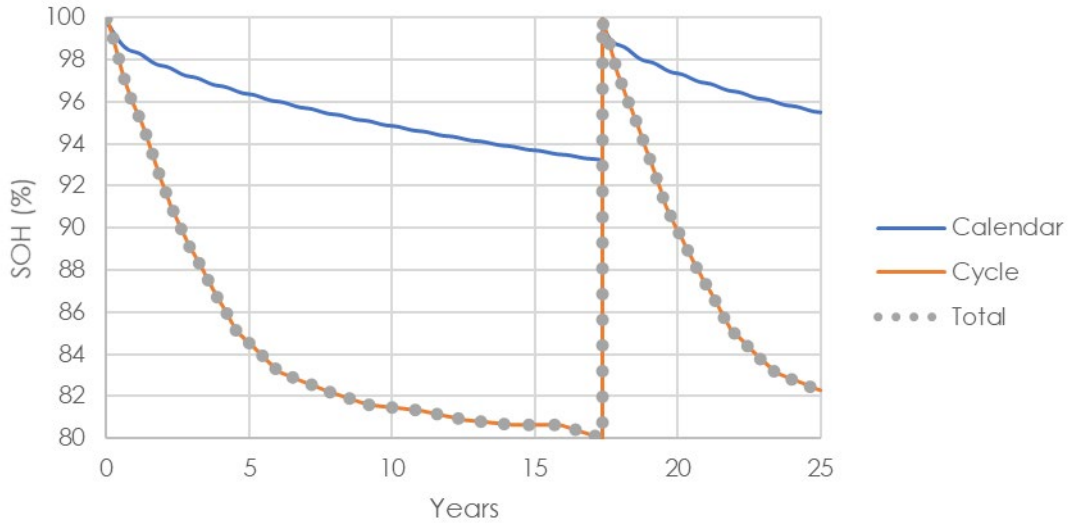

Figure 59. Calendar and cycling aging in SAM at Scenario 2 using the reference parameters.

On the other hand, in Figure 60 the same effects as in scenario 1 is observed, with the SOH evolution being very similar to the one of Figure 34.

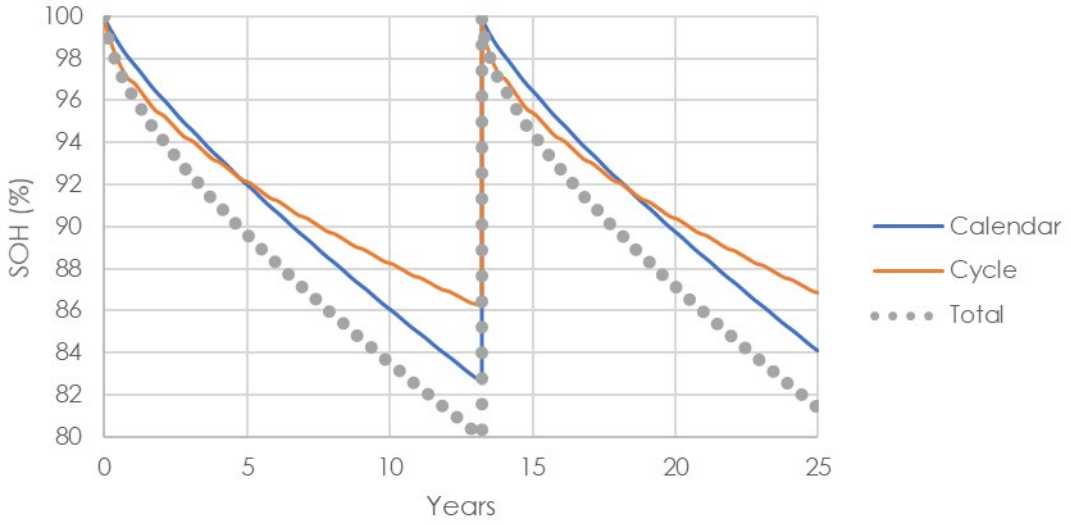

Figure 60. Calendar and cycling aging in simSES at Scenario 2 using the reference parameters.

The histogram of Figure 61 shows the frequency of each SOC. The same behaviour than for scenario 1 is observed, with the histogram being very similar to Figure 35.

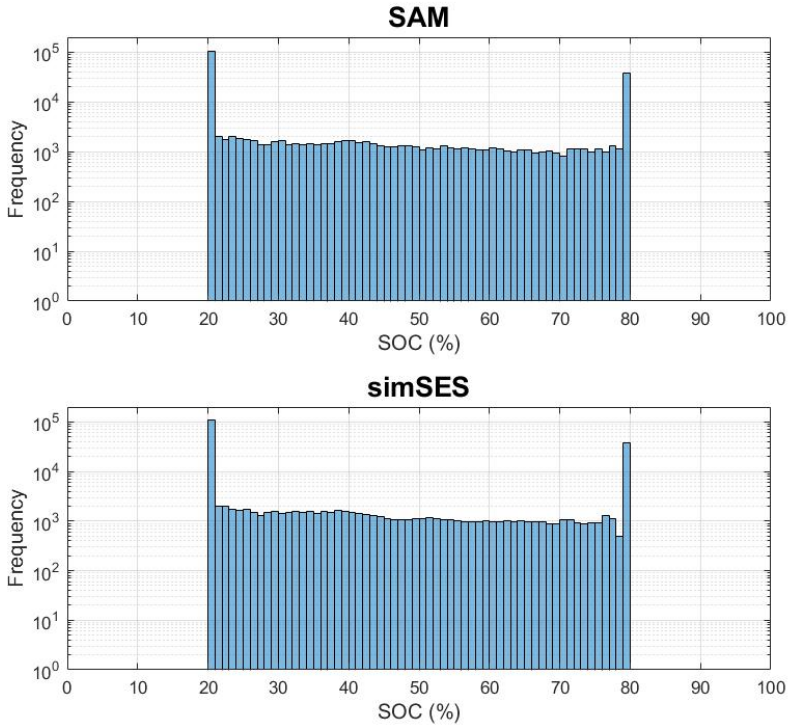

Figure 61. Frequency distribution of the different SOCs in SAM and simSES at Scenario 2 using the reference parameters.

On the other hand, Figure 62 shows the histogram of the different DOD. As with the SOC, the behaviour is very similar to the one obtained in scenario 1, being this plot very similar to Figure 36.

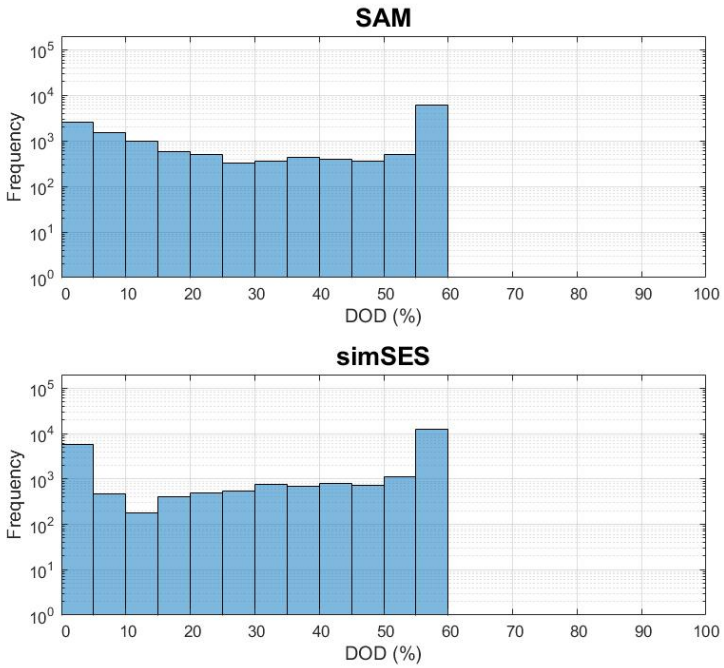

Figure 62. Frequency distribution of the different DODs in SAM and simSES at Scenario 2 using the reference parameters.

4.2.2 SOC Range

The influence of different SOC ranges was studied in Polysun, SAM and simSES.

The expected lifetime for each SOC limits is in Polysun is represented in Figure 63. The plot depicts the same tendency of smaller SOC ranges having better lifetime predictions, although the performance is better than for Scenario 1. This is probably a consequence of the profiles having a smaller mismatch in this case, which leads to more direct consumption and less cycling of the battery. In this case, all SOC ranges of 40% or less have the maximum 20 years calendar prediction.

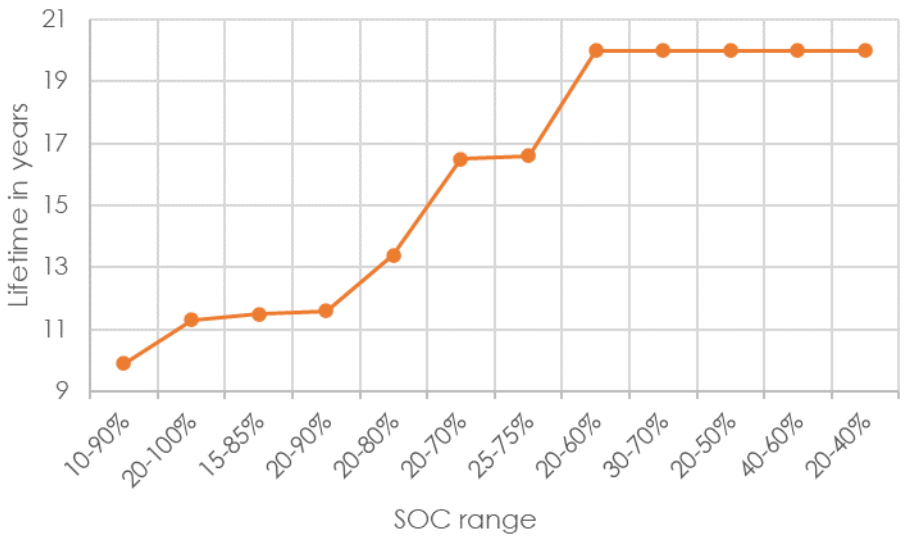

Figure 63. Expected lifetime in Polysun for different SOC ranges at Scenario 2.

The SOH evolution in SAM is represented in Figure 64. This figure is very similar to the corresponding Figure 39 from Scenario 1. As observed in Polysun, the aging is slightly less as in this case as the battery cycles less, although the difference is small.

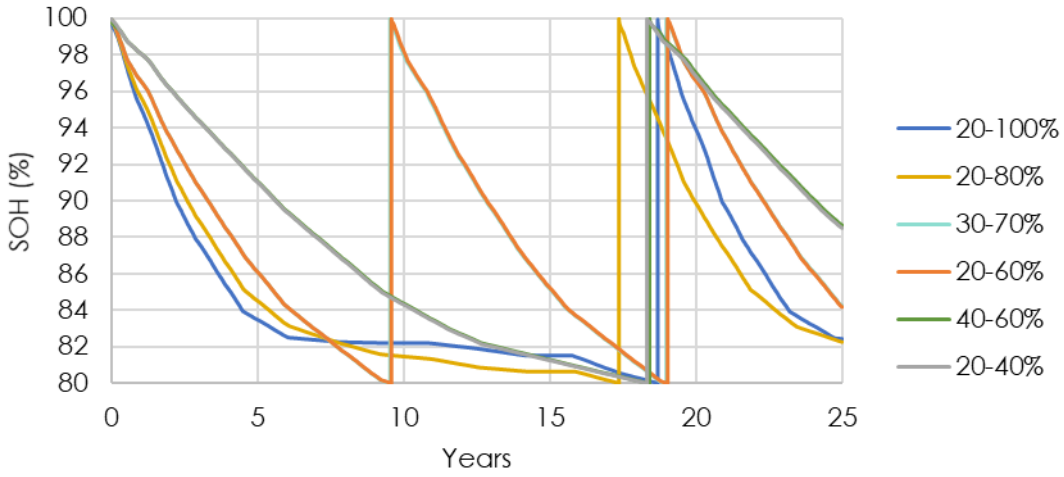

Figure 64. Evolution of the SOH in SAM for different SOC ranges at Scenario 2.

Similarly, simsSES' result shown in Figure 65 is almost the same as Figure 40. This happens because calendar aging dominates in all the ranges and in Figure 61 it was shown that the SOC distribution of Scenario 2 was very similar to the one of Scenario 1. This way, having the same SOC, ambient temperature and elapsed time than Scenario 1 the predicted calendar aging is the same.

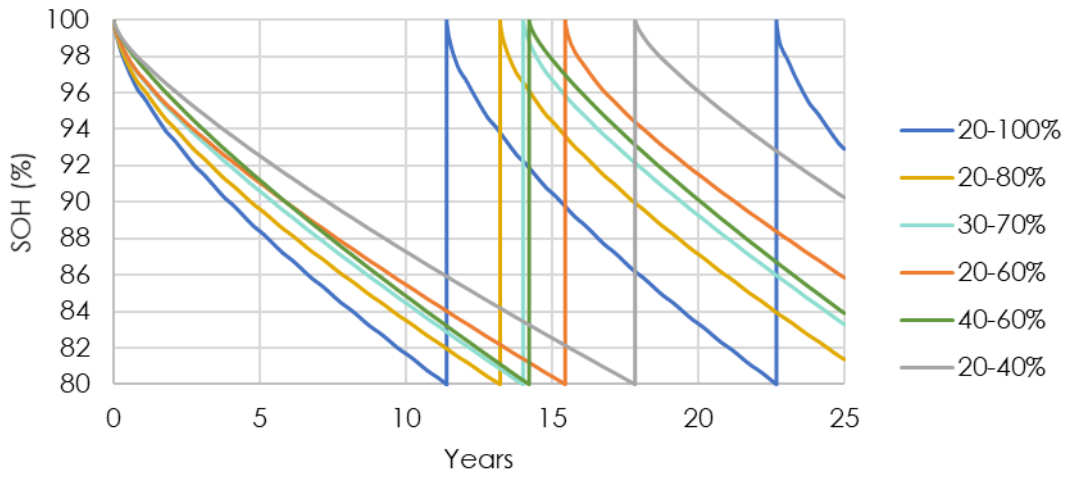

Figure 65. Evolution of the SOH in simSES for different SOC ranges at Scenario 2.

4.2.3 Charge and discharge rate

The influence of the charge/discharge rates depicted in Figure 66 shows the same behaviour than Figure 42 from Scenario 1.

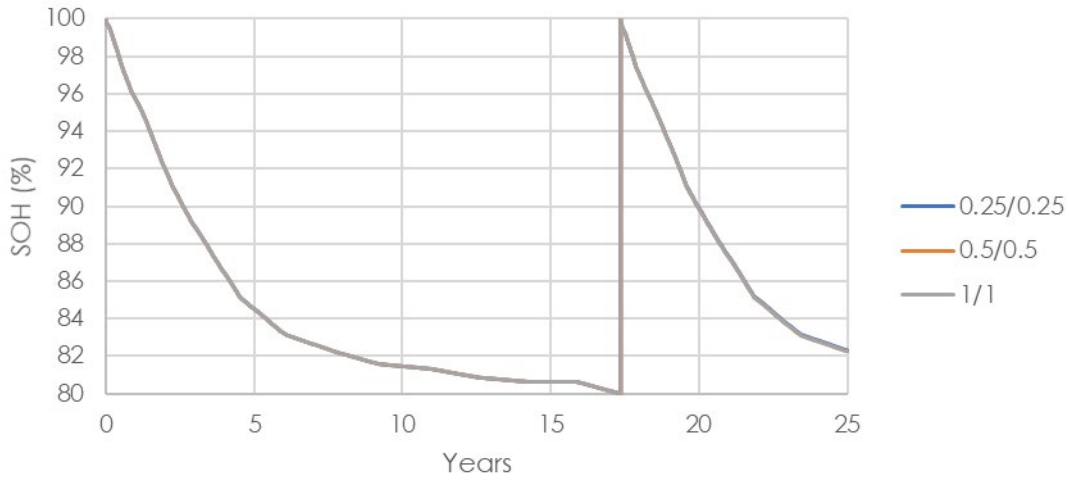

Figure 66. Evolution of the SOH in SAM for various C-rate limits at Scenario 2.

The histogram in Figure 67 shows the distribution of C-rates in SAM and simSES when there is no rate limit. This Figure is also similar to Figure 43 from Scenario 1.

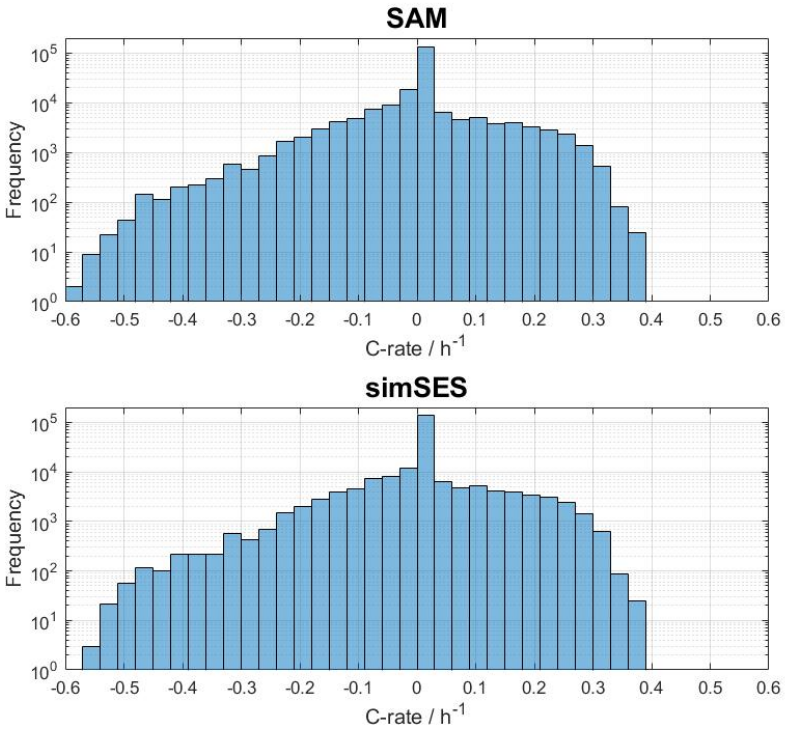

Figure 67. Frequency distribution of the different charge (positive) and discharge (negative) C-rates with no rate limit in SAM and simSES at Scenario 2.

4.2.4 Battery size

The effect of the battery size was studied keeping the same 3.6kWh usable capacity as explained for the previous scenario. The resulting plot represented in Figure 68 is very similar to Figure 47 previously obtained for Scenario 1.

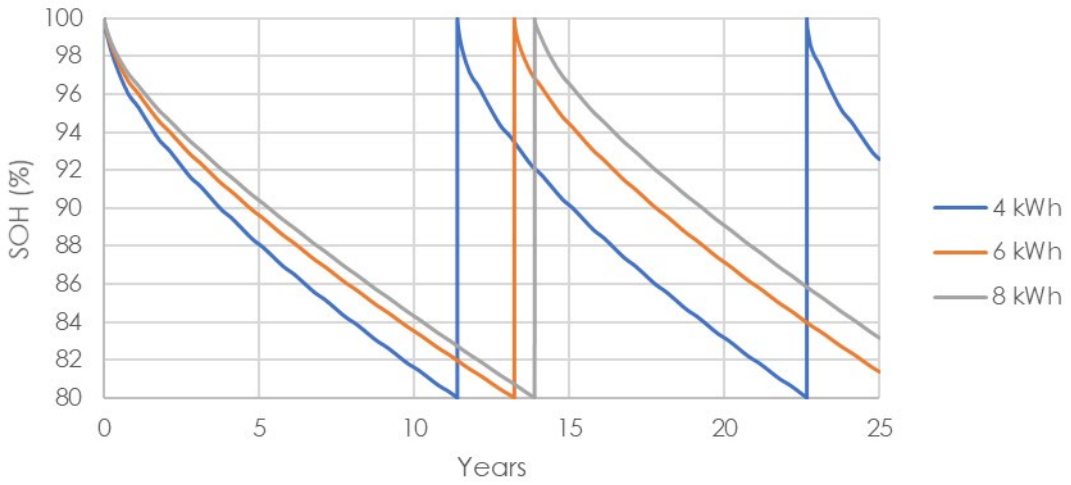

Figure 68. Evolution of the SOH in simSES for different battery sizes while keeping the same usable capacity at Scenario 2.

4.2.5 Dispatch method

The three studied dispatch methods studied in SAM are shown in Figure 69 showing a very similar behaviour to Figure 48 from Scenario 1.

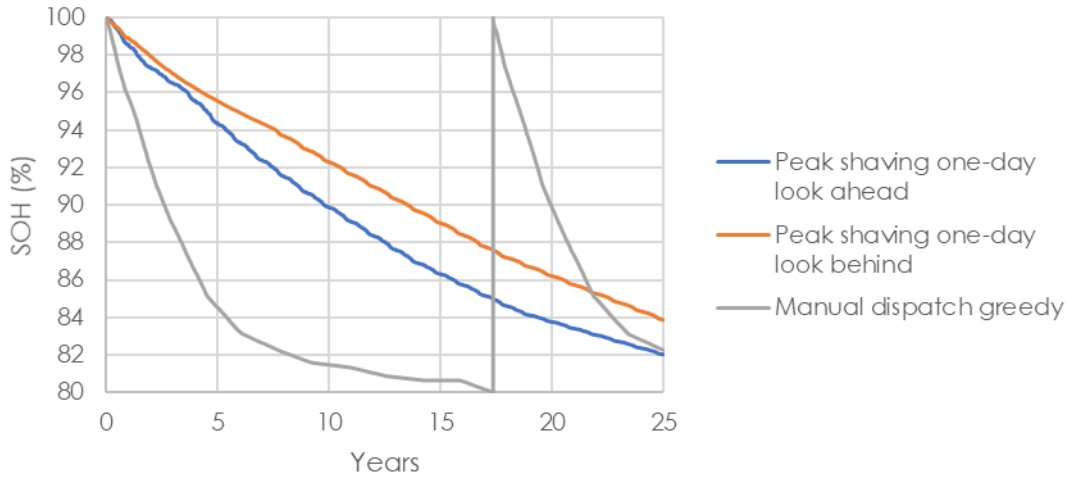

Figure 69. Evolution of the SOH in SAM under different dispatch methods at Scenario 2.

On the other hand, Figure 70 shows the state of health evolution under different dispatch methods in simSES. The result is very close to the previous Figure 49, again because of calendar aging being the dominant degradation mechanism.

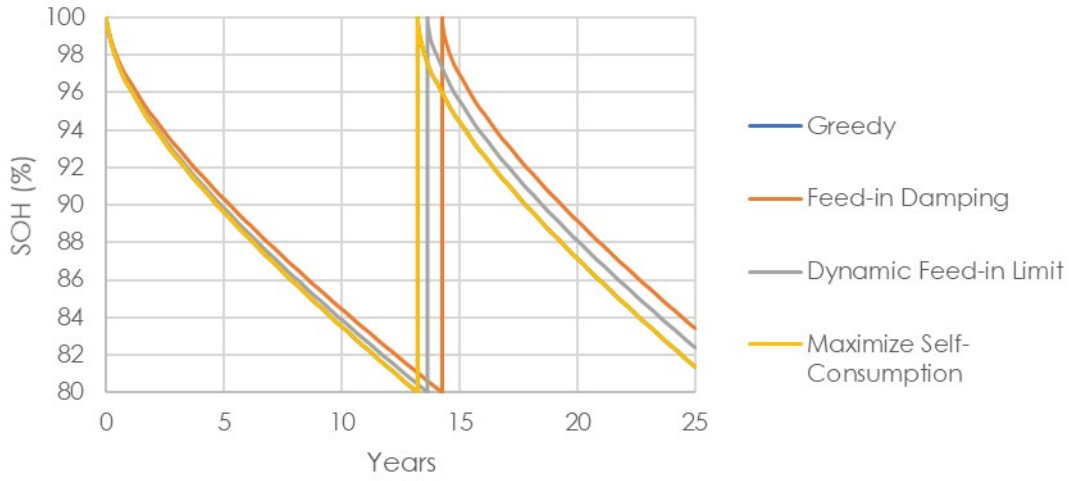

Figure 70. Evolution of the SOH in simSES under different dispatch methods at Scenario 2.

4.2.6 Chemistry

The next effect studied was the influence of the chemistry. Figure 71 shows the result for SAM. The resulting plot is similar to Figure 50 from the previous scenario, with both chemistries showing lightly less aging due to the smaller cycling in this scenario. As before the LFP chemistry experiences a great deceleration in aging because of its lifetime curve and the actual lifetime will probably be considerably shorter.

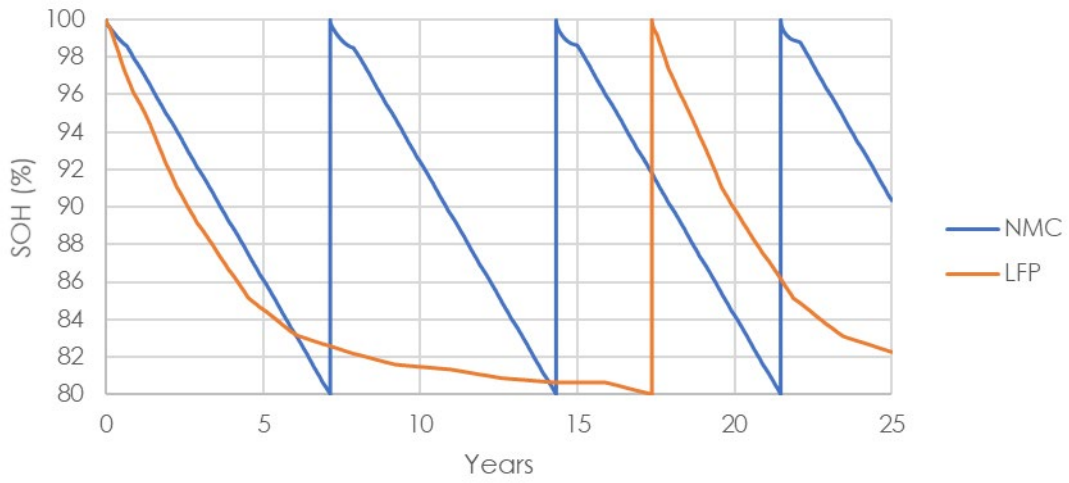

Figure 71. Evolution of the SOH in SAM for different battery chemistries at Scenario 2.

On the other hand, the result from simSES is shown in Figure 72. This figure is very similar to Figure 51 from Scenario 1.

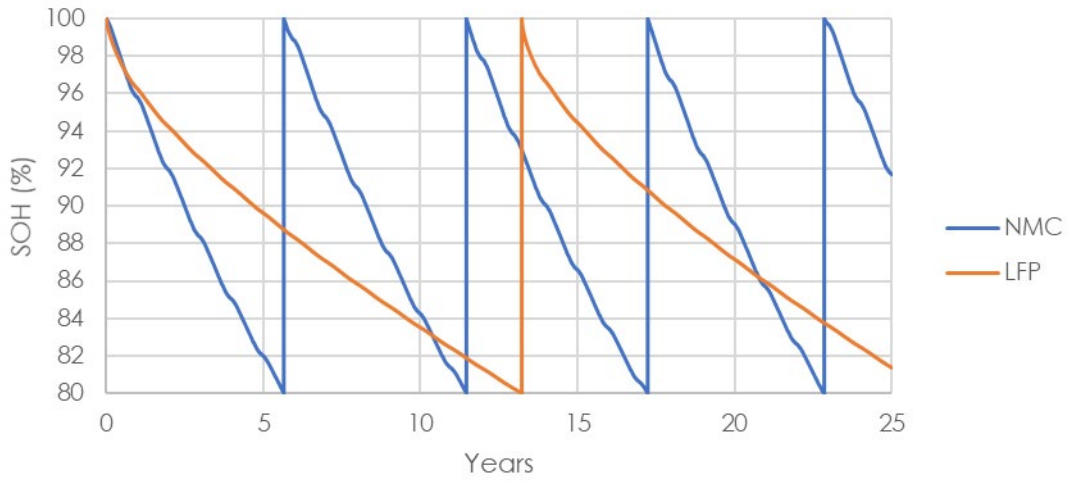

Figure 72. Evolution of the SOH in simSES for different battery chemistries at Scenario 2.

4.2.7 Temperature

Lastly, the SOH evolution of the battery at various ambient temperatures for SAM is represented in Figure 73. Once again, the same behaviour as in Scenario 1 in Figure 52 is observed with a slightly slower aging because of the lower cycle count.

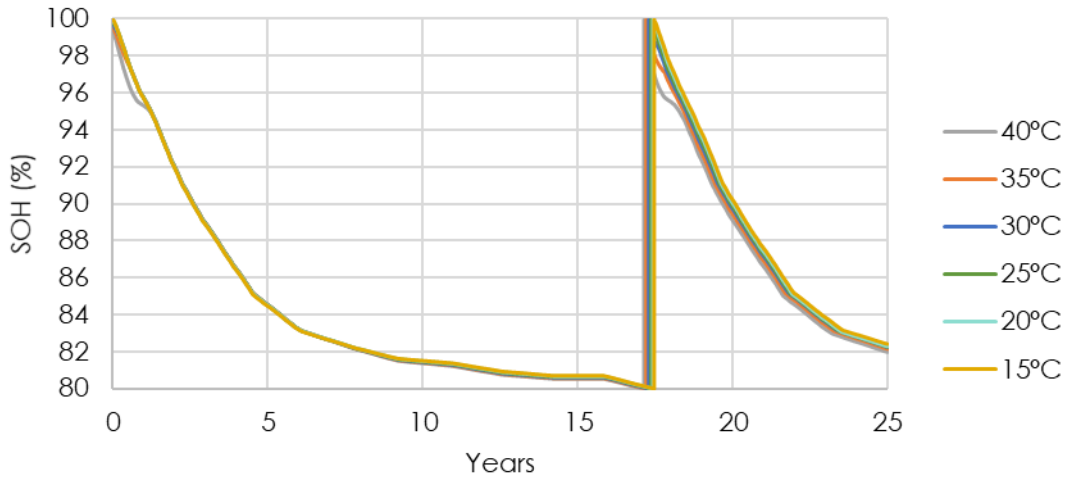

Figure 73. Evolution of the SOH in SAM at different ambient temperatures at Scenario 2.

On the other hand, the results from simSES are shown in Figure 74. The same trends as for Figure 53 is observed with temperature accelerating the SOH loss.

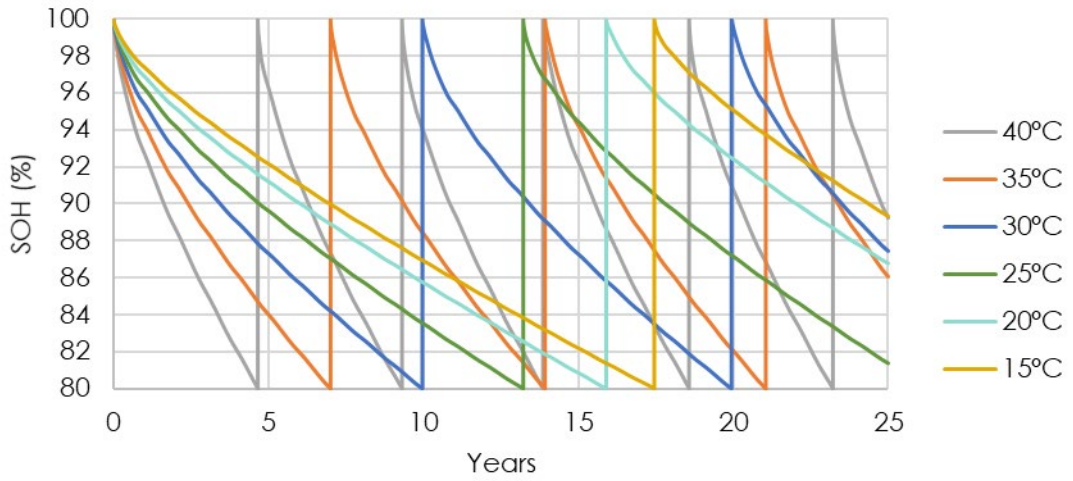

Figure 74. Evolution of the SOH in simSES at different ambient temperatures at Scenario 2.

4.3 Scenario 3: One person working

As with the previous scenarios, the profiles in the same summer and winter weeks are represented in Figure 75 and Figure 76

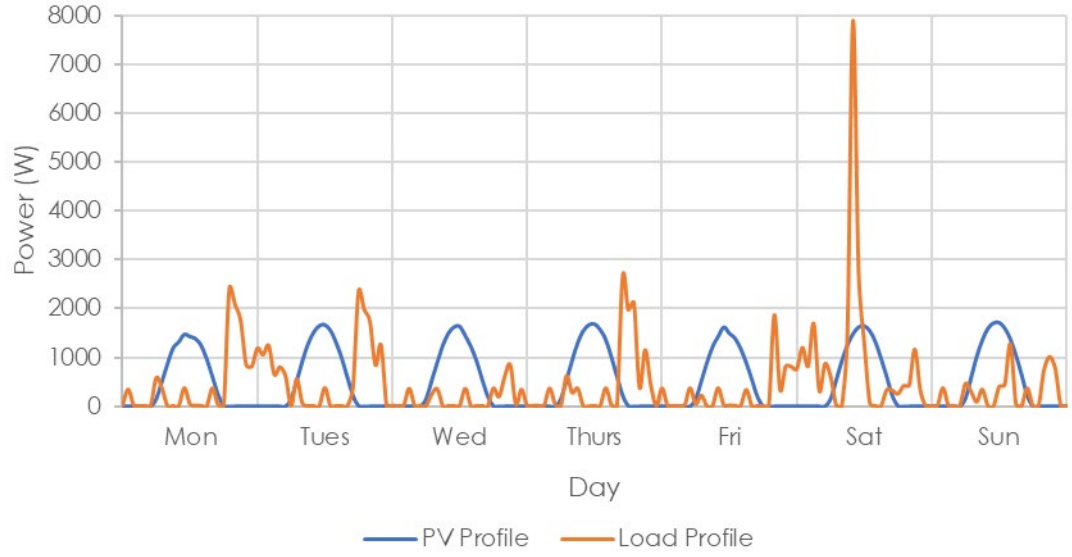

Figure 75. Consumption and generation profiles of Scenario 3 during a summer week.

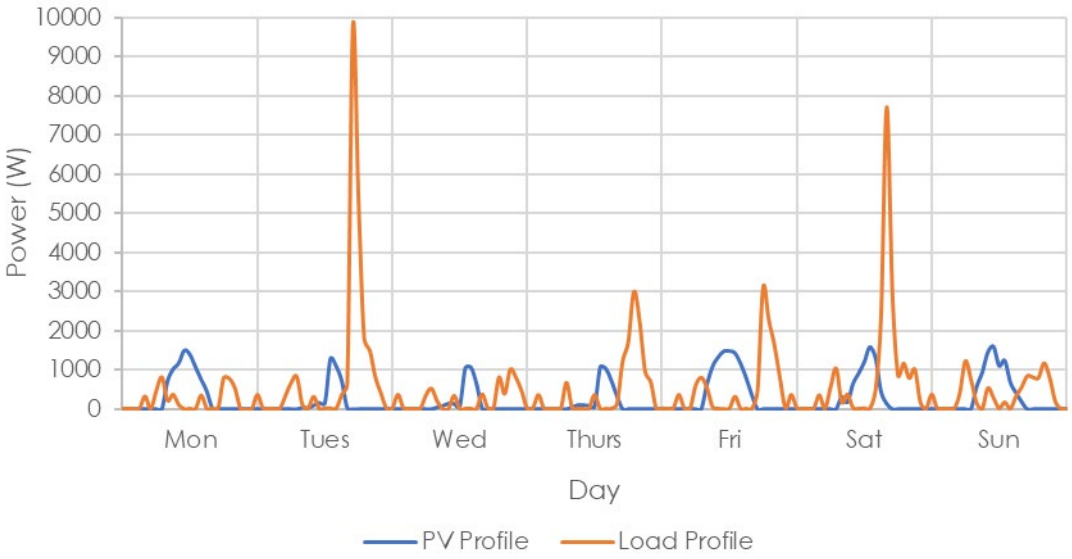

Figure 76. Consumption and generation profiles of Scenario 3 during a winter week.

Comparing these figures with Figure 28 and Figure 29 from Scenario 1 and Figure 54 and Figure 55 from Scenario 2 it is shown that in the one-person scenarios there are less demand spikes, as there is only one person consuming. This leads to a slightly bigger mismatch between the profiles. Also, the profiles show a difference between the weekdays and the weekends, similarly to Scenario 1, as it is also working scenario, being the demand during the central hours of the weekdays low and the consumption greater at the evenings and early in the morning. The PV system size for the one-person scenarios was 2.25 kWp and thus they show a lower generation.

4.3.1 Reference parameters

The summary of the simulations performed using both SAM and simSES is presented in Table 13. As for the previous scenarios, both models obtain similar values for cycle, average SOC and average DOD, while the counting algorithm obtains a very high cycle number.

Table 13. Summary of Scenario 3 with reference parameters

	SAM	simSES
Total Cycles (Counting algorithm)	5547 (12838)	5546
Average Cycles/day	0.61	0.61
Average DOD	43.20%	42.89%
Average SOC	42.81%	42.16%
Battery replacements	1 (22nd year)	1 (13th year)
SOH Calendar Aging	96.77%	83.04%
SOH Cycling Aging	83.34%	85.55%
Total SOH	83.34%	80.35%

The SOC evolution for the summer and winter week is shown in Figure 77 and Figure 78. When compared with the Scenario 1 (Figure 30 and Figure 31) and Scenario 2 (Figure 56 and Figure 57) it is observed that its behaviour is quite similar to the working scenario, with the battery being charged without interruption in summer's weekdays and with more interference during the winter.

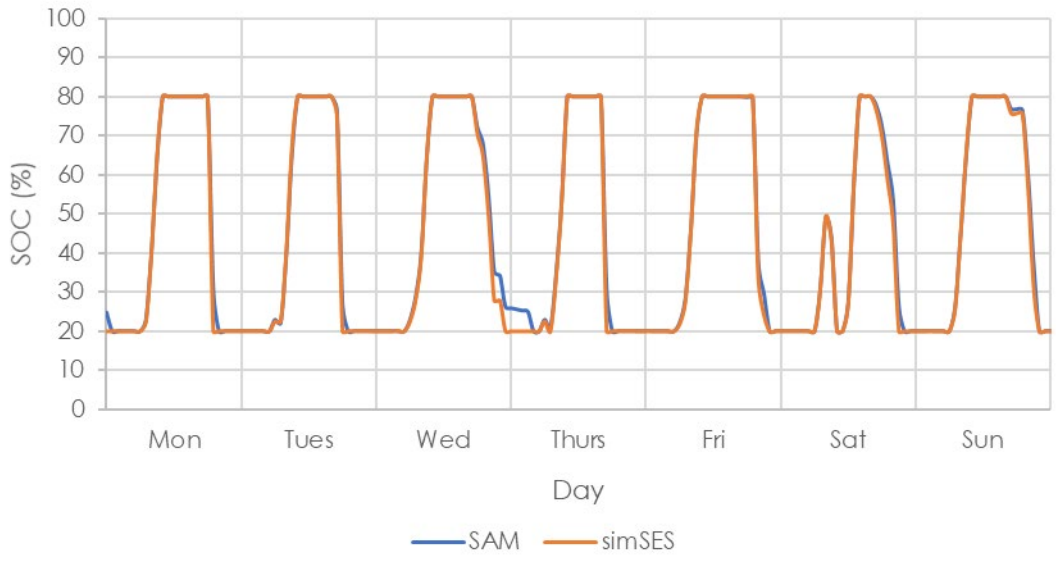

Figure 77. SOC in SAM and simSES at Scenario 3 during a summer week using the reference parameters.

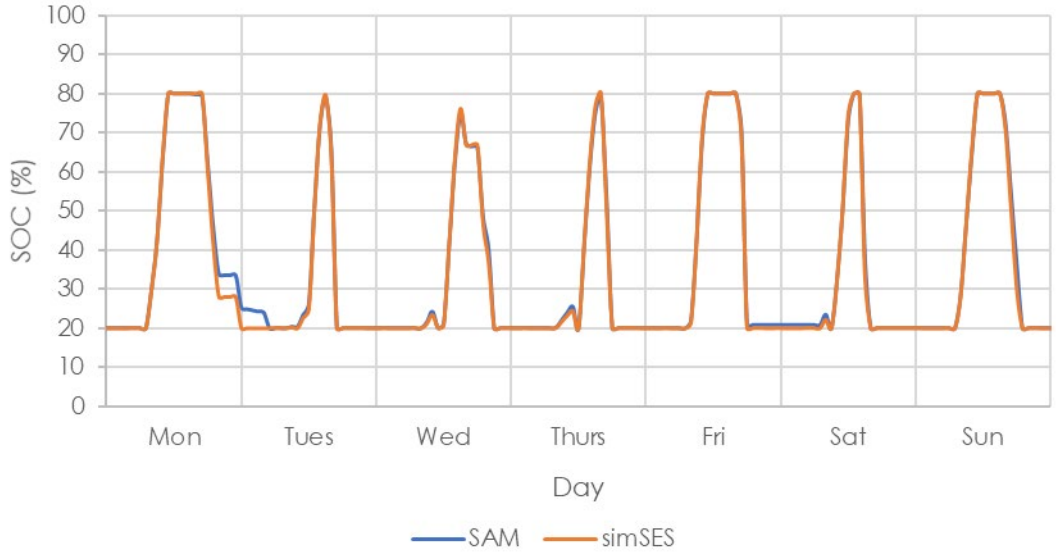

Figure 78. SOC in SAM and simSES at Scenario 3 during a winter week using the reference parameters.

Figure 79 shows the modelled SOH evolution in each software. As in previous cases simSES predicts a faster aging. However, cycle aging is predicted outside of the lifetime curves as has happened in previous occasions and is probably leading to a much slower aging than it should.

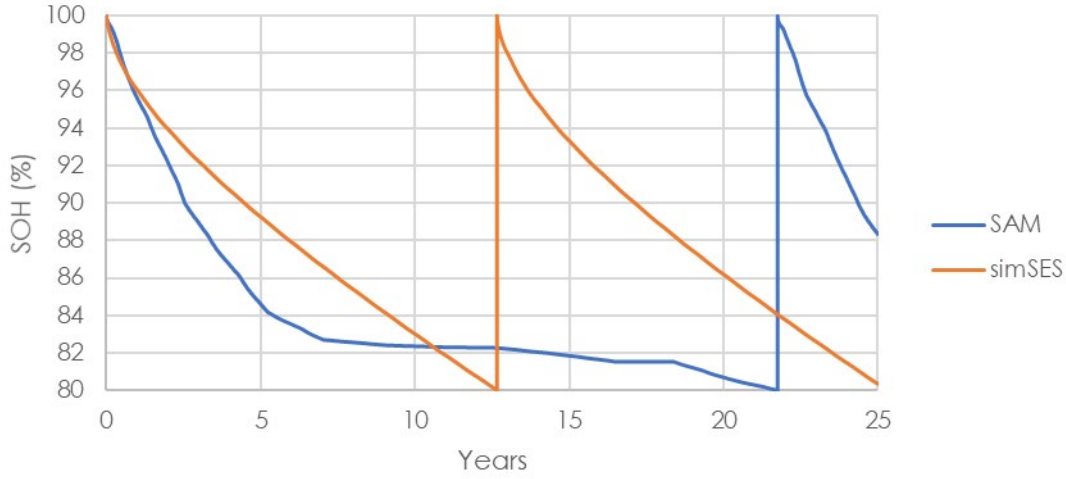

Figure 79. Evolution of the SOH in SAM and simSES at Scenario 3 using the reference parameters.

Studying the aging mechanism in SAM in Figure 80 it shows a similar evolution than in the Scenarios 1 and 2 (Figure 33 and Figure 59). However now the aging is slower as the number of computed cycles by the counting algorithm shown in Table 13 is smaller.

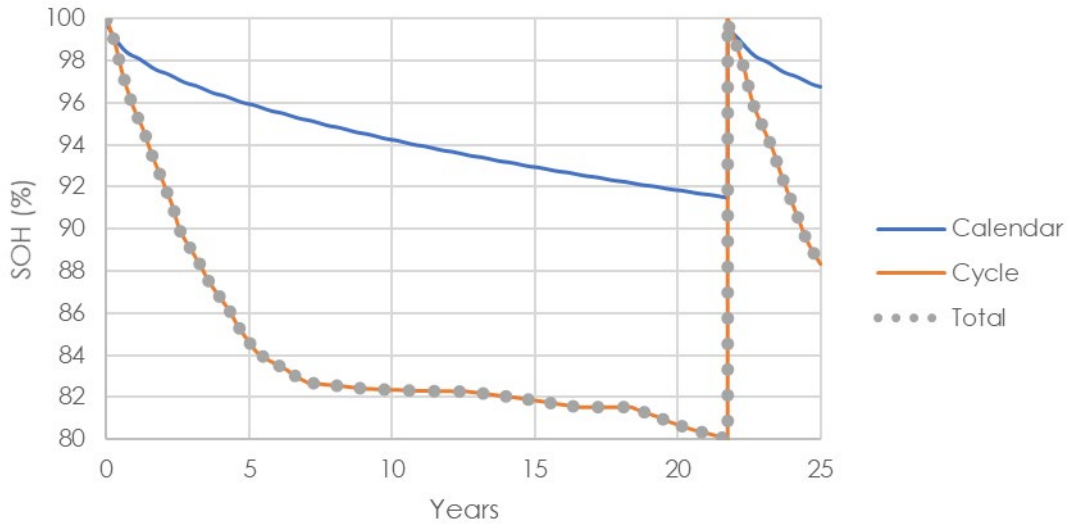

Figure 80. Calendar and cycling aging in SAM at Scenario 3 using the reference parameters.

In simSES calendar aging is the dominating aging mechanism as in as depicted in Figure 81 like in the previous scenarios (Figure 34 and Figure 60). However, the aging happens faster as the average SOC shown in Table 13 is higher.

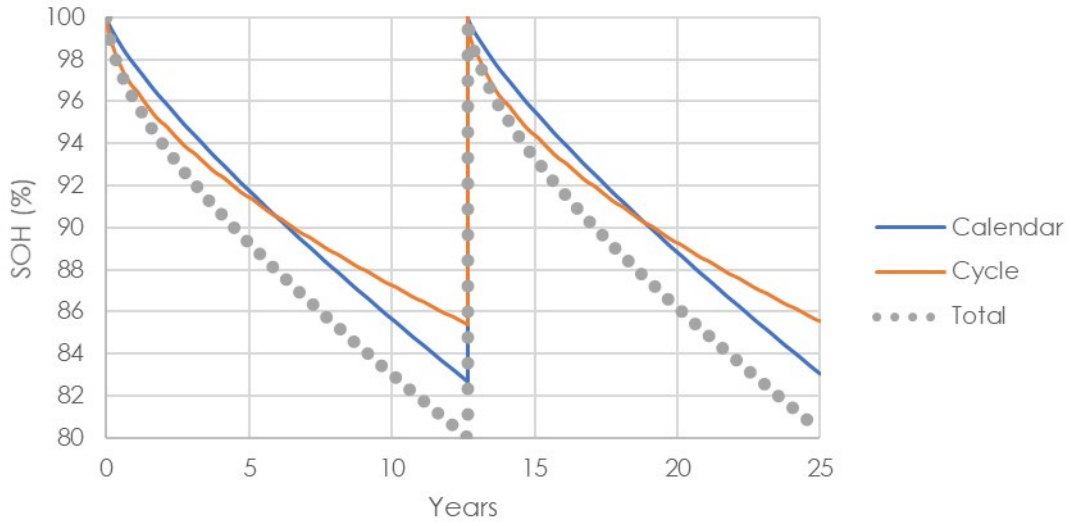

Figure 81. Calendar and cycling aging in simSES at Scenario 3 using the reference parameters.

The SOC and DOD distributions can help to understand how the role of the battery has changed for one person. The histogram of Figure 82 shows that the general shape of the SOC distribution is the same as in the family scenarios in Figure 35 and Figure 61, but the frequency of high SOC has slightly increased.

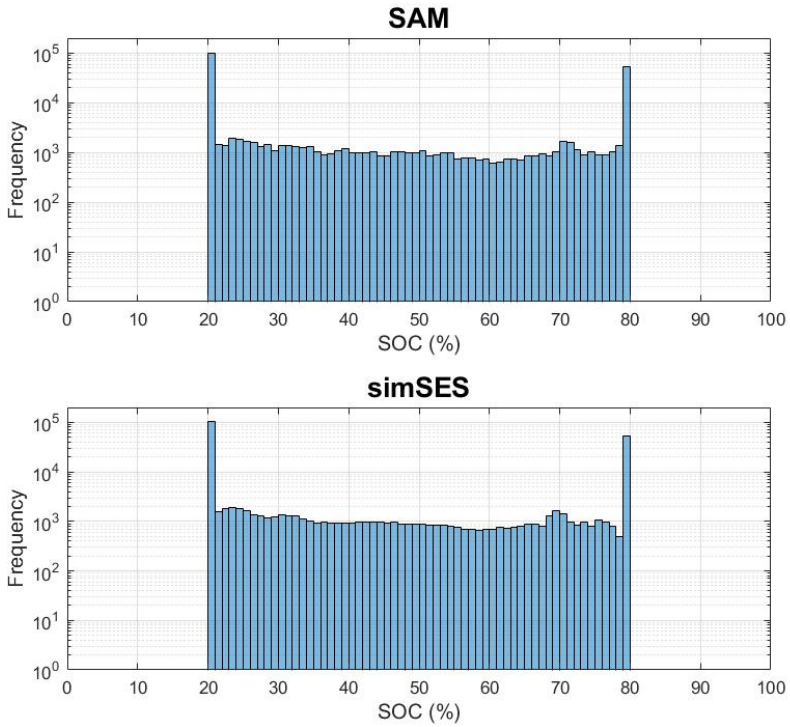

Figure 82. Frequency distribution of the different SOCs in SAM and simSES at Scenario 3 using the reference parameters.

On the other hand, Figure 83 shows that now bigger DODs are slightly more frequent than in the family scenarios displayed in Figure 36 and Figure 62, which might be a consequence of the bigger mismatch of the demand of one person with the PV generation, making full discharges more likely.

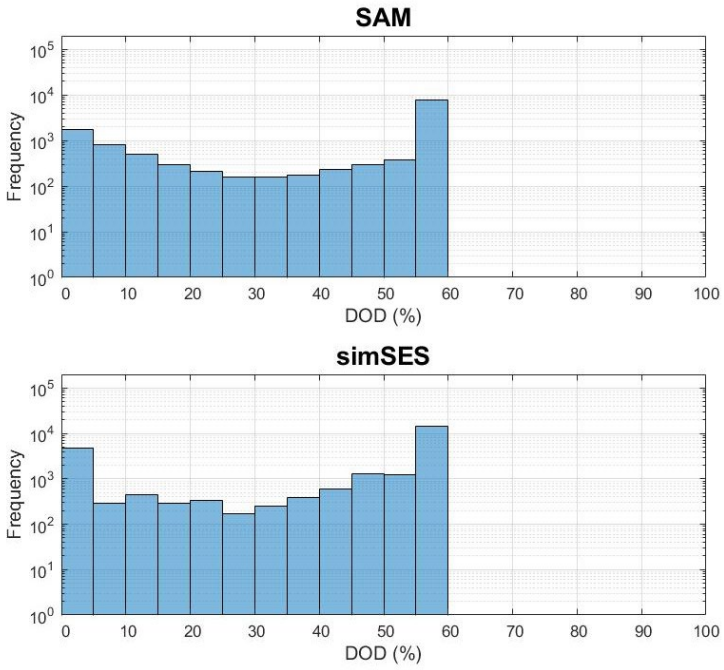

Figure 83. Frequency distribution of the different DODs in SAM and simSES at Scenario 3 using the reference parameters.

4.3.2 SOC Range

Figure 84 shows the expected lifetime in Polysun. The same general trend is observed with the exception of the 20-100% range which performs better than other smaller ranges.

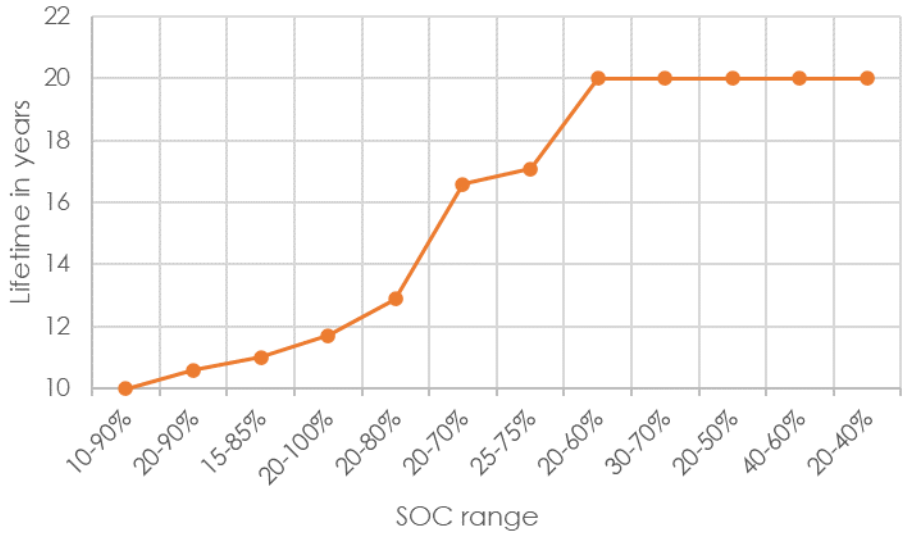

Figure 84. Expected lifetime in Polysun for different SOC ranges at Scenario 3.

Figure 85 shows the predicted SOH evolution in SAM. The same tendencies than in the previous scenarios are observed, with this scenario having a slower cycling as a consequence of the smaller number of cycles.

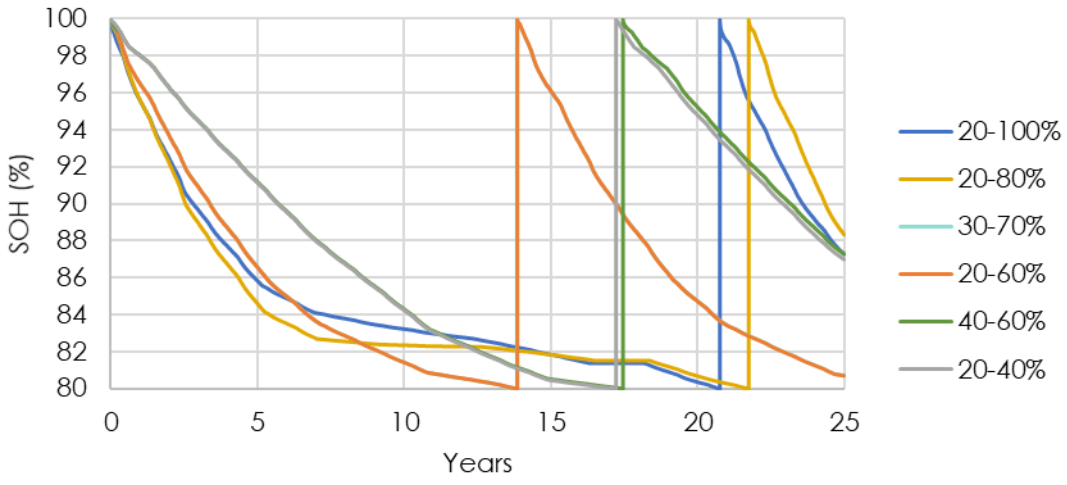

Figure 85. Evolution of the SOH in SAM for different SOC ranges at Scenario 3.

On the other hand, in simSES the results are similar to the previous scenarios as represented in Figure 86, as in all of them calendar aging dominates. In this case the

aging is slightly slower than in the family scenarios because this scenario has a higher average SOC, although the difference is small.

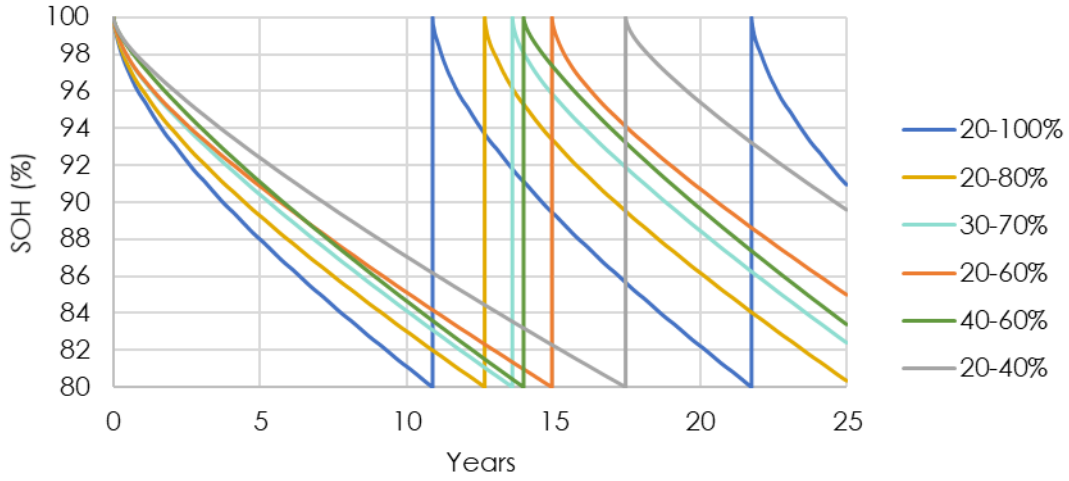

Figure 86. Evolution of the SOH in simSES for different SOC ranges at Scenario 3.

4.3.3 Charge and discharge rate

As shown in Figure 87, the behaviour of this scenario is very similar to the previous scenarios, with C-rate limit having almost no effect.

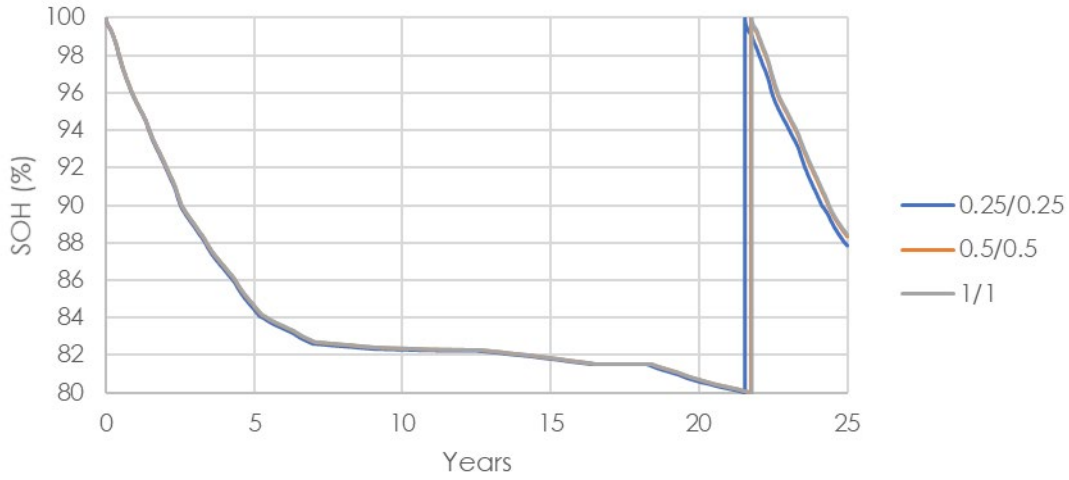

Figure 87. Evolution of the SOH in SAM for various C-rate limits at Scenario 3.

The C-Rate distribution of the histogram in Figure 88 shows that high discharge rate is more frequent than in the Scenarios 1 and 2 shown in Figure 43 and Figure 67. However, it still does not show a perceptible influence on the lifetime.

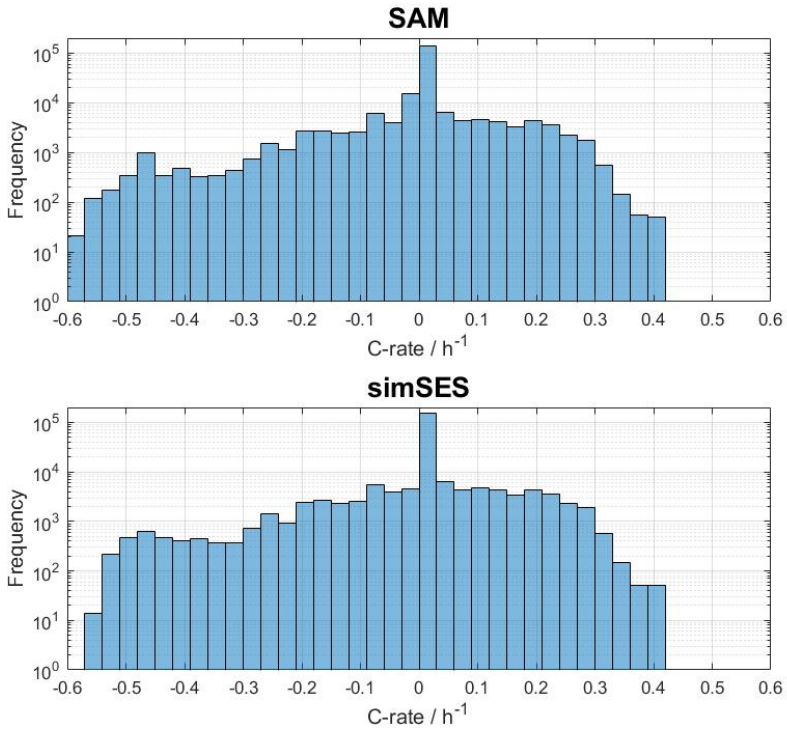

Figure 88. Frequency distribution of the different charge (positive) and discharge (negative) C-rates with no rate limit in SAM and simSES at Scenario 3.

4.3.4 Battery size

The effect of the battery size was studied keeping the same usable capacity. In the 4.5 kWh battery the 60% SOC range represents 2.7 kWh. The proportions are kept, and this energy still represents the same 90% and 45% SOC range for the 3kWh and 6kWh batteries, so the same SOC intervals as before are used.

Figure 89 shows that SOH degrades at a lower rate in larger batteries, as also happened in the previous scenarios.

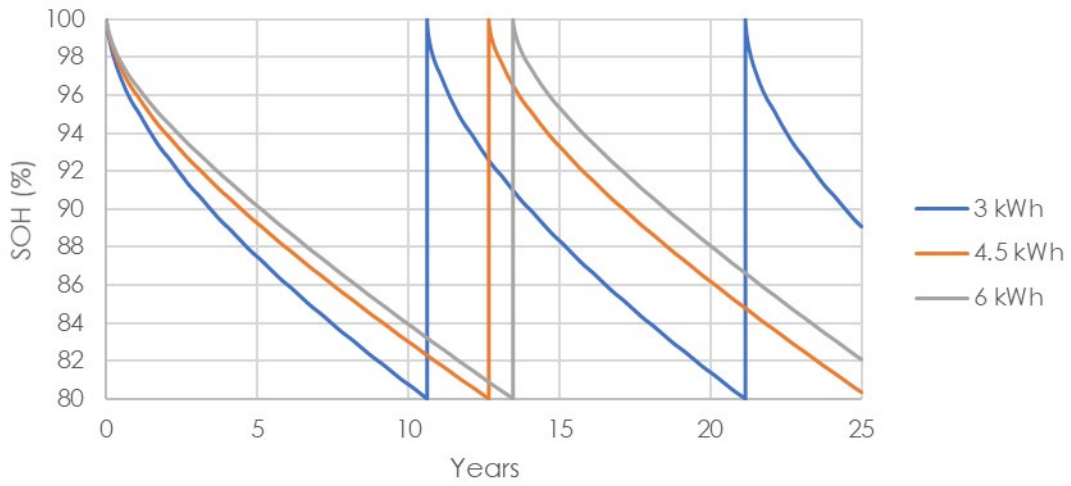

Figure 89. Evolution of the SOH in simSES for different battery sizes while keeping the same usable capacity at Scenario 3.

4.3.5 Dispatch method

Figure 90 shows that in SAM the difference between the dispatch methods is similar to the previous scenarios.

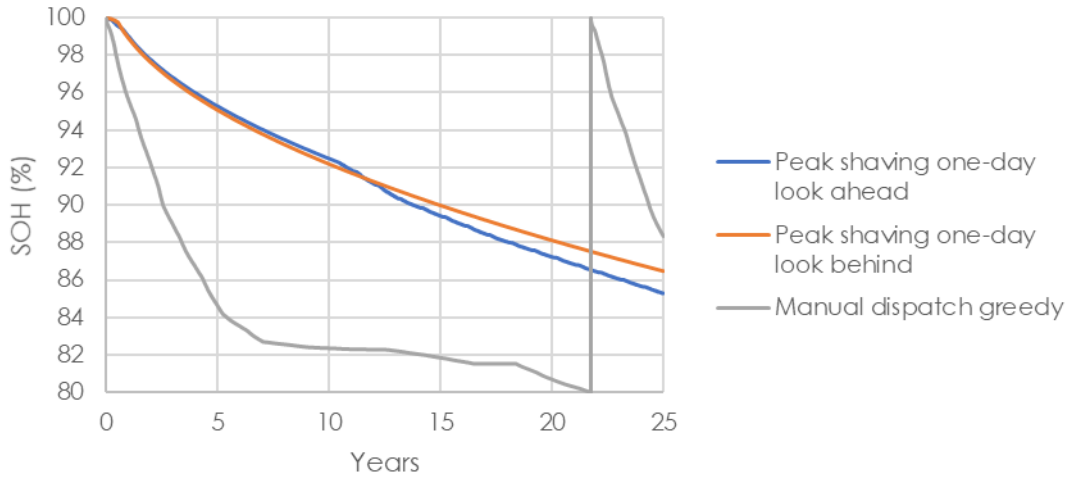

Figure 90. Evolution of the SOH in SAM under different dispatch methods at Scenario 3.

Similarly, Figure 91 shows that in simSES the results of all the dispatch models are very similar as shown in as in previous scenarios.

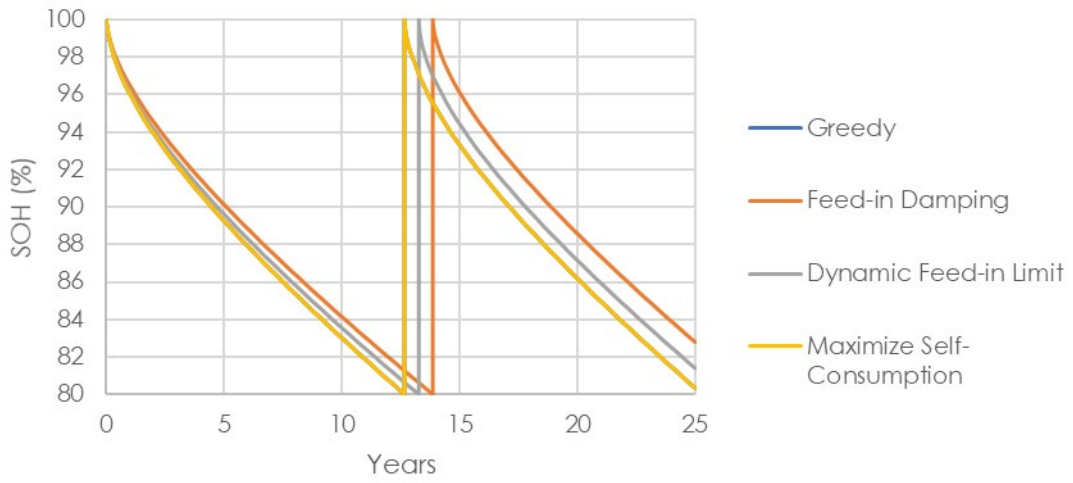

Figure 91. Evolution of the SOH in simSES under different dispatch methods at Scenario 3.

4.3.6 Chemistry

The NMC and LFP chemistries degradations are shown in Figure 92. As in the previous scenarios the NMC battery degrades much faster.

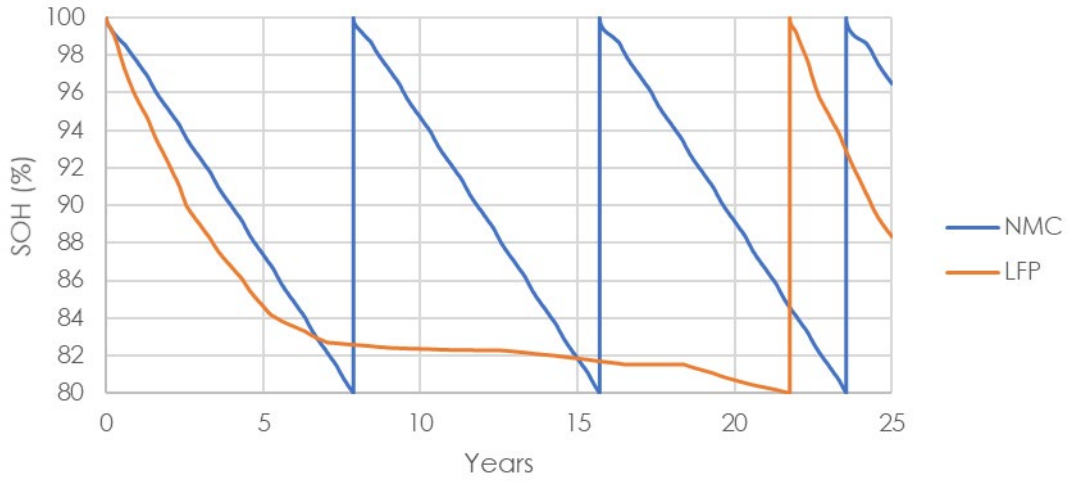

Figure 92. Evolution of the SOH in SAM for different battery chemistries at Scenario 3.

Figure 93 represents the SOH evolution of each chemistry in simSES. The result is similar to Figure 50 and Figure 71 from the Scenarios 1 and 2 with the aging in the NMC chemistry depending on the cycles of each scenario (as it only models calendar aging).

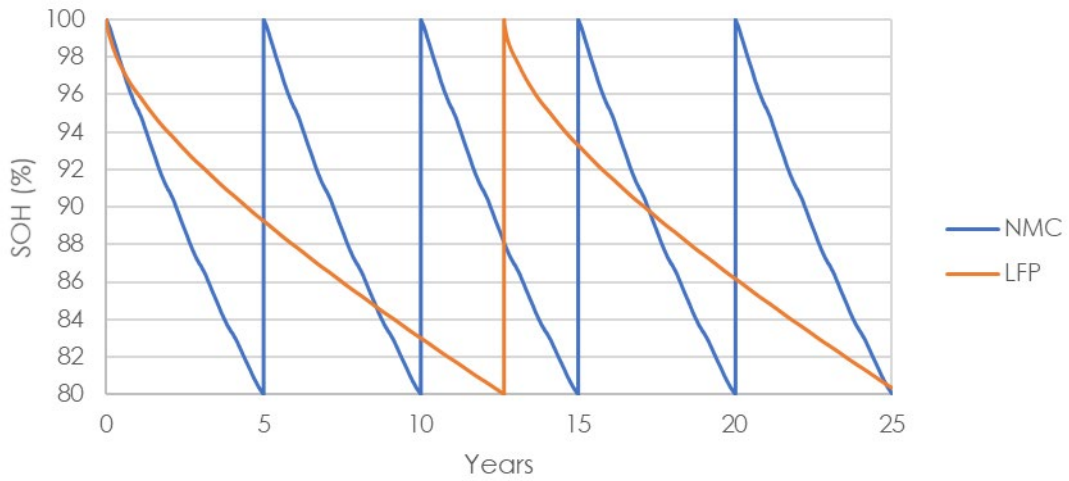

Figure 93. Evolution of the SOH in simSES for different battery chemistries at Scenario 3.

4.3.7 Temperature

Finally, the temperature dependence in SAM is the same as in previous scenarios as shown in Figure 94, although in this case and because of the smaller cycle aging the less favourable 40°C shows a much faster aging.

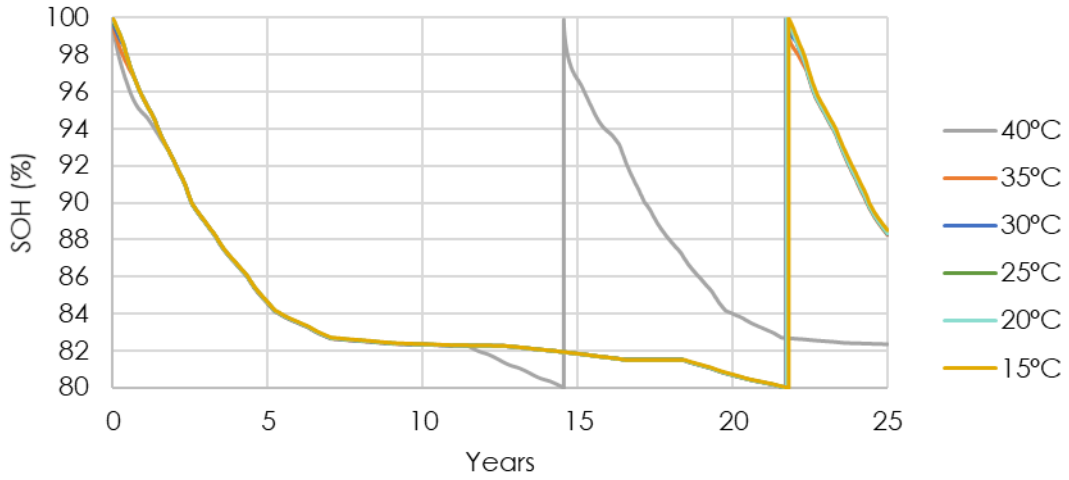

Figure 94. Evolution of the SOH in SAM at different ambient temperatures at Scenario 3.

On the other hand, Figure 95 shows that in simSES the results do not differ from previous scenarios.

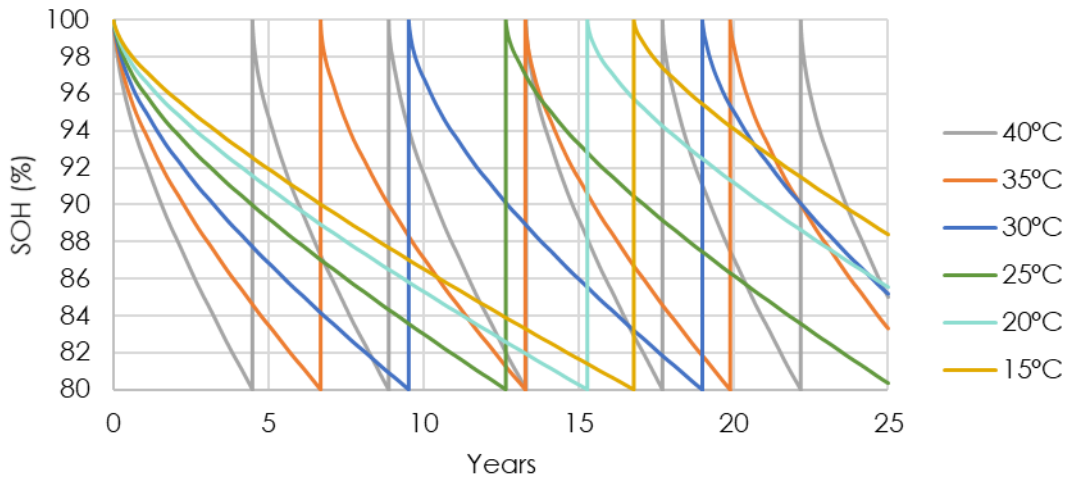

Figure 95. Evolution of the SOH in simSES at different ambient temperatures at Scenario 3.

4.4 Scenario 4: One person unemployed

As with the previous scenarios, the profiles in the same summer and winter weeks are represented in Figure 96 and Figure 97.

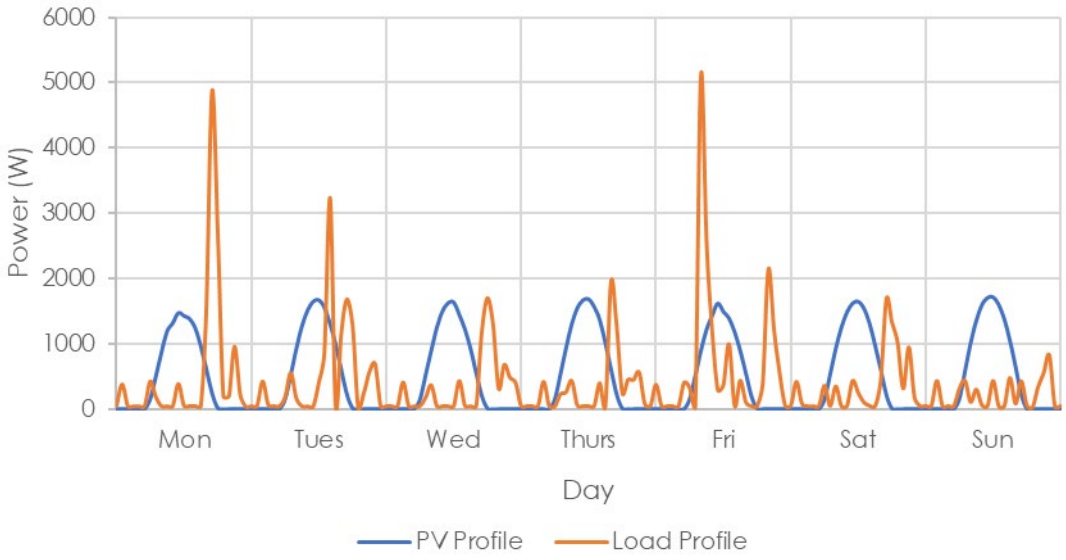

Figure 96. Consumption and generation profiles of Scenario 4 during a summer week.

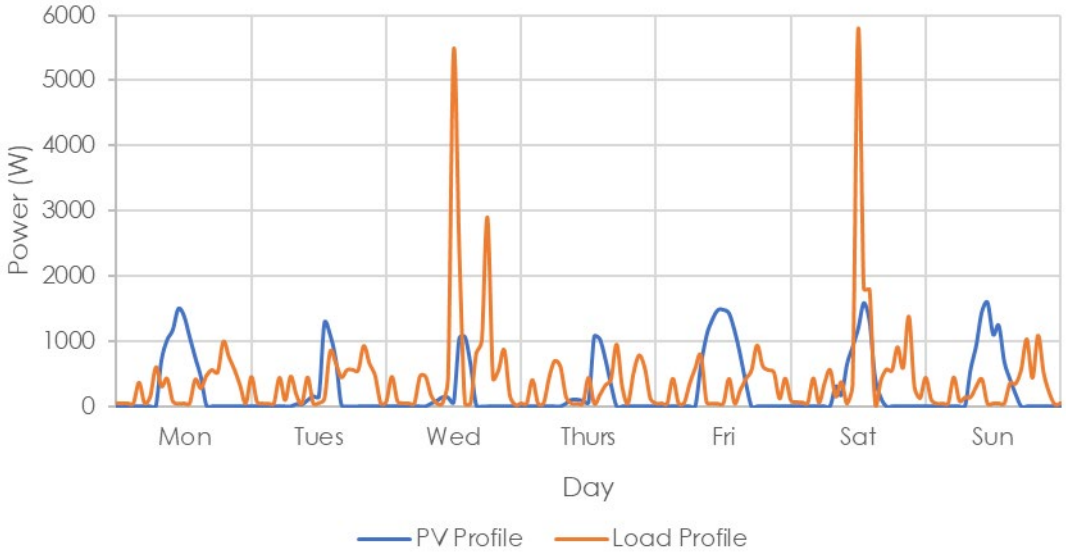

Figure 97. Consumption and generation profiles of Scenario 4 during a winter week.

Comparing these figures with Figure 75 and Figure 76 from Scenario 3 it is shown that in the "unemployed scenario" there is no difference between the weekdays and the weekend and the consumption is more distributed throughout the day rather than concentrated at some time of the day.

4.4.1 Reference parameters

The summary of the simulations performed using both SAM and simSES is presented in Table 14. As for the previous scenarios, both models obtain similar values for cycle, average SOC and average DOD, while the counting algorithm obtains a very high cycle number. Contrary to what happened with the family scenarios, now the unemployed scenario cycles more than the working scenario.

Table 14. Summary of Scenario 4 with reference parameters

	SAM	simSES
Total Cycles (Counting algorithm)	5725 (14823)	5720
Average Cycles/day	0.61	0.61
Average DOD	38.62%	43.13%
Average SOC	41.03%	39.93%
Battery replacements	1 (20th year)	1 (14th year)
SOH Calendar Aging	95.93%	83.86%
SOH Cycling Aging	82.91%	86.76%
Total SOH	82.91%	81.39%

The SOC evolution for the summer and winter week is shown in Figure 98 and Figure 99. When compared with the Scenario 3 (Figure 77 and Figure 78) the battery not fully being charged during the day is observed more often, especially during winter, as a greater share of the PV production is being directly consumed. This difference was also shown when comparing the Scenario 1 and Scenario 2.

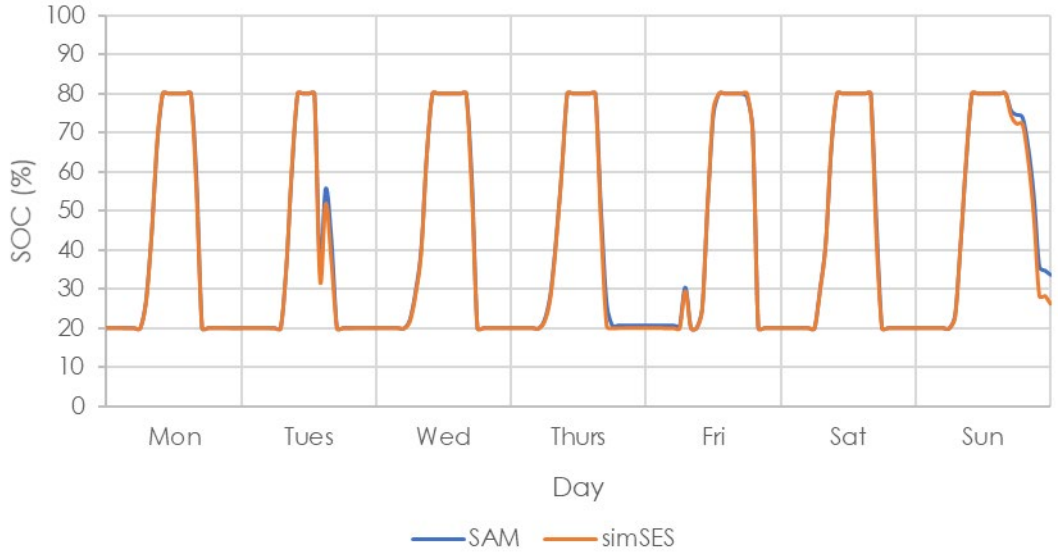

Figure 98. SOC in SAM and simSES at Scenario 4 during a summer week using the reference parameters.

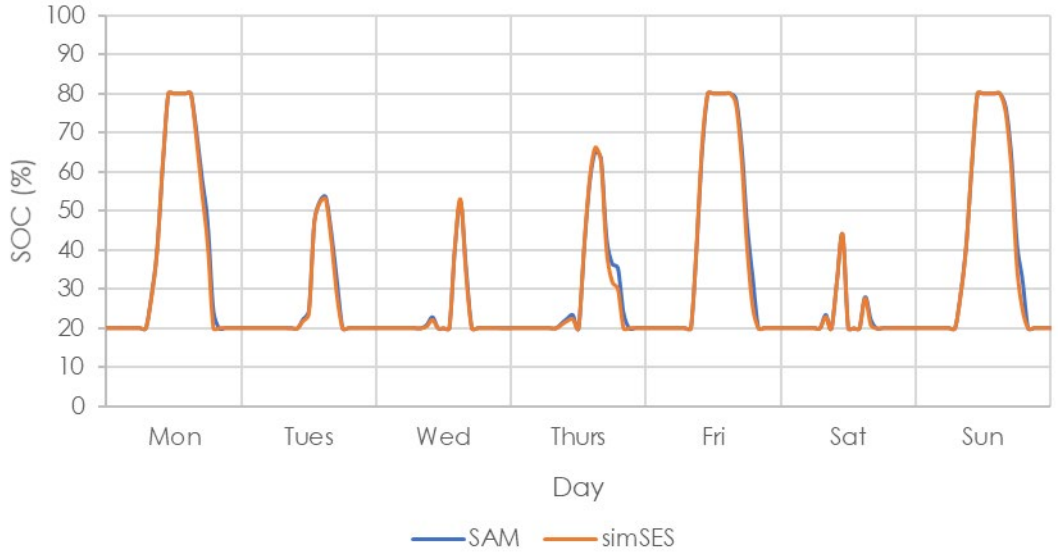

Figure 99. SOC in SAM and simSES at Scenario 4 during a winter week using the reference parameters.

The comparison of the SOH evolution in the two software is shown in Figure 100. As in all the previous scenarios simSES predicts a faster aging although the SAM keeps experiencing the high cycles problem.

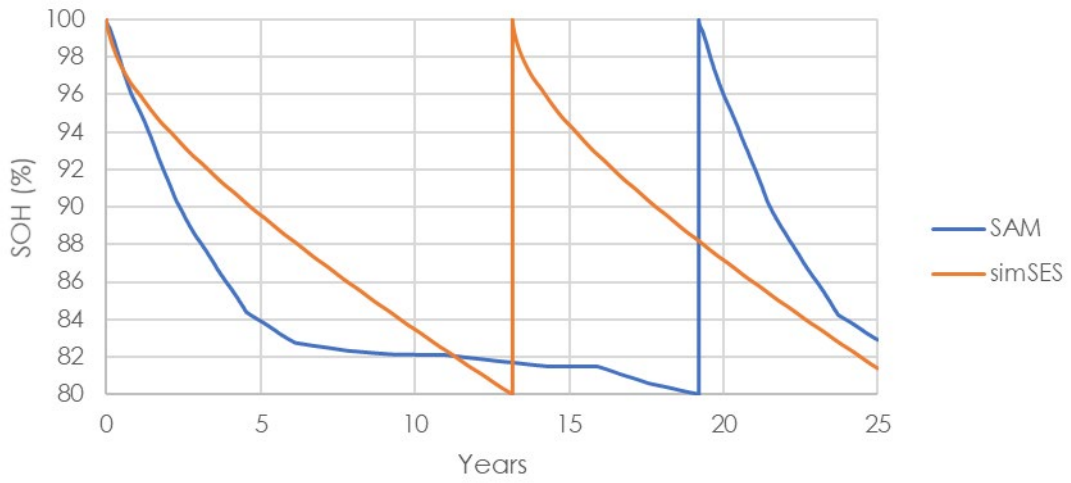

Figure 100. Evolution of the SOH in SAM and simSES at Scenario 4 using the reference parameters.

The aging mechanisms in SAM are studied in Figure 101, showing the same tendency as in the other three scenarios.

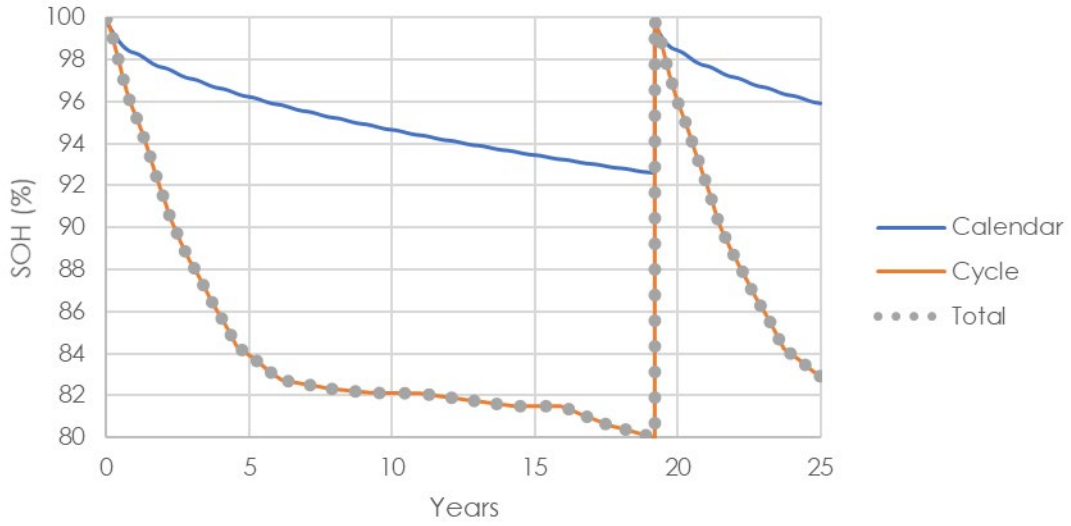

Figure 101. Calendar and cycling aging in SAM at Scenario 4 using the reference parameters.

The same happens in simSES with the resulting evolution shown in Figure 102 being very similar to the ones in Figures 34, 60 and 81.

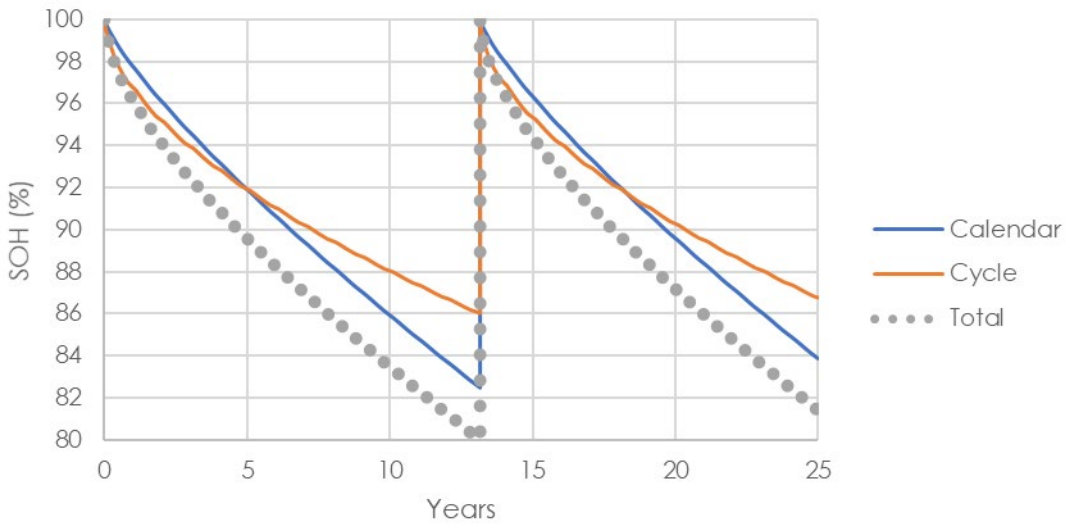

Figure 102. Calendar and cycling aging in simSES at Scenario 4 using the reference parameters.

After that, the SOC and DOD distributions were analysed. Figure 103 shows the frequency distribution of each SOC. This histogram is very similar to the ones of the other scenarios.

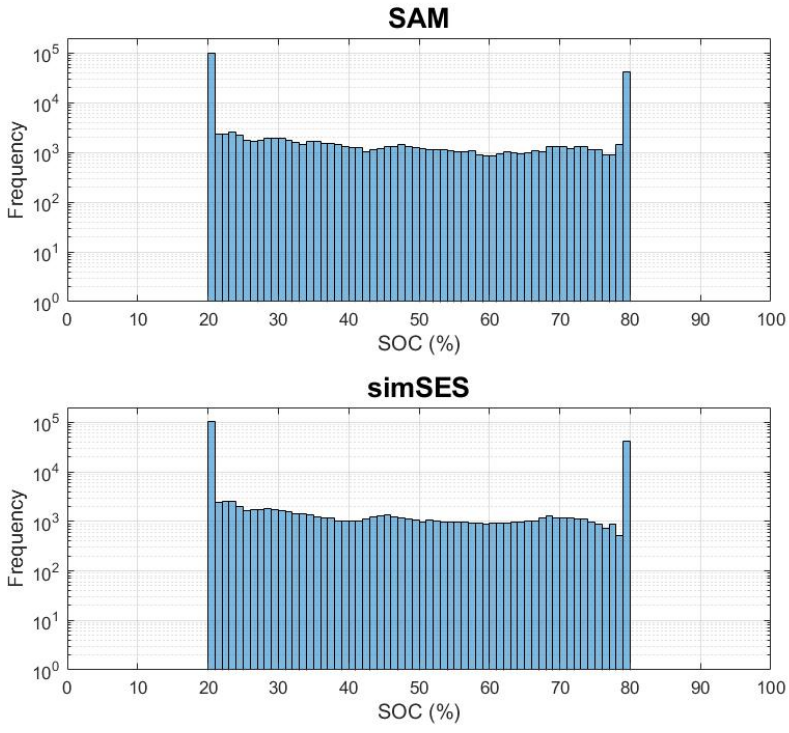

Figure 103. Frequency distribution of the different SOCs in SAM and simSES at Scenario 4 using the reference parameters.

On the other hand, the histogram of Figure 104 shows a very similar distribution to the other scenarios. However, as happened with the other one-person scenario in Figure 83, greater DODs are more frequent than in family scenarios.

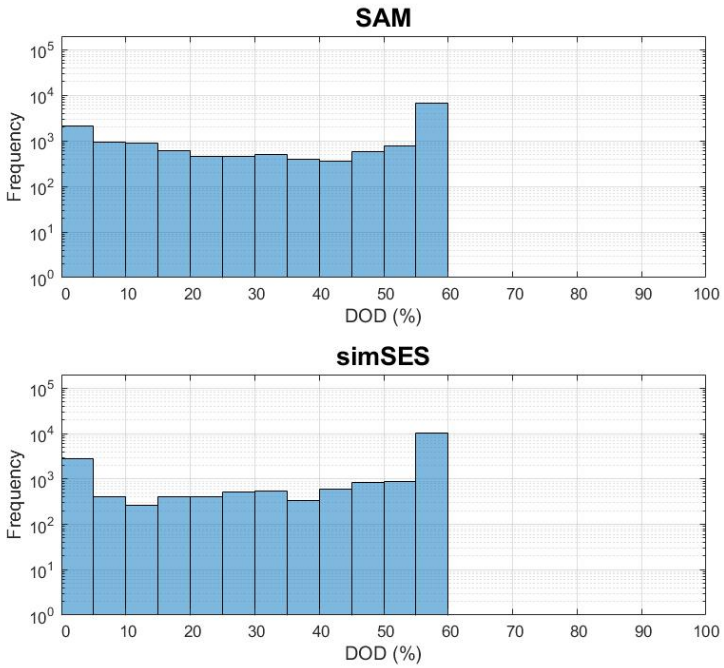

Figure 104. Frequency distribution of the different DODs in SAM and simSES at Scenario 4 using the reference parameters.

4.4.2 SOC Range

The analysis in Polysun once again exhibits the same trends. Figure 105 shows how the lifetime increases with decreasing SOC range until reaching the maximum 20 years lifetime. The expected lifetime of this scenario is slightly lower than the previous one, as the battery cycles more.

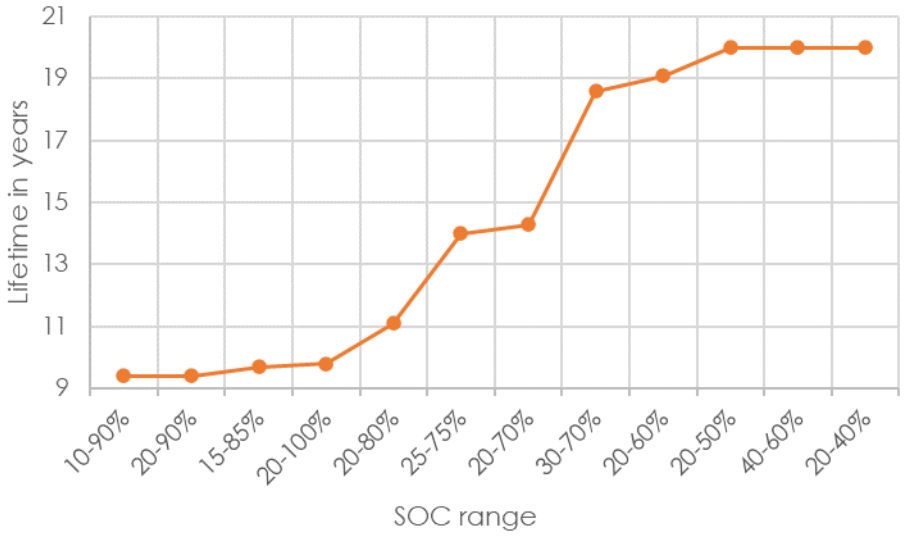

Figure 105. Expected lifetime in Polysun for different SOC ranges at Scenario 4.

Similarly, the results in SAM and simSES follow the same trend as in previous scenarios as shown in Figure 106 and Figure 107 respectively.

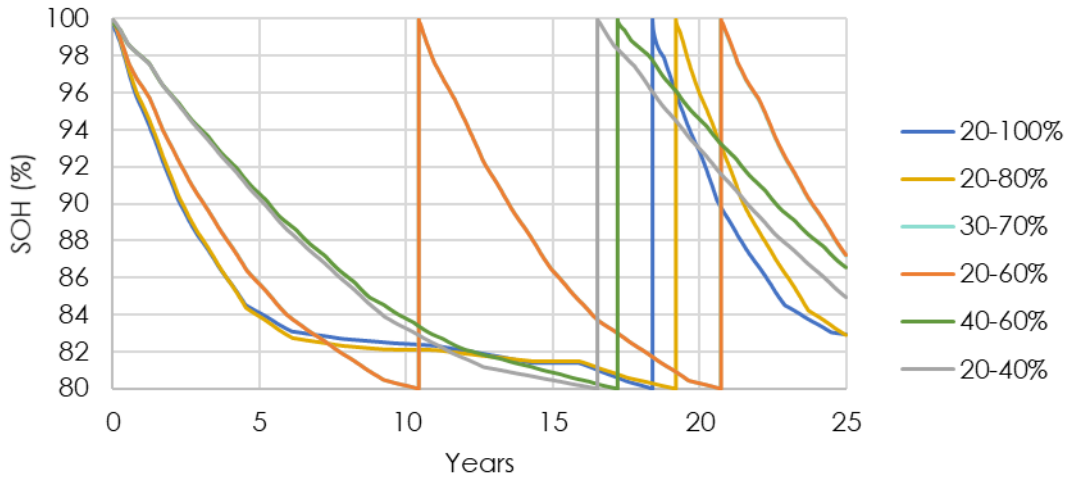

Figure 106. Evolution of the SOH in SAM for different SOC ranges at Scenario 4.

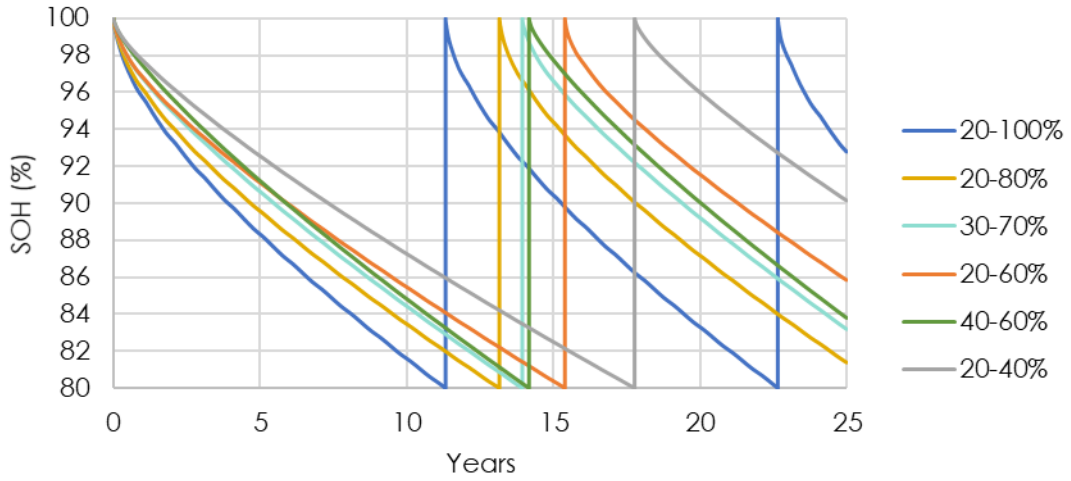

Figure 107. Evolution of the SOH in simSES for different SOC ranges at Scenario 4.

4.4.3 Charge and discharge rate

Figure 108 shows that the evolution of the SOH is almost the same for all C-rates, as happened in the other scenarios.

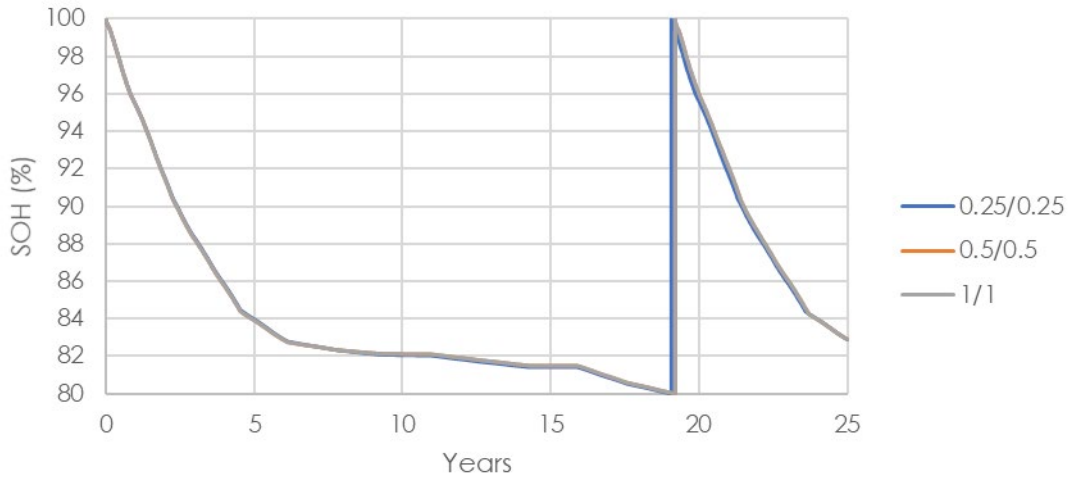

Figure 108. Evolution of the SOH in SAM for various C-rate limits at Scenario 4.

Analysing the histogram of C-rate distribution in Figure 109 it is observed a similar distribution than in the other scenarios. As the other one-person scenario in Figure 88, it shows a slightly higher frequency of higher discharge rates than the family scenarios of Figure 43 and Figure 67.

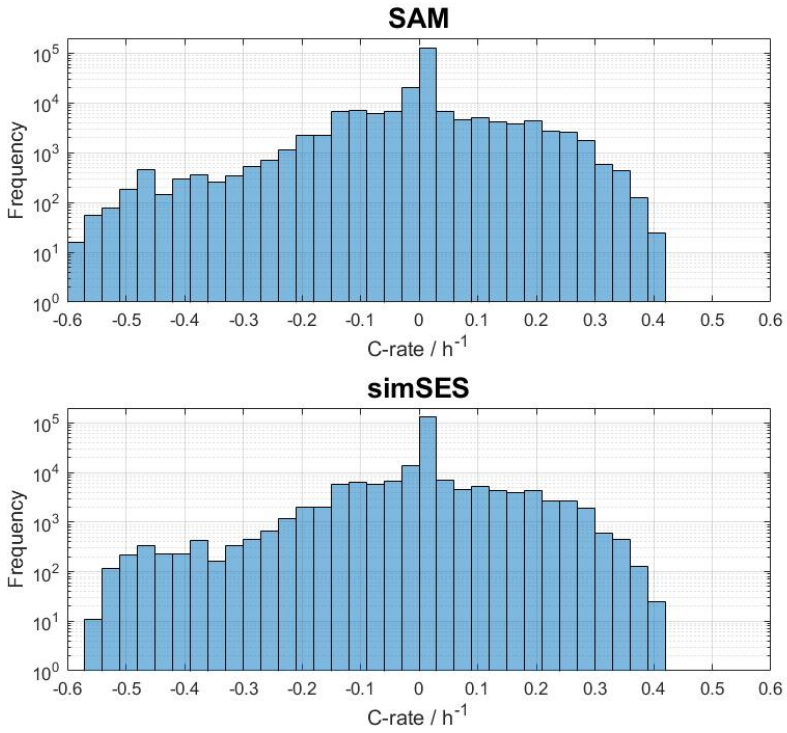

Figure 109. Frequency distribution of the different charge (positive) and discharge (negative) C-rates with no rate limit in SAM and simSES at Scenario 4.

4.4.4 Battery size

The battery size analysis in Figure 110 shows once again the same trends as in the previous scenarios.

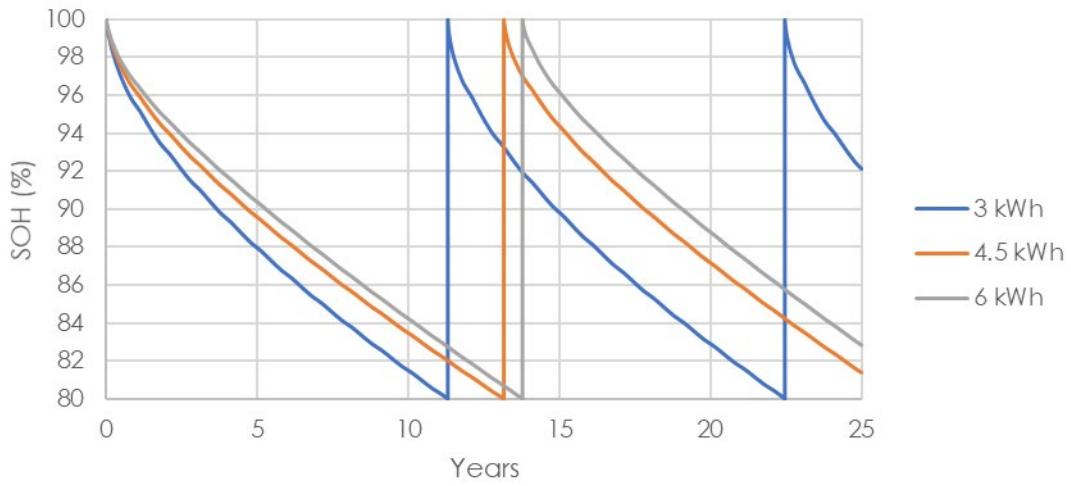

Figure 110. Evolution of the SOH in simSES for different battery sizes while keeping the same usable capacity at Scenario 4.

4.4.5 Dispatch method

Figure 111 and Figure 112 show the SOH evolution under the different dispatch methods in SAM and simSES, which exhibits the same trends as for the previous scenarios.

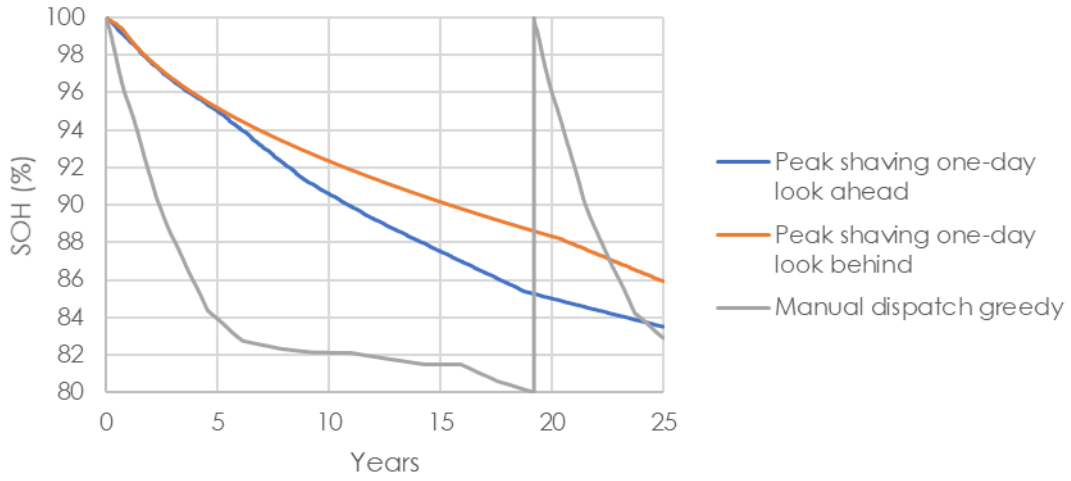

Figure 111. Evolution of the SOH in SAM under different dispatch methods at Scenario 4.

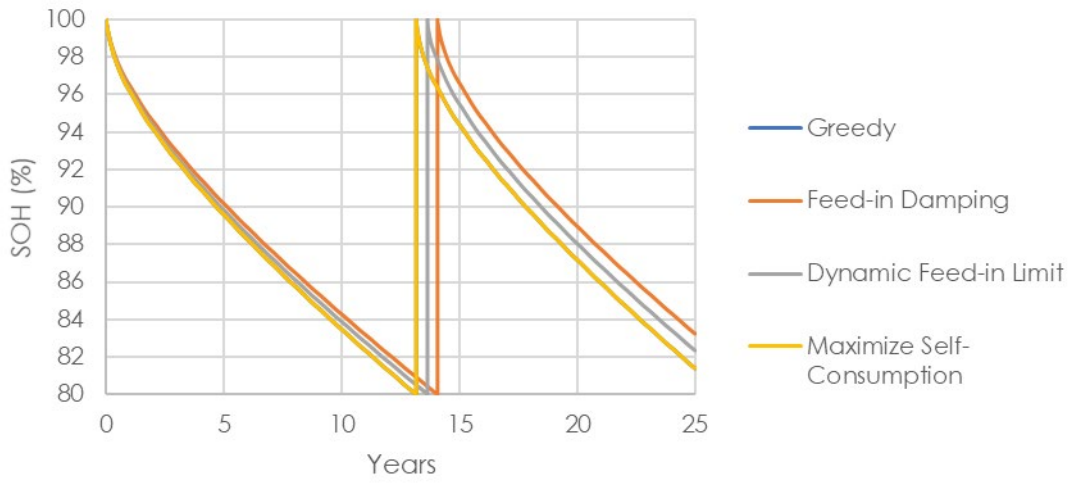

Figure 112. Evolution of the SOH in simSES under different dispatch methods at Scenario 4.

4.4.6 Chemistry

As in previous scenarios the NMC battery suffered a faster degradation as depicted in Figure 113, although presumably the LFP model would have had a similar evolution if it was not experiencing the slowed aging described before.

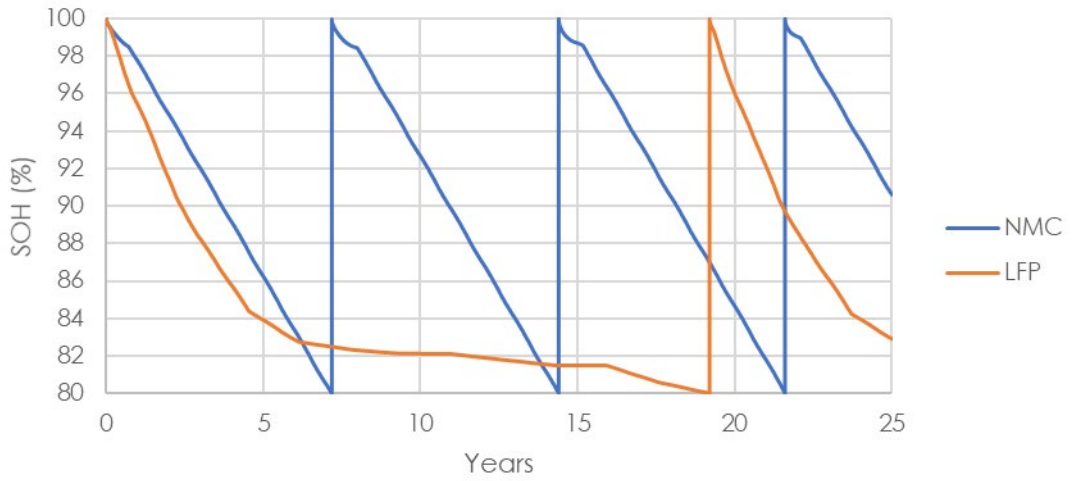

Figure 113. Evolution of the SOH in SAM for different battery chemistries at Scenario 4.

Similarly, Figure 114 shows the SOH evolution in simSES. As in previous cases, the SOH of the NMC model fades much faster, needing multiple replacements.

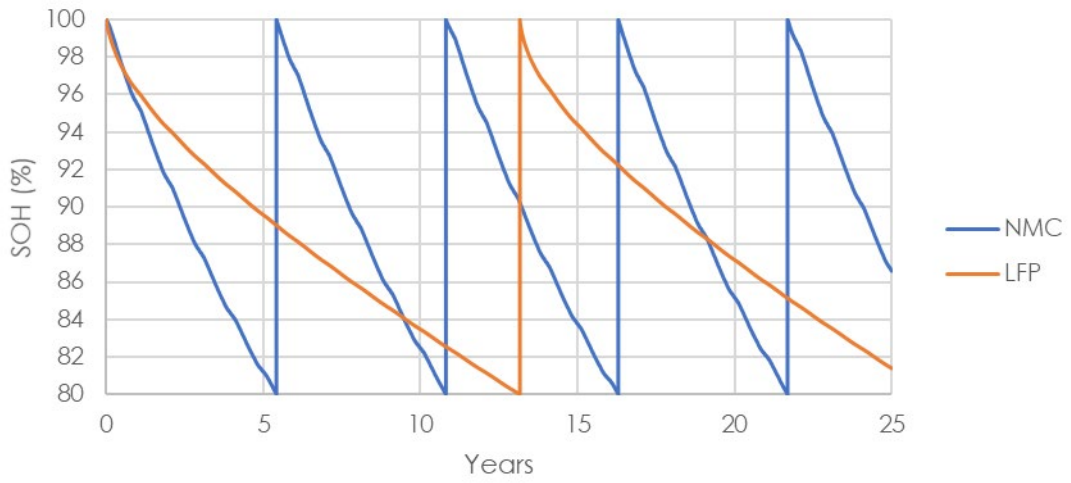

Figure 114. Evolution of the SOH in simSES for different battery chemistries at Scenario 4.

4.4.7 Temperature

Figure 115 shows the temperature dependence in SAM, being very similar to Figure 94 from Scenario 3 and following the general trend.

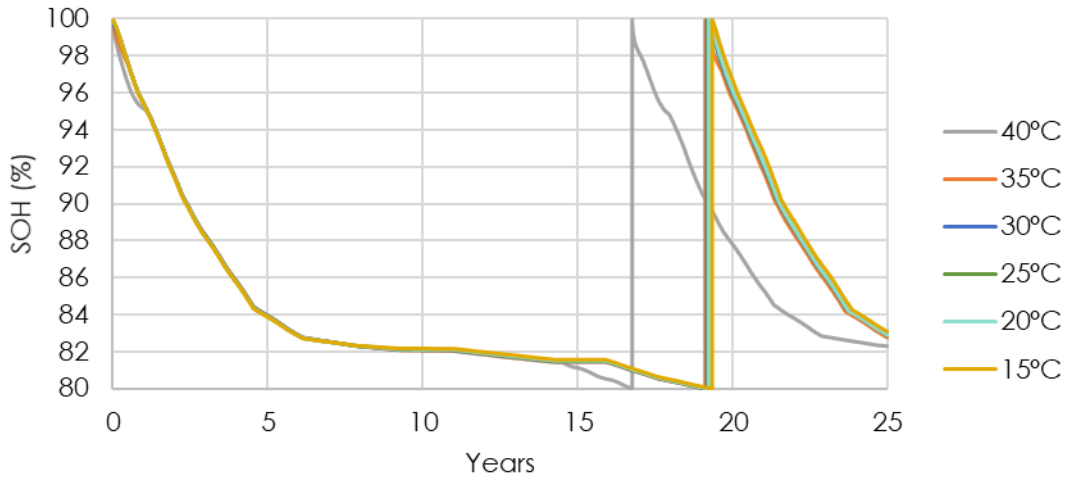

Figure 115. Evolution of the SOH in SAM at different ambient temperatures at Scenario 4.

Figure 116 shows the temperature dependence in simSES, which follows the same trend as the other scenarios with higher temperatures accelerating the degradation.

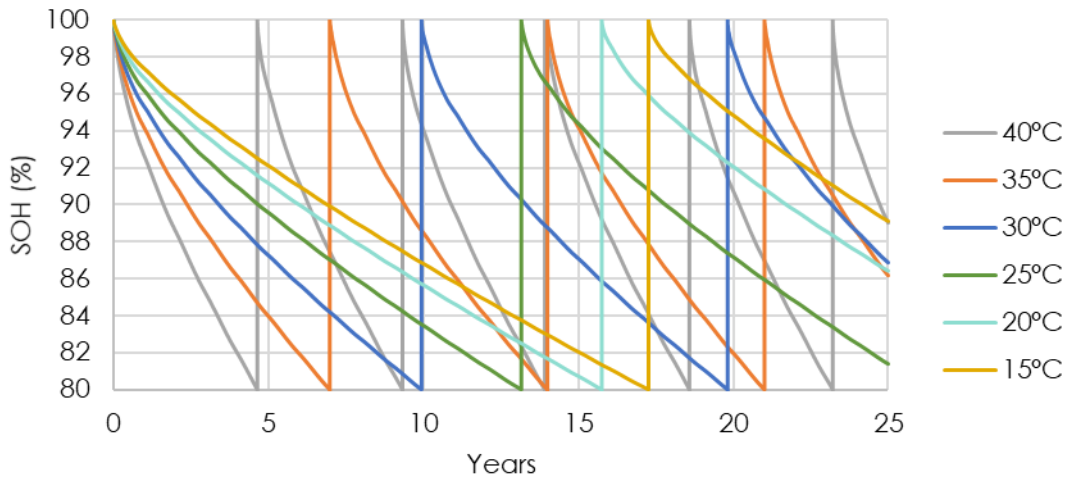

Figure 116. Evolution of the SOH in simSES at different ambient temperatures at Scenario 4.

4.5 Cross-scenario comparison

Through the analysis of each scenario the particularities of each one have been identified and compared. This last section aims to offer a more general comparison of the four scenarios studied by observing the aging evolution with the reference parameters as well as its calendar and cycling components. The scenarios included two one-person and two multi-person households with their working and unemployed variants. Multi-person households are expected to have higher and more variated load pattern while a higher mismatch between PV and load is expected in working cases. The scenarios were simulated in SAM as well as in simSES. For both models, there was no significant difference between the results of the four scenarios.

Table 15 shows how a battery bank enhances self-consumption from the PV system and significantly increases the rentability of the system. The most favourable situations are the unemployed cases over the working ones, as the energy consumption during the sun hours will be higher. Similarly, the family situation has a more varied demand, making it more likely to have consumption during the sun hours. Larger improvements in self-consumption should mean more duty for the battery, and thus might affect the lifetime.

Table 15. Self-consumption fraction in each scenario with and without battery.

	Family		One person	
	Working	Unemployed	Working	Unemployed
Self-consumption fraction without battery	22.4%	35.1%	14.9%	25.5%
Self-consumption fraction with battery	63.6%	70.9%	50.2%	63.6%

To compare the lifetime the simSES model will be used as SAM presented several limitations in the lifetime calculation.

Figure 117 shows the calendar aging for each scenario. The evolution of each case is very similar, as calendar aging is only slightly affected by some scenarios having more frequent high SOC. This way "family scenarios" perform better than "one-person scenarios" because the demand is more continuous and thus the battery spends less time idling at high SOC. For the same reason, unemployed cases age slower than their working counterparts, as in working scenarios the battery will often idle at high SOC having been charged while the residents are away from home. However, these differences are very small in all cases and do not have a pronounced effect in the lifetime.

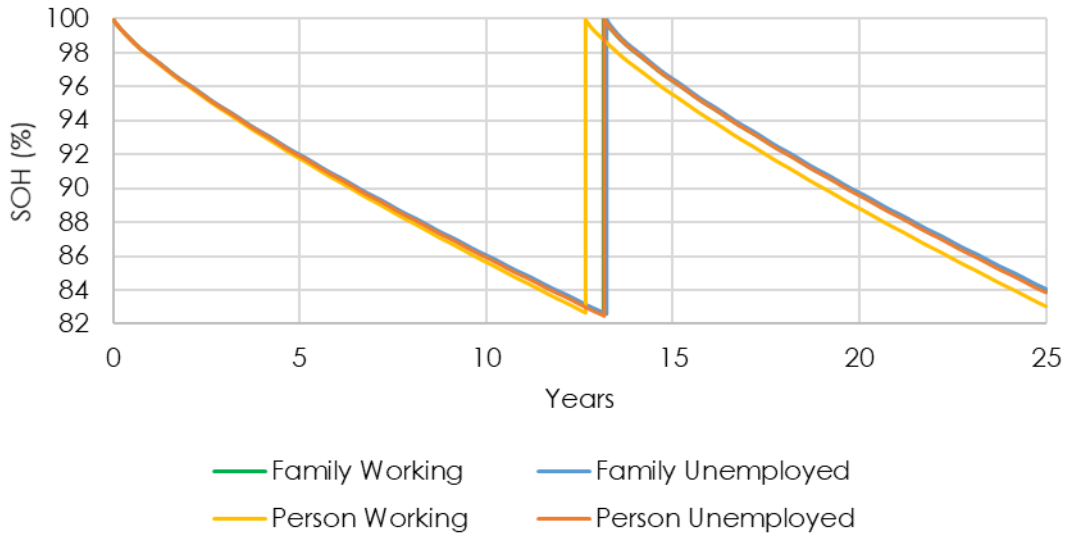

Figure 117. Evolution of the SOH due to calendar aging in simSES at the four studied scenarios.

Figure 118 shows the cycle aging in each scenario. Despite calendar aging dominating all scenarios the values for cyclic are not far from calendar ones. Cycle aging is more affected by the different scenarios although the effect is still very small, showing a 1% difference between the extreme cases. The difference between the scenarios is induced

by the different cycling and the different DODs in this case. In the same way as with calendar aging, "one-person scenarios" age faster than "family scenarios", as it was observed when analysing the DOD distribution in Figure 83 and Figure 104, which showed a higher frequency of high DODs. Similarly, the "working scenarios" show a faster aging than the "unemployed scenarios".

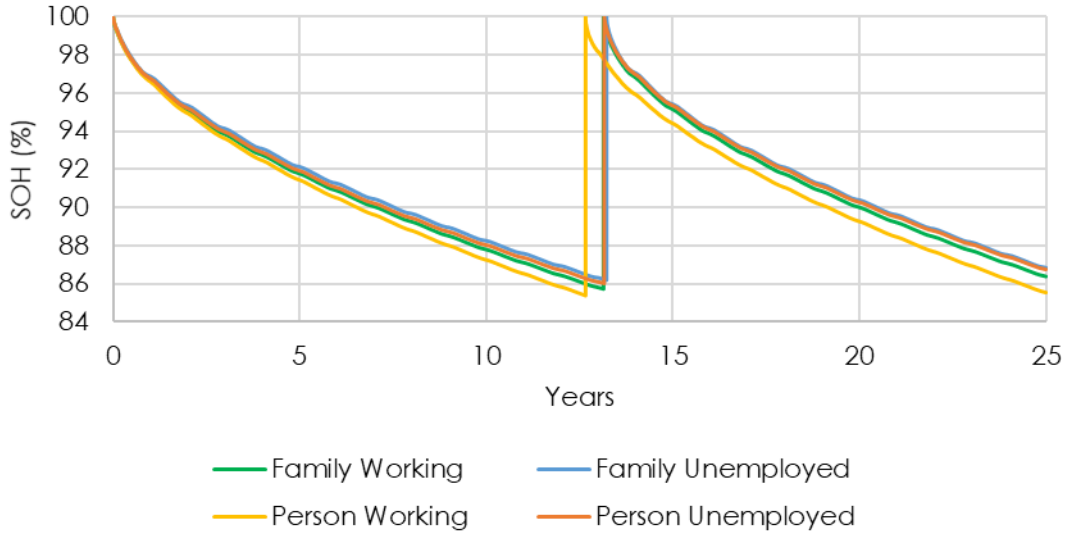

Figure 118. Evolution of the SOH due to cycle aging in simSES at the four studied scenarios.

The two effects are combined to obtain the total aging shown in Figure 119. In the four scenarios the calendar aging dominates. After combining the effects only, Scenario 4 shows a small difference with the rest of the scenarios, as it was the less favourable from a lifetime perspective.

Figure 119. Evolution of the SOH in simSES at the four studied scenarios

Lastly, Table 16 shows the estimated lifetime by each software. In SAM, the change in slope shown in Figures 39, 64, 85 and 106 in the SOH curves for the 20-100% and 20-80% seems to indicate that the SOH calculation malfunctions as the cycle count increases as discussed in Scenario 1. Since this did not happen for smaller ranges, the lifetime predictions at the end of the initial higher slope are extracted and shown in the table as well. On the other hand, simSES shows more continuity in the SOH progression and hence gives more confidence in the lifetime prediction. The values from Polysun and simSES are relatively similar while SAM tends to predict different values, as a consequence of the malfunction encountered. The values from Polysun and simSES seem relatively reasonable, being in line with the warranties from manufacturer provided in Table 7 and the values from the literature.

Table 16. Lifetime prediction for each scenario for the reference parameters.

	Family		**One person**	
	Working	Unemployed	Working	Unemployed
Polysun	9.7 years	13.4 years	12.9 years	11.1 years
SAM (Value at the end of the initial slope)	15.8 years (5.7 years)	17.4 years (6.7 years)	21.8 years (7.3 years)	19.2 years (7.7 years)
simSES	13.1 years	13.2 years	12.7 years	13.2 years

The effect of the operating parameters will be discussed in depth in the next chapter but to conclude this section it will be briefly discussed and compared with the literature reviewed in the next points:

- The effect on the lifetime of different consumption and generation profiles is small. This was also previously reported by Beltran et al. [49].
- Calendar aging is increased by high SOC. This effect has been extensively observed in the literature [37], [41], [46].
- Cycle aging is favoured by high DODs. This effect has also been extensively observed in the literature [30], [37], [41].
- The SOC ranges can limit cyclic aging by limiting DOD and calendar aging by limiting the allowable SOCs. This is a very common strategy in the literature and

multiple studies have been made looking for the optimum SOC range [30], [41], [44], [47], [48].

- The C-rate did not show noticeable influence in any of the scenarios, although this could be a consequence of the inaccuracy experienced in SAM. In the literature higher C-rates are harmful to the lifetime of the battery [30], [37].
- The increase on battery size while maintain same useable capacity showed a positive effect on the lifetime. This effect was also reported by Mishra et al. [41].
- The dispatch method influences cycling and SOC distribution and thus affects the lifetime. In SAM the two "Peak shaving" methods showed very little operation of the battery and thus suffered less aging. In simSES the four dispatch methods studied obtained similar aging values, as the strategy of these dispatch methods is relatively similar.
- The LFP batteries performed much better in terms of lifetime than the NMC batteries. However, this is probably because of the limitations identified in SAM and simSES models. In the literature both chemistries usually experience a similar aging, with the LFP often performing slightly better [30], [37], [41], [49].
- High temperatures strongly increased calendar aging. This effect has also been extensively reported in the literature [30], [37], [41], [46].

5 Conclusions

In this dissertation the mechanisms affecting the lifetime of Li-ion batteries and the corresponding parameters set in PV battery systems were identified. Four scenarios were considered in order to study the effect of the settings through simulations, a family with the parents either unemployed or working and one person either unemployed or working.

Through them it was observed that in the models the aging is the result of the dominating degradation mechanism at each step. The different parameters as well as the generation and demand can promote either of the aging mechanisms or both. Overall, the lifetimes estimated in Polysun and simSES are similar to the ones observed in the literature for similar situations. Out of the two, simSES predictions are probably more reliable, as the model is more complex and considers the influence of more parameters like ambient temperature, charge and discharge rates or calendar aging. In SAM, the results are limited because of the cycle count malfunction and thus the reliability of the prediction cannot be properly discussed, as presumably once this malfunction was corrected the lifetime prediction would improve.

The generation and consumption profile had a small influence in lifetime, mainly affecting the cycle aging, with a lesser effect on calendar aging. “Family scenarios” showed a better performance, as their demand was more distributed throughout the day, leading to spending less time at high SOC and undergoing more partial charge and discharge cycles instead of full ones. Similarly, “unemployed scenarios” perform better because they have consumption during the central hours of the day allowing for partial SOC and charges and discharges as a greater share of the demand is directly consumed from the PV. These effects were discussed in Figures 117 and 118 and can be explained using the SOC and DOD distribution shown in the histograms from each scenario.

The SOC range impacts both cycling aging and calendar aging. Smaller SOC ranges limit the maximum DOD reducing the cycling aging, as shown in the cycling aging dominated cases of SAM represented in Figures 39, 64, 85 and 106. On the other hand, the limits restrict the possible SOC and therefore lower limits can reduce the calendar aging as depicted by the calendar aging dominated cases of simSES represented in Figures 40, 65, 86 and 107.

Restricting the charge and discharge rates did not show a noticeable effect as shown in Figures 42, 66, 87 and 108, possibly because this effect was eclipsed by the very high cycling experienced in SAM.

The battery size affects the cycling aging and calendar aging. For the same SOC range increasing the battery size generally improves the performance as the battery is able to operate in situations where a smaller battery would be either full or depleted. However, this makes the battery cycle more and can hurt the lifetime. If the goal is to improve the lifetime of the battery by using a bigger battery, the usable capacity must be restricted to be the same as before. In this case the SOC limits are reduced, limiting the maximum DOD and SOC, and thus reducing the cycling aging and calendar aging. This way a similar effect than regulating the SOC limits is achieved without reducing the usable energy. This was shown in Figures 45, 47, 68, 89 and 110.

The dispatch method mainly affects the cycling aging. Efficient dispatch methods can achieve a greater energy usage, therefore cycling more the battery and causing a faster cycle degradation. This was clearly observed in SAM as “Manual dispatch greedy” achieved a much higher cycling of the battery.

The effect of the chemistry on calendar aging could not be studied because of the limitations of the models. In cycle aging the LFP chemistry showed a much slower degradation than the NMC both in SAM, as in Figure 50 and simSES as in Figure 51. However, this is probably consequence of the difference in lifetime curves in SAM, which led to the NMC technology not suffering the inaccurate slower aging, and the limitation of the model in simSES.

Temperature showed a strong effect only in calendar aging, being the effect of temperature noticeable in simSES as in Figures 53, 74, 95 and 116. This way high temperatures greatly accelerated aging. This effect was less significant as temperature decreased, with batteries aging similarly at temperatures below 20°C.

Lastly, some general guidelines can be extracted from the simulations and the tendencies identified:

- A tighter SOC range can extend the lifetime but limits the usable energy. The 20-80% range seems reasonable, as it offers a reasonable usable capacity and tighter 40% DOD ranges only offered 1 or 2 years more of lifetime.

- The charge and discharge rate did not show a strong influence, possibly because of limitations in the models. The rate limit of 0.5C can be obtained from the literature, which improves the lifetime with small performance loss, as higher rates were very infrequent.
- Oversizing the battery can greatly extend the lifetime but increases the initial cost of the battery.
- The study of the NMC chemistry was not conclusive by the limitations of the models. From the literature it can be concluded that both LFP and NMC chemistries have their advantages and do not show important difference in terms of lifetime, so both are valid choices.
- Temperature can greatly hurt the lifetime of the battery. Because of this the battery should be protected from sources of heat. Room temperature of 20-25°C is adequate as lower temperatures show very similar aging.

This way the objectives of the dissertation have been met, having realized a comprehensive review of the degradation mechanisms in Li-ion batteries, identifying and analysing the main operating parameters affecting Li-ion aging and extracting guidelines from this analysis to extend the lifetime of Li-ion batteries.

Suggestions for future work

This study has shown that most strategies to minimize the battery aging have associated a loss of performance or an increase in the cost of the system. In order to evaluate them, the next logical step to this study would be to perform an economic analysis, seeking the optimal set of parameters to maximize the rate of return of the system.

Moreover, this work is conditioned by the accuracy of the models and the limited experimental lifetime data available. In the future the limitations of these models should be addressed, and more experimental/field tests should be carried out in order to support these models. Specifically, the models and lifetime data for NMC batteries for energy storage application is limited. In particular the limitation of the lifetime prediction in SAM software needs further investigation.

6 References

[1] European Parliament, “Directive 2009/28/EC of the European Parliament and of the Council of 23 April 2009,” *Off. J. Eur. Union*, vol. 140, no. 16, 2009.

[2] European Parliament, “Directive 2018/2001 of the European Parliament and of the Council of of 11 December 2018,” *Off. J. Eur. Union*, vol. 328, no. 82, 2018.

[3] European Commission, “The European Green Deal,” *Eur. Comm.*, vol. 53, no. 9, 2019, doi: 10.1017/CBO9781107415324.004.

[4] R. Boddula, Inamuddin, R. Pothu, and A. M. Asiri, Eds., *Rechargeable Batteries: History, Progress and Applications*. Beverly, USA: Wiley, 2020.

[5] M. J. Piernas Muñoz and E. Castillo Martínez, “Introduction to Batteries,” in *Prussian Blue Based Batteries*, SpringerBriefs in Applied Sciences and Technology, 2018, pp. 1–8.

[6] Battery University Group, “Battery Definitions,” 2017. https://batteryuniversity.com/learn/article/battery_definitions (accessed Mar. 23, 2021).

[7] MIT Electric Vehicle Team, “A Guide to Understanding Battery Specifications.” 2008, [Online]. Available: http://web.mit.edu/evt/summary_battery_specifications.pdf.

[8] T. B. Reddy and D. Linden, Eds., *Linden’s Handbook of Batteries*, 4th ed., no. 8. New York, USA: McGraw-Hill Professional Publishing, 2010.

[9] National Research Council, *Overcoming Barriers to Plug-in Electric Vehicle*. Washington, USA: National Academies Press, 2015.

[10] S. Hussain, M. U. Ali, S. H. Nengroo, I. Khan, M. Ishfaq, and H. J. Kim, “Semiactive hybrid energy management system: A solution for electric wheelchairs,” *Electron.*, vol. 8, no. 3, 2019, doi: 10.3390/electronics8030345.

[11] P. H. Huang, J. K. Kuo, and C. Y. Huang, “A new application of the UltraBattery to hybrid fuel cell vehicles,” *Int. J. Energy Res.*, vol. 40, no. 2, pp. 146–159, 2016, doi: 10.1002/er.3426.

[12] H. Chen, G. Cong, and Y. C. Lu, “Recent progress in organic redox flow batteries: Active materials, electrolytes and membranes,” *J. Energy Chem.*, vol. 27, no. 5,

pp. 1304–1325, 2018, doi: 10.1016/j.jechem.2018.02.009.

[13] Lightning Global, “Lithium-ion Batteries Part I: General Overview and 2019 Update,” 2019.

[14] T. Horiba, “Lithium-ion battery systems,” *Proc. IEEE*, vol. 102, no. 6, pp. 939–950, 2014, doi: 10.1109/JPROC.2014.2319832.

[15] IEEE Power and Energy Society, *IEEE Guide for the Characterization and Evaluation of Lithium-Based Batteries in Stationary Applications*. 2018.

[16] J. Spangenberger, “Introduction to lithium ion battery,” *EPA*, 2018, [Online]. Available: https://www.epa.gov/sites/production/files/2018-03/documents/spanenberger_epa_webinar_-_3-22-18_-_argonne.pdf.

[17] Battery University Group, “Types of Lithium-ion,” 2021. https://batteryuniversity.com/learn/article/types_of_lithium_ion (accessed Apr. 12, 2021).

[18] Avicenne energy, “The Rechargeable Battery Market and Main Trends 2012-2025,” 2019, [Online]. Available: https://www.bpifrance.fr/content/download/76854/831358/file/02-PresentationAvicenne-Christophe0Pillot-28Mai2019.pdf.

[19] Battery University Group, “Summary Table of Lithium-based Batteries,” 2019. https://batteryuniversity.com/learn/article/bu_216_summary_table_of_lithium_based_batteries (accessed Apr. 12, 2021).

[20] Battery University Group, “Lithium-polymer: Substance or Hype?,” 2017. https://batteryuniversity.com/learn/article/the_li_polymer_battery_substance_or_hype (accessed Apr. 12, 2021).

[21] Battery University Group, “Types of Battery Cells,” 2020. https://batteryuniversity.com/learn/article/types_of_battery_cells (accessed May 31, 2021).

[22] LG Chem, “RESU 6.5 specifications sheet.” 2019.

[23] Tesla, “Powerwall 2 datasheet.” 2019.

[24] VARTA, “VARTA pulse Datasheet.” 2020.

[25] SENEC, “SENEC.Home V3 Hybrid Specs and Data Sheet,” 2020.

[26] ReLiON, “ReLiON RB48V100 Datasheet.” 2021.

[27] ByD, “BYD Energy Storage Products (B-Box) Specifications,” 2020.

[28] SimpliPhi, “PHI 3.4 smart-tech battery specifications,” 2016.

[29] PowerPlus Energy, “LiFe Premium Specifications,” 2020.

[30] Y. Preger *et al.*, “Degradation of Commercial Lithium-Ion Cells as a Function of Chemistry and Cycling Conditions,” *J. Electrochem. Soc.*, vol. 167, no. 12, p. 120532, 2020, doi: 10.1149/1945-7111/abae37.

[31] M. M. Kabir and D. E. Demirocak, “Degradation mechanisms in Li-ion batteries: a state-of- the-art review,” *Int. J. Energy Res.*, vol. 41, no. 14, pp. 1963–1986, 2017, doi: https://doi.org/10.1002/er.3762.

[32] B. Balagopal, C. S. Huang, and M. Y. Chow, “Effect of calendar ageing on SEI growth and its impact on electrical circuit model parameters in Lithium ion batteries,” *Proc. - 2018 IEEE Int. Conf. Ind. Electron. Sustain. Energy Syst. IESES 2018*, vol. 2018-Janua, pp. 32–37, 2018, doi: 10.1109/IESES.2018.8349846.

[33] A. Pérez, V. Quintero, H. Rozas, F. Jaramillo, R. Moreno, and M. Orchard, “Modelling the degradation process of lithium-ion batteries when operating at erratic state-of-charge swing ranges,” *2017 4th Int. Conf. Control. Decis. Inf. Technol. CoDIT 2017*, vol. 2017-Janua, no. September, pp. 860–865, 2017, doi: 10.1109/CoDIT.2017.8102703.

[34] K. Smith, Y. Shi, and S. Santhanagopalan, “Degradation mechanisms and lifetime prediction for lithium-ion batteries - A control perspective,” *Proc. Am. Control Conf.*, vol. 2015-July, pp. 728–730, 2015, doi: 10.1109/ACC.2015.7170820.

[35] A. H. Zimmerman and M. V. Quinzio, “Lithium plating in lithium-ion batteries,” *NASA Battery Workshop*. 2010, [Online]. Available: https://www.nasa.gov/sites/default/files/atoms/files/1-lithium_plating_azimmerman.pdf.

[36] F. Hoffart, “Proper care extends li-ion battery life,” *Power Electronics Technology*, 2008. https://www.powerelectronics.com/markets/mobile/article/21859861/proper-care-extends-liion-battery-life (accessed Mar. 13, 2021).

[37] A. Gailani, R. Mokidm, M. El-Dalahmeh, M. El-Dalahmeh, and M. Al-Greer, “Analysis of Lithium-ion Battery Cells Degradation Based on Different Manufacturers,” *UPEC 2020 - 2020 55th Int. Univ. Power Eng. Conf. Proc.*, 2020, doi: 10.1109/UPEC49904.2020.9209759.

[38] J. Erickson, “Tips for extending the lifetime of lithium-ion batteries,” *University of Michigan*, 2020. https://news.umich.edu/tips-for-extending-the-lifetime-of-lithium-ion-batteries/ (accessed Mar. 13, 2021).

[39] Energsoft, “Improving the longevity of lithium-ion batteries,” 2020. https://energsoft.com/blog/f/improving-longevity-of-lithium-ion-batteries (accessed Mar. 13, 2021).

[40] S. Grolleau, A. Delaille, and H. Gualous, “Lithium-ion battery aging: Representative EV cycling profiles compared to calendar life.” 27th International electric vehicle symposium & exhibition, 2013, [Online]. Available: https://www.evs27.org/download.php?f=defpresentations/EVS27-3B-3650181.pdf.

[41] P. P. Mishra *et al.*, “Analysis of degradation in residential battery energy storage systems for rate-based use-cases,” *Appl. Energy*, vol. 264, no. February, p. 114632, 2020, doi: 10.1016/j.apenergy.2020.114632.

[42] Battery University Group, “How to Prolong Lithium-based Batteries.” https://batteryuniversity.com/learn/article/how_to_prolong_lithium_based_batteries/2 (accessed Mar. 13, 2021).

[43] G. Angenendt, S. Zurmühlen, R. Mir-Montazeri, D. Magnor, and D. U. Sauer, “Enhancing Battery Lifetime in PV Battery Home Storage System Using Forecast Based Operating Strategies,” *Energy Procedia*, vol. 99, no. March, pp. 80–88, 2016, doi: 10.1016/j.egypro.2016.10.100.

[44] I. K. Won, K. M. Choo, S. R. Lee, J. H. Lee, and C. Y. Won, “Lifetime management method of lithium-ion battery for energy storage system,” *J. Electr. Eng. Technol.*, vol. 13, no. 3, pp. 1173–1184, 2018, doi: 10.5370/JEET.2018.13.3.1173.

[45] M. Dubarry, A. Devie, K. Stein, M. Tun, M. Matsuura, and R. Rocheleau, “Battery Energy Storage System battery durability and reliability under electric utility grid operations: Analysis of 3 years of real usage,” *J. Power Sources*, vol. 338, no. March 2016, pp. 65–73, 2017, doi: 10.1016/j.jpowsour.2016.11.034.

[46] S. Grolleau, A. Delaille, and H. Gualous, “Predicting lithium-ion battery degradation for efficient design and management,” *World Electr. Veh. J.*, vol. 6, no. 3, pp. 549–554, 2013, doi: 10.3390/wevj6030549.

[47] C. Goebel, H. Hesse, M. Schimpe, A. Jossen, and H. A. Jacobsen, “Model-Based Dispatch Strategies for Lithium-Ion Battery Energy Storage Applied to Pay-as-Bid Markets for Secondary Reserve,” *IEEE Trans. Power Syst.*, vol. 32, no. 4, pp. 2724–2734, 2017, doi: 10.1109/TPWRS.2016.2626392.

[48] Y. Tian, A. Bera, J. Mitra, B. Chalamala, and R. H. Byrne, “Effect of operating strategies on the longevity of lithium-ion battery energy storage systems,” *2018 IEEE Ind. Appl. Soc. Annu. Meet. IAS 2018*, pp. 1–8, 2018, doi: 10.1109/IAS.2018.8544518.

[49] H. Beltran, P. Ayuso, and E. Pérez, “Lifetime Expectancy of Li-Ion Batteries used for Residential Solar Storage,” *Energies*, vol. 13, no. 3, p. 568, 2020, doi: doi:10.3390/en13030568.

[50] Vega Solaris AG, “Polysun.” .

[51] G. Said, “Development of Detailed Statistics on Energy Consumption in Households,” *Natl. Stat. Off. Malta*, 2012.

[52] Association of European Automotive and Industrial Battery Manufacturers, “Battery energy storage for smart grid applications,” *Rep. Smart Grids Task Force EUROBAT’s Ind. Batter. Comm.*, vol. 15, no. 2, p. 8, 2013.

[53] J. Weniger, T. Tjaden, and V. Quaschning, “Sizing of residential PV battery systems,” *Energy Procedia*, vol. 46, pp. 78–87, 2014, doi: 10.1016/j.egypro.2014.01.160.

[54] National Renewable Energy Laboratory, “System Advisor Model Version 2020.11.29 (SAM 2020.11.29) User Documentation.” 2020.

[55] M. Naumann, N. Truong, M. Schimpe, M. Müller, A. Jossen, and H. C. Hesse, “SimSES: Software for techno-economic Simulation of Stationary Energy Storage Systems,” no. October, pp. 1–2, 2017, doi: 10.3390/batteries20200.

[56] Vela Solaris AG, “Polysun software User Manual.” 2020.

[57] N. Diorio *et al.*, “Technoeconomic Modeling of Battery Energy Storage in SAM,” *NREL Tech. Rep.*, no. September, 2015, [Online]. Available: http://www.nrel.gov/docs/fy15osti/64641.pdf.

[58] S. D. Downing and D. F. Socie, “Simple rainflow counting algorithms,” *Int. J.*

Fatigue, vol. 4, no. 1, pp. 31–40, 1982, doi: 10.1016/0142-1123(82)90018-4.

[59] K. Smith, A. Saxon, M. Keyser, B. Lundstrom, Z. Cao, and A. Roc, "Life prediction model for grid-connected Li-ion battery energy storage system," *Proc. Am. Control Conf.*, pp. 4062–4068, 2017, doi: 10.23919/ACC.2017.7963578.

[60] A. Zeh and R. Witzmann, "Operational strategies for battery storage systems in low-voltage distribution grids to limit the feed-in power of roof-mounted solar power systems," *Energy Procedia*, vol. 46, pp. 114–123, 2014, doi: 10.1016/j.egypro.2014.01.164.

[61] J. Wang *et al.*, "Cycle-life model for graphite-LiFePO4 cells," *J. Power Sources*, vol. 196, no. 8, pp. 3942–3948, 2011, doi: 10.1016/j.jpowsour.2010.11.134.